A NEURAL CIRCUIT FOR RESOLVING

SENSORY CONFLICT IN *DROSOPHILA*

Laurence Lewis

2016

A NEURAL CIRCUIT FOR RESOLVING SENSORY CONFLICT IN *DROSOPHILA*

Dissertation der Graduate School of Systemic Neurosciences

der Ludwig-Maximilians-Universität München

Laurence Lewis

Die vorliegende Arbeit wurde im Max-Planck-Institut für Neurobiologie in Martinsried unter der Aufsicht von Dr. Ilona Grunwald Kadow in der Zeit vom Oktober 2011 bis November 2015 durchgeführt.

Erstgutachter: Dr. Ilona Grunwald Kadow

Zweitgutachter: Prof. Dr. Mark Hübener

Datum der Einreichung: 08 Februar 2016

Datum der Verteidigung: 31 Mai 2016

Contents

II

IV

List of figures

List of tables

List of abbreviations

OR	Olfactory receptor
GR	Gustatory receptor
IR	Ionotrophic receptor
OSN	Olfactory sensory neuron
AL	Antennal lobe
PN	Projection neuron
MB	Mushroom body
LH	Lateral horn
KC	Kenyon cell
MBON	Mushroom body output neuron
DAN	Dopaminergic neuron
PAM	Protocerebral anteromedial cluster (DAN)
PPL	Protocerebral posteriolateral cluster (DAN)
SMP	Superior medial protocerebrum
SIP	Superior intermediate protocerebrum
SLP	Superior lateral protocerebrum
CRE	Crepine
CS	Conditioned stimulus
US	Unconditioned stimulus
GFP	Green fluorescent protein
RFP	Red fluorescent protein
AD	Activation domain
DBD	DNA-binding domain
GRASP	GFP reconstitution across synaptic partners
JFRC	Janelia farm research campus

Abstract

Animal habitats are highly complex and encode a surfeit of potentially meaningful information relevant to an animal's immediate and future survival. Animals must sense and decode this complex environmental information in order to initiate an optimal behavioural response capable of meeting its survival requirements. Some environmental stimuli may elicit innate or learned attraction or aversion, while others may trigger courtship behaviour or grooming. However, the same stimuli may have different meaning to the animal depending on its internal state and the presence or absence of other stimuli. Thus, sensory cues often conflict with one another, requiring the animal to decide on which sensory objects to respond to.

Like all animals, the fruit fly *Drosophila melanogaster* must resolve this sensory conflict within its olfactory environment. An ecologically relevant example of this is the conflict between the strongly aversive odour carbon dioxide (CO_2), which is emitted by fermenting fruit, *Drosophila's* primary food source, and vinegar volatiles, which include many attractive products of fermentation. It has been shown that when starved, the fruit fly *Drosophila melanogaster* is capable of overcoming its innate aversion to CO_2 to approach the conflicting food odour vinegar (Bräcker et al., 2013). This implies a neural mechanism whereby a neural representation of vinegar is able to suppress the innate capability of CO_2 to drive aversion behaviour. It was found that a structure in the fly brain commonly associated with olfactory learning, the mushroom body (MB), is required for processing innate CO_2 aversion in a starvation dependent manner (Bräcker et al., 2013). This suggested a possible common neural substrate for both learned and innate sensory processing and behaviour execution.

To examine a possible role for the *Drosophila* MB in weighing conflicting olfactory inputs I conducted a systematic olfactory behavioural screen in which I tested responses to CO_2, vinegar, and the conflicting CO_2 plus vinegar. During testing MB neurons were thermogenetically inactivated via the targeted expression of UAS-Shibire[ts1] to the three primary populations of neurons composing the MB: MB output neurons (MBON), MB neuromodulatory input neurons, and MB Kenyon cell (KC) interneurons. The behavioural screen recapitulated data previously obtained in our lab identifying the

α'/β' KCs as playing the dominant role in representing CO_2 (Bräcker et al., 2013). The screen also identified MBONs innervating the β'2 region of the MB horizontal lobe as being required for CO_2 avoidance. Subsequent optogenetic behavioural experiments demonstrated that the same MBONs were sufficient to drive aversive behaviour, providing a putative MB circuitry for mediating CO_2 aversion. Additional behavioural experiments and calcium imaging revealed that dopaminergic neurons (DAN) innervating the same β'2 anatomical compartment represent vinegar, and that their activation is sufficient to reduce CO_2 aversion. This observation suggests DAN inhibition of the flow of CO_2 olfactory information from the presynaptic KCs to the postsynaptic MBONs. Indeed, these findings are consistent with our current understanding of MB neuromodulation by DANs, which are known to represent contextual information in the formation of associative memory and impinge on the KC-MBON synapse. Critically, it is demonstrated here that MBONs respond more weakly to a combination of vinegar and CO_2 than they do to CO_2 alone.

Taken together my findings suggest that the β'2 MBONs are sufficient to mediate CO_2 aversion, and that this sufficiency is dampened by vinegar responsive β'2 DANs, thus allowing flies to overcome their innate CO_2 aversion in the context of appetitive vinegar stimulus. The implication of my work is that the processing of sensory information to drive immediate behavioural responses is carried out by the same structure responsible for forming lasting associations, the MB. The economy of energy and neural substrates available for performing the processing tasks required of brains often results in a convergence of multiple functions onto few brain structures. In the present case the inherent similarities between the tasks of immediate and lasting modulation of behaviours supports this parsimony.

1.0 Introduction

1.1 Sensory neuroscience

The body of an observer, animal or human, is continually awash with energy in the form of light and heat, and in physical contact with various forms of matter: solid, liquid, and gas. Diverse sensory systems evolved to allow animals to detect, process, and attach meaning to their interactions with environmental features relative to their biological needs. The sensory channels available to an animal converge in its brain and form multimodal representations of its environment (Cappe et al., 2009; Frye, 2010; Hidaka et al., 2015; Recanzone, 2009). Based on the information contained within these representations animals can execute behavioural programs via their motor systems and navigate through their surroundings (Sarlegna & Mutha, 2014). The ability to sense and respond to their environment means that animals are continually faced with decisions: where to move, what to eat, when to sleep. However, these decisions are not free but are constrained by the necessities of biological maintenance and reproduction, and these constraints are part of an animal's evolutionary heritage; they are adaptations to the particular ecology in which it has evolved to survive. For example, if hungry, the smell of food will be a particularly prominent feature of an animal's sensorium, and will dominate its decision-making processes (Huetteroth & Waddell, 2011; Hunter, 2013; Rolls, 2015). In this way, the perceptual and behavioural characteristics of all animals are tuned by their evolution, and by immediate and remembered sensory information.

The ability to adapt behaviour on a moment-by-moment basis is crucial to ensuring survival. But which factors determine the optimal behavioural adaptation? Animals must decide which behavioural program to enact in response to a given sensory stimulus, and the decision is usually influenced by a combination of nutritive, reproductive, and homeostatic requirements (Ejima et al., 2007; Huetteroth & Waddell, 2011; Hunter, 2013; Yang et al., 2015). The fruit fly, *Drosophila melanogaster*, is as constrained by these biological imperatives as are humans. To help them secure necessary food and water and to respond to social cues, flies must be experts in their own chemical ecology, and as such their chemical senses play a crucial role in guiding their behaviour. They spend their entire

lives on and around fruit where they develop from larvae, feed, court, mate, and lay eggs. It is therefore extremely important for flies that they correctly judge the quality of their potential habitat, and they do so by contrasting external olfactory stimuli against their internal state. For a decision to be made, diverse and often conflicting information must converge from the sensory organs and be prioritized by the fly based on prescient biological requirements.

Despite the fundamental nature of these questions, the neural circuitry through which conflicting motivational drives are resolved is poorly understood. The genetic and experimental tools available to *Drosophila* researchers allow unparalleled control over the state of neural circuits in the fly brain, and offer an opportunity to investigate the processing strategies underlying decision-making.

1.2 Chemical environments

All organic life is composed of material that was once part of the environment, or indeed, part of other organisms. The system as a whole is in a continual state of flux as bacteria, plants, and animals exchange their chemical components with the environment around them. As a consequence, all environments inhabited by organic life are saturated with the chemical products of metabolism and decay. These products are distributed throughout the local ecology in various forms: they can be solid (an animal carcass), in solution (a piece of fruit rotting in shallows at the edge of a lake), or airborne (the smell of rain falling on dry soil). In all of these cases microorganisms, insects, and mammals contribute to a complex chemical ecology simply by performing their biological functions.

1.2.1 Chemical environments as chemosensory environments

Despite the vast complexity of chemical environments there is also some degree of order. Due to the high reproducibility of chemical reactions the appearance of a compound A in an environment co-occurs with the products of its decomposition or catabolism: compounds B and C. For example, fruit fallen from a tree (A) is initially fresh and gives off a plume of volatile gasses, but as bacteria and yeast on its surface begin to multiply

2

and metabolize sugars and proteins, the chemical composition of both the fruit itself (B) and the odour plume it gives off (C), changes dramatically. Despite there being many alterations in the chemical composition of the fruit, the process of decomposition and its products are similar every time it occurs. Many organisms take advantage of this consistency by detecting and evaluating these chemical by-products (chemical cues) and taking their composition to mean something about the state of the fruit, i.e. rotten, or fresh (Becher et al., 2012; Zhu et al., 2003).

The products of biological metabolism are not only released through decay, but also by living animals. Predatory species take advantage of odours released by their prey to identify it as an appropriate food source and to locate it in space. Cats, foxes, and snakes, for example, have all been observed to visit mouse-scented locations up to six days after an initial odour cue was placed (Hughes et al., 2010). Individuals within a prey species presumably give off similar chemical signatures, meaning a predator can reliably identify its sources of food. Insects display similar adaptations. The leaf feeding pea aphid, *Acyrthosiphon pisum*, has been observed to drop from leaves upon detection of the elevated heat and humidity indicative of herbivore breath. Such a simple adaptation ensures that the aphids aren't consumed by the feeding herbivore (Gish et al., 2010).

The chemical environment is not only a product of bacterial, plant, and non-human animal life. Human biological processes also produce a wide variety of chemical by-products that find their way into our immediate environments. Human exhaled breath alone contains more than 3,500 chemical components (Buszewski et al., 2007), with the exact composition being a unique representation of the biological state of the individual. The particular composition of this compound mix can be indicative of what the person recently ate, their emotional state, and whether or not they are suffering from a particular disease, an observation currently being exploited as a method of disease detection and diagnosis (Lourenço & Turner, 2014; Whittle et al., 2007).

The above examples all illustrate that many biotic features of an environment produce specific chemical signatures, and that biological features of an environment can be identified by their chemical signatures. The accumulated chemical output of all biological life results in a vastly complex olfactory landscape that encodes information as to whether food is safe to eat or water safe to drink, or whether a predator is lurking in

bushes 30 meters away. Animal nervous systems are equipped to detect and decode this information, with a staggering diversity of mechanisms and behavioural responses having evolved simply to help animals appraise and navigate their chemical environment. *Drosophila melanogaster* is one such animal highly dependent on its chemical senses to guide its myriad behaviours.

1.3 *Drosophila* as a model organism

Largely thanks to the Columbia University professor Thomas Hunt Morgan, and his discovery of the White mutation in 1910 (Morgan, 1910), *Drosophila* has been rigorously studied in laboratories for well over 100 years. It is only in recent decades however that the accessibility and genetic tractability of the fruit fly has been exploited for the advancement of our understanding of neurobiology and olfaction. In the late 1960s and early 1970s Seymour Benzer used forward genetic approaches to identify genes important in fly behaviour. It was observed that chemical mutation of flies could lead to genetically heritable behavioural phenotypes in olfactory learning and memory. The mutants *dunce* (*dnc*) (Byers et al., 1981; Dudai et al., 1976) and *rutabaga* (*rut*) were identified in Benzer's laboratory and were later shown to code for adenylate cyclase and phosphodiesterase respectively, both of which are proteins required for synaptic potentiation and therefore memory acquisition. Thanks to this work, and much that has been done in the following decades, *Drosophila* is now a powerful tool for understanding the relationship between the structure and function of neural circuits and the behaviours they generate.

Experimental tools developed on the back of advances in genetics now allow the dissection of neural circuits via the targeted expression of reporter and effector proteins to specific cell types. The commonly used GAL4-UAS binary expression system has made it possible to uninvasively manipulate and visualize cells with a previously unattainable level of spatial and temporal resolution. In one fly line a GAL4 transgene is inserted downstream of an endogenous promoter element, thus targeting expression of the GAL4 yeast transcription factor to a specific population of cells. In a second fly line an upstream activation sequence is inserted in to the genome along with a downstream transgene. If these two lines are crossed the transgene is expressed only in the cells expressing GAL4

(Brand & Perrimon, 1993; Fischer et al., 1988) (Figure 1A). This system, and others like it, allows an experimenter to drive the expression of transgenes such as *UAS-Shibire^{ts1}* (Kitamoto, 2001), a temperature sensitive allele of dynamin which blocks synaptic transmission upon exposure to an increased temperature, or *UAS-dTrpA1* (Rosenzweig et al., 2005), a heat-activated transient receptor potential (TRP) ion channel protein, which can be used to transiently activate neurons.

Being able to activate or block synaptic transmission of specific neurons allows gain of function and loss of function experiments to be conducted, thus establishing the necessity or sufficiency of a particular set of neurons for the functional output of a circuit. The expression of green fluorescent protein (GFP) can also be driven using the GAL4-UAS system allowing the visualization of cells via microscopy. A newer technology based on the GAL-UAS system allows even more spatially defined expression of the desired transgene. The Split-GAL4-UAS system (Luan et al., 2006) works on the same principle of intersectional expression except that the GAL4 transcription factor is split into two stable domains, the DNA-binding domain (DBD), and the activation domain (AD).
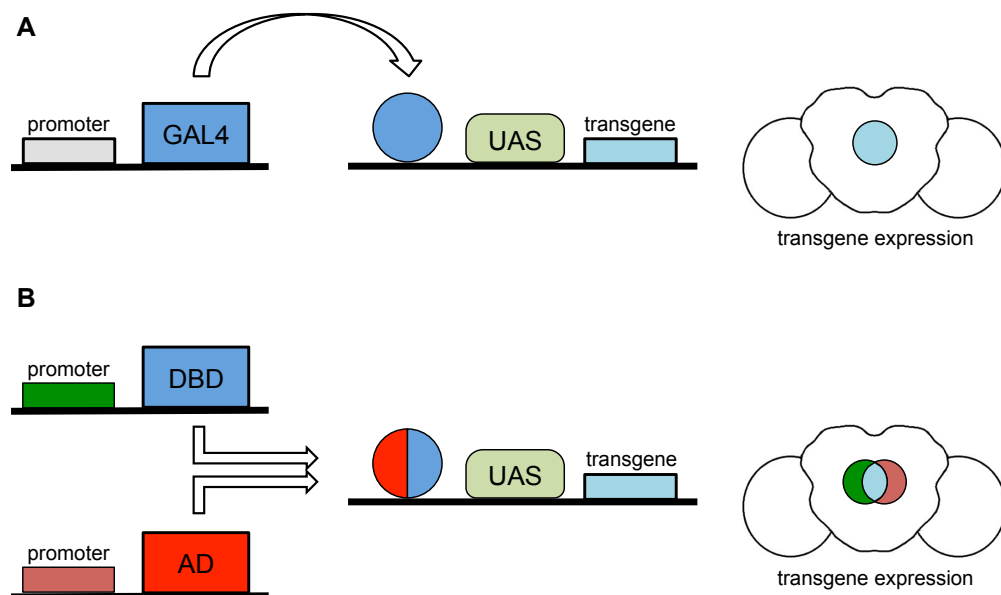
Figure.1 GAL4-UAS and Split-GAL4-UAS expression systems

  (A) The expression of the GAL4 transcription factor is under the control of an endogenous promoter. In cells in which it is expressed GAL4 binds to the UAS and triggers expression of the downstream transgene.
  (B) The DBD and AD form a functional GAL4 transcription factor in cells in which they are both expressed triggering transgene expression. The Split-GAL4 system allows for more specific targeting of cells.

The transgene for each GAL4 protein domain can be put under the control of a different endogenous promoter element, meaning that expression of the UAS-transgene only occurs in cells in which the DBD and AD are both expressed (Figure 1B). The addition of a third promoter element allows an even higher degree of specificity of transgene expression, and therefore more fine-grain manipulation of neural circuits. Other expression systems, such as the LexA-LexAop system (Lai & Lee, 2006; Szüts & Bienz, 2000), can be utilized within a single fly allowing the simultaneous expression of more than one transgene. For example, the expression of two different effector or fluorescence proteins can be driven in two different populations of cells in one fly.

As well as its enormous utility as a genetic system *Drosophila* is well established as a model system for studying the neurobiology of olfaction. As a result, a great deal is now understood about the anatomy and physiology of the olfactory pathways that allow the fruit fly to detect and respond to the odour cues important in its ecology.

1.4 Insect chemoreception

In order for environmental chemical information to be a useful driver of behaviour an animal must be 'irritable' to the compounds it comes into contact with, and be able to transduce and process the chemical information it senses. Most organisms have been endowed by evolution with the ability to sample chemical cues via the chemical senses, smell and taste. Both can be used to identify an object, but the sense of smell has the benefit of being able to function remotely, allowing an animal to appraise distant objects of biological and behavioural significance. For insects the sense of smell is particularly important and has been implicated in odour tracking during both flight (Chow et al., 2011; Stewart et al., 2010; S. Wasserman et al., 2012) and ground based locomotion, courtship (Grosjean et al., 2011; Tompkins et al., 1983; K. Wang et al., 2014), and aggression (W. Liu et al., 2011). Their olfactory sense provides an important window onto their environment with olfactory stimuli often describing environmental features critical to the fly's survival. In comparison to mammals, a significant portion of the insect brain is given over to processing olfactory information, but despite this divergence the neurobiological solutions to olfactory sensation and processing are relatively conserved across animal kingdoms (reviewed in Laurent 2002; Ache & Young 2005). Given these attributes the

study of insect neurobiology is a particularly useful tool when trying to understand more general cross-species neurobiological phenomena.

1.4.1 Conservation across vertebrate and invertebrate olfactory systems

Pioneering work published in 1991 by Linda Buck and Richard Axel identified a large family of G-protein coupled receptors (GPCR) expressed in the rat olfactory epithelium. They proposed and demonstrated that these GPCRs were the olfactory receptors (OR) allowing animals to respond to environmental odour cues (Buck & Axel, 1991). Bioinformatic comparison across species revealed a high degree of similarity between the general features of OR families in mammals, fish, birds, and amphibians. They also observed that the OR families found in invertebrate species shared this conservation, although to a lesser extent. At the detailed proteomic level there is a higher
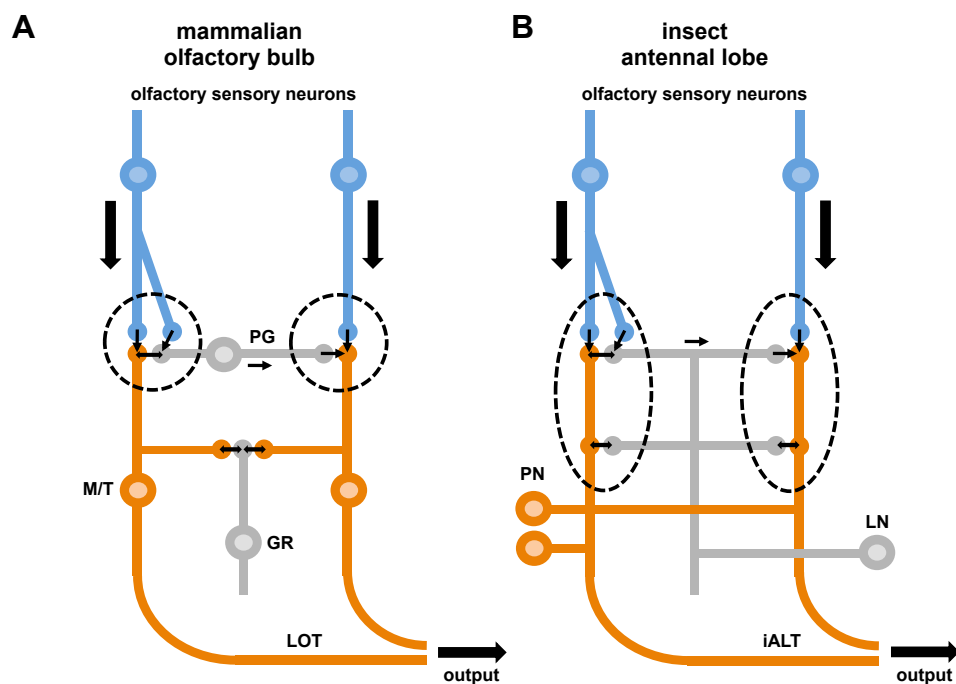
Figure 2. The mammalian olfactory bulb and insect antennal lobe share similar circuit morphology

(A) The mammalian OB is composed of sensory receptor neurons synapsing with mitral/tufted cells (M/T) and periglomerular cells (PG). Glomerular neuropil indicated by dashed circles. The lateral olfactory tract (LOT) is transected by and receives dual level lateral inhibition from the PG cells and the granular cells (GR). (B) The insect AL has largely the same circuit format with the exception that PNs receive lateral inhibition from one set of LNs only, which form synapses exclusively within the AL.

level of divergence between species, likely reflecting the different ecological demands on the olfactory systems of difference animals.

The olfactory pathways of different species are also similar in terms of the neural circuitry that processes olfactory information transduced at the periphery. Both the mammalian olfactory bulb (OB) and the insect antennal lobe (AL) share a glomerular structure whereby one glomerulus is innervated by olfactory sensory neurons (OSN) expressing similar ORs that synapse with downstream output neurons and local interneurons (Boeckh et al., 1990) (Figure 2). The anatomical conservation of this primary circuit structure indicates a perhaps critical role in olfactory signal processing. The genetic and structural similarities contribute to *Drosophila* being an ideal system in which to study the generalized neural systems and behaviours related to olfactory sensation.

1.4.2 Peripheral odour detection

Despite invertebrates not possessing noses, their olfactory systems are remarkably analogous to those of mammals (Figure 2.). In the case of the fruit fly, odours are absorbed directly into perilymph held in porous sensilla protruding from the third antennal segment and maxillary palps, the fruit fly's olfactory sensory organs (Figure 3). There are three types of morphologically and functionally distinct sensilla: trichoid, basiconic, and ceoloconic, and each encases the dendritic projections of up to four OSNs. The antenna hosts all three sensilla types, whereas the maxillary palps only the basiconic type. This anatomical divergence likely relates to the types of odours processed by the respective organs, but as yet, little is known about what this means functionally.

The sensilla and the OSNs they contain are tuned to specific odours that diffuse throughout the perilymph and either bind directly to the heterodimeric receptor complexes on the OSN dendrites or to soluble odour binding proteins (OBPs) that facilitate odour signal transduction (Xu et al., 2005). A combination of ORs and ionotrophic receptors (IR) are expressed in subpopulations of OSNs with each OSN expressing one to two ORs or IRs. All ORs are expressed alongside a co-receptor (Or83b / ORCO), without which the OSN is rendered anosmic (Larsson et al., 2004). IRs are typically formed of more monomeric subunits and as a result there are more IR co-receptors (e.g., IR8a, IR25b) than

there are OR co-receptors (Benton et al., 2009; P J Clyne et al., 1999). Some specialized sensilla house OSNs that, instead of ORs or IRs, express gustatory receptors (GR). GRs are typically expressed in gustatory sensory neurons in the labellum, tarsae, ovipositor, and wing tips, and facilitate taste sensation (P. J. Clyne, 2000; Nayak & Singh, 1983; Scott et al., 2001). However, they are also expressed by ab1C OSNs in the large basiconic ab1 sensilla. The ab1C OSNs express the GRs Gr63a and Gr21a, and allow *Drosophila* to detect and respond to environmental and biogenic CO_2 (Jones et al., 2007), an important molecule in *Drosophila*'s ecology and an experimental odour used in this study.

The 60 OR genes (Buck & Axel, 1991; Vosshall et al., 1999), 61 IR genes (Benton et al., 2009), and 68 GR genes (Chyb, 2004; Dunipace et al., 2001; Scott et al., 2001), and their expression in the ~1300 OSNs (unilaterally), allow the fruit fly to detect and process odours across broad concentration ranges (Asahina et al., 2009), to distinguish single odours from complex mixtures (Parnas et al., 2013), and to initiate behavioural responses appropriate to nutritive, reproductive, and survival requirements. However, it is clear that ~189 genes are not sufficient to convey sensitivity to the vast number of compounds the fly will encounter in its environment and has been shown to be sensitive to. To accommodate this complexity ORs, GRs, and IRs are usually sensitive to multiple ligands (Stortkuhl & Kettler, 2001; J. W. Wang et al., 2003), which hugely multiplies the number of possible detectible odours.

1.4.3 The antennal lobe

Many studies have sought to elucidate the mechanisms of olfactory information processing in the AL, the first processing substrate in the olfactory pathway. Much progress has been made in understanding the physiological mechanisms through which AL circuits respond uniquely and reliably to single or combinations of odours, maintain dynamic range of sensory neurons, and propagate processed olfactory information to higher brain centres (Bhandawat et al., 2007; Chou et al., 2010; Silbering & Galizia, 2007). It should be noted that all anatomical nomenclature used in this text are as laid out by the Insect Brain Name Working Group (Ito et al., 2014).

Olfactory information is propagated to the AL from the antenna and maxillary palps via the antennal nerve (Figure 3), which is composed of fasciculated OSN axonal projections. OSN axons innervate one or more of the AL glomeruli, which are tuned to specific odours or groups of odours (Semmelhack & Wang, 2009). The ventral most glomerulus, or V-glomerulus, is solely responsible for processing aversive CO_2 and is innervated only by OSNs expressing Gr63a and Gr21a (Jones et al., 2007; Suh et al., 2004). Other glomeruli are dominantly involved in representing attractive cues. Upon inactivation of synaptic transmission in Or42b and Or92a expressing OSNs, which innervate the DM1 and VA2 glomeruli respectively, behavioural attraction to vinegar was almost completely abrogated (Semmelhack & Wang, 2009). Also innervating the 43 AL glomeruli are inhibitory and excitatory local interneurons (LN), which are involved in dynamic range control and lateral inhibition between glomeruli and olfactory PNs (J. Barth et al., 2014; Root et al., 2007).
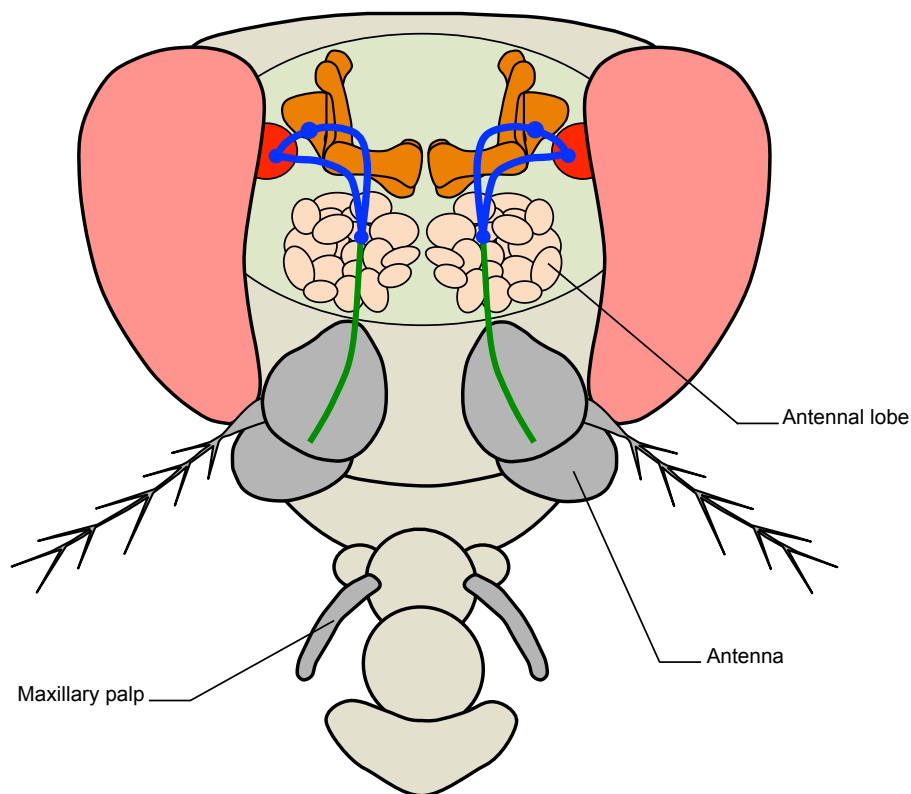
Figure 3. The *Drosophila* olfactory pathway

Schematic of the *Drosophila* olfactory sensory organs, olfactory pathway, and higher brain centres. The antennal nerve is represented in green, the PNs in blue, the MB in orange, and the LH in red. The iALT innervates the MB calyx prior to innervating the LH. The mALT projects directly from the AL to the LH.

10

PNs output olfactory information from one or more glomeruli and propagate it primarily to two higher brain regions: the mushroom body (MB) (*corpora pedunculata*), and the lateral horn (LH) (Figure 2) (H.-H. Lin et al., 2013; Marin et al., 2002; Stocker et al., 1997). They do this via three tracts; the inner antennal lobe tract (iALT), which first innervates the MB calyx and then the LH, the medial antennal lobe tract (mALT), which projects primarily to the LH but sends some collaterals to the MB calyx, and the outer antennal lobe tract (oALT) (not shown in Figure 3), which represents fewer PNs and innervates the LH directly (H.-H. Lin et al., 2013; Wong et al., 2002). Individual PNs diverge from these tracts to innervate various parts of the fly brain. It is not known what the precise functions of the non-MB/LH innervating PNs are, although it is likely that they relay odour specific information to parts of the brain for the purpose of neuromodulation.

1.4.4 The mushroom body

The MB was first described in 1850 by French biologist Felix Dujardin, who proposed it as the insect's centre of intelligence due to variability in its morphology between eusocial and non-social insects. Largely due to its irregular and characteristic morphology, the MB has long drawn attention and been central to the study of insect olfactory neurobiology.

The MB is a second-order olfactory processing centre and anatomically pronounced neuropil structure found across most insect and some annelid species (Strausfeld et al., 1998), with it's size, morphology, and function varying depending on an insect's specific sensory ecology. In *Drosophila* it is associated with various functions including the sparsening of olfactory representation (Honegger et al., 2011), learning and memory (de Belle & Heisenberg, 1994; Perisse et al., 2013; Tully & Quinn, 1985), and multi-modal sensory integration (S. Lin et al., 2014; Vogt et al., 2014). However, across different insect species the MB plays a lesser or greater role in these functions depending on the specific processing tasks demanded by the animal's ecological niche. In hymenoptera such as the honeybee *Apis melifora* the MB plays a significant role in integrating visual and olfactory information; the honeybee MB calyx has defined visual and olfactory input regions (Gronenberg, 2001). This contrasts strongly with the *Drosophila* MB, which receives comparatively little input from the optic lobes, although

the existence of dedicated visual projection neurons and a role in visual learning has recently been demonstrated (Vogt et al., 2014). These differences almost certainly reflect the differing requirements on the respective sensory systems between the two organisms. Similar functional properties have also been ascribed to the MB in the Hawkmoth *Manduca sexta* (Balkenius & Hansson, 2012), while studies of the Cockroach *Periplaneta americana* suggests a possible role for the MB in cancelling out self-generated motion via efference copy (Mizunami, Okada, et al., 1998). Interestingly, secondarily anosmic insects such as the diving beetle (*Dytiscus*) and cicadas, which don't possess antennal lobes, still have MBs. In these cases however, the MBs lack calyces due to absence of olfactory input and presumably process information from other sensory systems (Strausfeld et al., 1998).

This flexibility of function across species makes it clear that the MB is a complex structure sitting at or near the apex of the sensory information processing hierarchy. Indeed, it is often described as the insect equivalent of the mammalian cortex (Tomer et al., 2010), piriform cortex (N. K. Tanaka et al., 2009), hippocampus (Qi & Lee, 2014), and cerebellum (Farris, 2011), due respectively to its anatomical location, association with particular sensory systems, its role in learning and memory, and its specific neural circuit motifs.

Due to its diversity of function, study of the MB presents many challenges, some of which can be immediately addressed through the choice of model organism. *Drosophila* is a largely olfactory animal with a significantly smaller brain than many of its arthropod cousins. The brain of a honeybee is composed of ~960,000 neurons (Randolf & Giurfa, 2001), whereas the fruit fly brain is an order of magnitude smaller with ~100,000 neurons. This difference is also reflected at the level of the MB: the honeybee MB is composed of ~170,000 interneurons compared to the fruit fly's ~2000 unilaterally.

The numerical simplicity of the *Drosophila* MB makes it an excellent tool for understanding fundamental neural processing features required to perform complex sensory integration tasks. This is reflected in the vast literature that has been published in recent decades, with great advances being made in our understanding of both the anatomical and functional aspects of *Drosophila* neurobiology.

1.4.5 The MB and LH: Innate and learned behavioural responses

The stereotyped responses of flies to aversive odours such as CO_2 (Suh et al., 2004), geosmin (Stensmyr et al., 2012), and vinegar (Faucher et al., 2006; Semmelhack & Wang, 2009) are generally considered to be innate as opposed to learned. That is to say that these behavioural responses are genetically and developmentally encoded into the architecture of the fly brain without the fly having to learn that the odours are aversive or attractive. It was traditionally supposed that innate behaviours were 'hardwired' responses in which stimuli directly trigger the initiation of a motor program corresponding to the hedonic valence of the odour. However, that view is beginning to shift as neurobiologists acknowledge that the function and dynamics of even simple neural networks are highly dependent upon environmental and biological context.

In contrast to innate behaviours, learned responses allow the fly to retain acquired information over time and to execute behaviour upon reoccurrence of the initial stimulus conditions. In the laboratory, classical Pavlovian conditioning (Pavlov, 1927) is used to associate a conditioned stimulus (CS), such as a weakly aversive odour (e.g., octonol, methylcyclohexanol), with an unconditioned stimulus (US) in the form of negatively reinforcing electric shock, or positively reinforcing sugar reward. For example, the simultaneous exposure of flies to electric shock and the odour causes flies, when later tested, to express an increased avoidance of the odour compared to unconditioned flies (Owald et al., 2015a).

Over the past three decades, much research has gone into understanding what sets apart innate and learned behavioural responses. In the early 1980s researchers working with Martin Heisenberg, and following up work done in the laboratory of Seymour Benzer (Dudai et al., 1976), identified the fruit fly MB as a structure without which the fly's ability to learn was impaired (de Belle & Heisenberg, 1994), although the first indication that the insect MB may be involved in learning came from work done on honeybees by Menzel et al. in 1974 (R. Menzel, J. Erber, 1974). It was typically thought that the MB was dispensable for innate odour processing, and indeed the data seemed to confirm this: upon ablation of the larval MB with hydroxyurea, adult flies were still able to respond to basic odour and light stimuli but were unable to form learned associations (de Belle & Heisenberg, 1994). It was therefore thought that the LH was the brain region responsible

for driving naïve olfactory behaviours. This idea was given further credence after the observation by Heimbeck et al. (Heimbeck et al., 2001) that upon blockade of both the MB and LH innate behavioural responses were also diminished. Furthermore, it has been observed that the LH has segregated pathways for processing pheromones and driving reproductive behaviours (Jefferis et al., 2007; Ruta et al., 2010). Since the early experiments much work has been done on the MB in the context of olfactory learning, but only recently has it been implicated in more fundamental processing tasks related to modulation of innate behaviours by various internal state conditions (e.g., hunger, thirst) (Bräcker et al., 2013; Krashes et al., 2009; S. Lin et al., 2014) and conflicting odour stimuli (DasGupta et al., 2014; Lewis et al., 2015).

Research carried out in our laboratory demonstrated that the KCs are required for CO_2 avoidance only when the fly is starved, implying that a MB-independent pathway processes CO_2 when the fly is fed (Bräcker et al., 2013). It is likely that these different pathways are composed of the multiple V-glomerulus PNs and the brain regions they innervate (H.-H. Lin et al., 2013). It is also possible that the starvation dependent switch between the MB-independent and -dependent pathways is facilitated by the V-glomerulus PNs and their synaptic partners. The LH is therefore a good candidate structure for processing MB independent CO_2 avoidance. The LH receives much of the PN output from the AL, but it also recurrently connects to the MB calyx and lobes, meaning it may potentially drive downstream motor signals. In addition to hunger there are other internal states that could potentially modify innate behaviours. Indeed another study has recently shown that the MB is involved in processing innate water search behaviour. When flies are thirsty they prefer humid air to dry air, but when water sated they avoid humid air. Inactivation of a subset of MB input neurons switched attraction to humid air in sated flies to aversion (S. Lin et al., 2014). Food and water are important motivators of behaviour, but so too is external temperature. As such it has been shown that the MB is also involved in processing hot and cold avoidance in *Drosophila* (Frank et al., 2015; Tomchik, 2013).

All of these behaviours function independently of learning, suggesting a role for the MB in instantaneous innate behaviour modulation as well as in the formation of lasting associations, and that perhaps these two functions have a common basis in MB circuitry. In the case of hunger and thirst the MB only seems to play a significant role in either immediate odour processing or memory formation when flies are either hungry or thirsty,

implying that the MB or its input neurons integrate internal state information with external sensory information. How these two functions are both implemented in the MB circuitry is not yet understood. It may be the case that to maintain maximum behavioural flexibility innate preferences and learned associations interact and compete to drive behaviour. It has been suggested that certain innate responses might over time erode learned associations as a strategy to keep the MB representation of past and present olfactory environmental features up to date (Cohn et al., 2015).

1.5 Functional anatomy of the *Drosophila* mushroom body

1.5.1 Olfactory input to Kenyon cell interneurons

The MB consists mainly of Kenyon cell (KC) interneurons with cell bodies located at the anterior of the fly's brain. KCs send both dendritic and axonal projections anteriorly through the brain to form the MB's primary input structure, the calyx, and its characteristic bifurcated lobe structure respectively (Figure 4). The calyx receives direct olfactory input from 3-4 PNs from each of the AL glomeruli. Connectivity between PNs and KCs is facilitated via claw-like structures found on KCs (Butcher et al., 2012), with each claw being innervated by one PN. Each KC has on average 6.4 input claws, which means that connectivity between PNs and KCs is very sparse. KCs are known to have very low spontaneous activity and act as coincidence detectors between odour evoked patterns of activation across PN populations (Gruntman & Turner, 2013), thus the physiological purpose for the KC input claws is likely to strengthen the synaptic input from the PNs. This KC odour representation and readout by downstream MB output neurons likely underlies *Drosophila*'s ability to discriminate and generalise similar odours (Campbell et al., 2013).

1.5.2 Mushroom body lobe structure

KC axons project anteriorly through the calyx and fasciculate to form the MB peduncle that bifurcates to form the vertical and horizontal lobes (Figure 4). The vertical lobe is itself composed of two separate sub-lobes, the α lobe and the α' lobe. The horizontal lobe

is composed of three separate sub-lobes: β, β', and γ (Figure 4). KCs can be broadly divided into three anatomically and genetically distinct groups based on which sub-lobes they compose: α/β, α'/β', and γ (Crittenden et al., 1998). Each lobe within the MB, and therefore also the KCs, can be further subdivided. The α and β lobes can each be divided into posterior (p), central (c), and superior (s) regions with the corresponding KC named accordingly (e.g., α/βp). The α' and β' lobes are divided into medial (m), anterior (a), and posterior (p), and the γ lobe into main (m), and dorsal (d) (Aso, Hattori, et al., 2014; Nobuaki K Tanaka et al., 2008; Yao Yang et al., 1995). Both the vertical and horizontal lobes of the MB are sheathed in supportive glia (Awasaki et al., 2008). It is generally considered in the MB field that different populations of KCs making up both lobes of the MB might represent segregated channels representing input from different categories of odours and input from other sensory systems (visual, proprioceptive), and that MBONs innervating the MB lobes sample across all of these modalities to facilitate associative memory formation and drive behaviour (Figure 5).
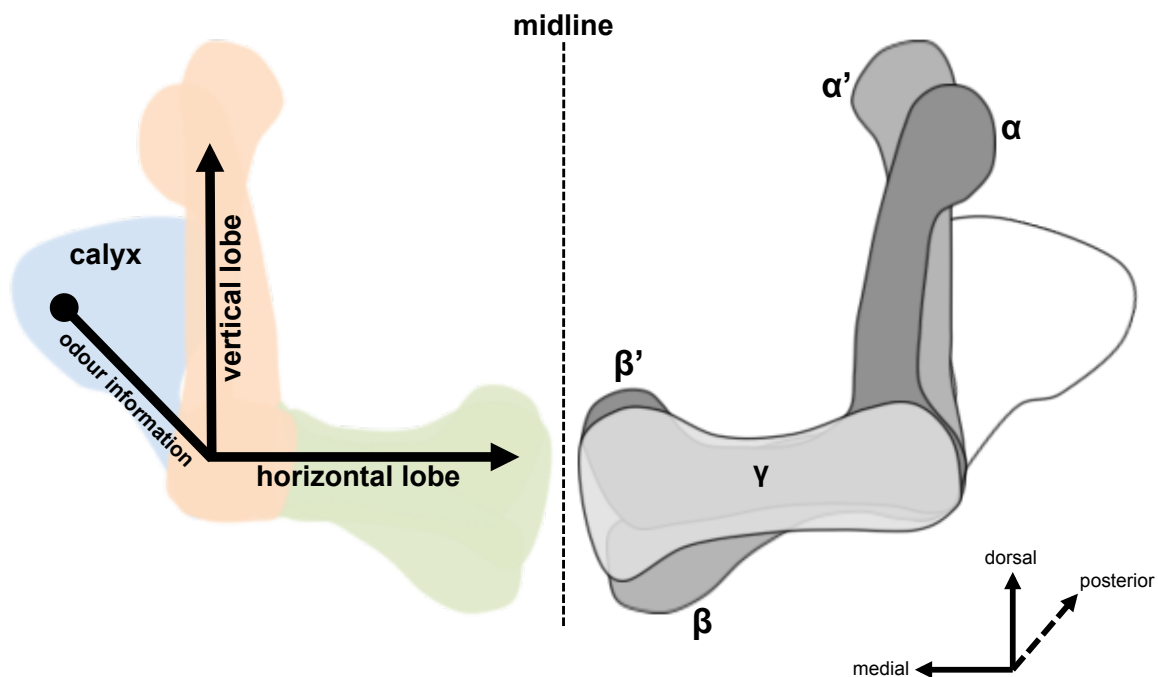
Figure 4. The *Drosophila* mushroom body (MB)

Olfactory information is input to the MB via PN-KC synapses in the MB calyx. It then propagates along anteriorly projecting KC axons into the horizontal and vertical lobes. The horizontal lobe is subdivided in three further lobes: the β, β', and γ lobes. The vertical lobe is subdivided into two further lobes: the α and α' lobes. The KC populations innervating each of these lobes are genetically distinct and can be further subdivided based on a more fine-grained analysis of their innervation patterns.

1.5.3 Mushroom body dopaminergic input neurons (DAN)

If the calyx is the MB's input structure, then the lobes are its output structures. They are also the sites at which neuromodulatory input impinges on the KC-MBON synapse (Aso, Hattori, et al., 2014; Cohn et al., 2015; Ichinose et al., 2015; Nobuaki K Tanaka et al., 2008). The MB lobes are innervated by two primary populations of neurons: approximately 200 cells comprising 20 types of dopaminergic neurons (DAN) of the protocerebral anteromedial (PAM) and protocerebral posteriolateral (PPL) clusters, and 34 cells comprising 21 types of mushroom body output neurons (MBON) (Aso, Hattori, et al., 2014; Ito et al., 1998; Kim et al., 2007; Schwaerzel et al., 2003). In addition to these
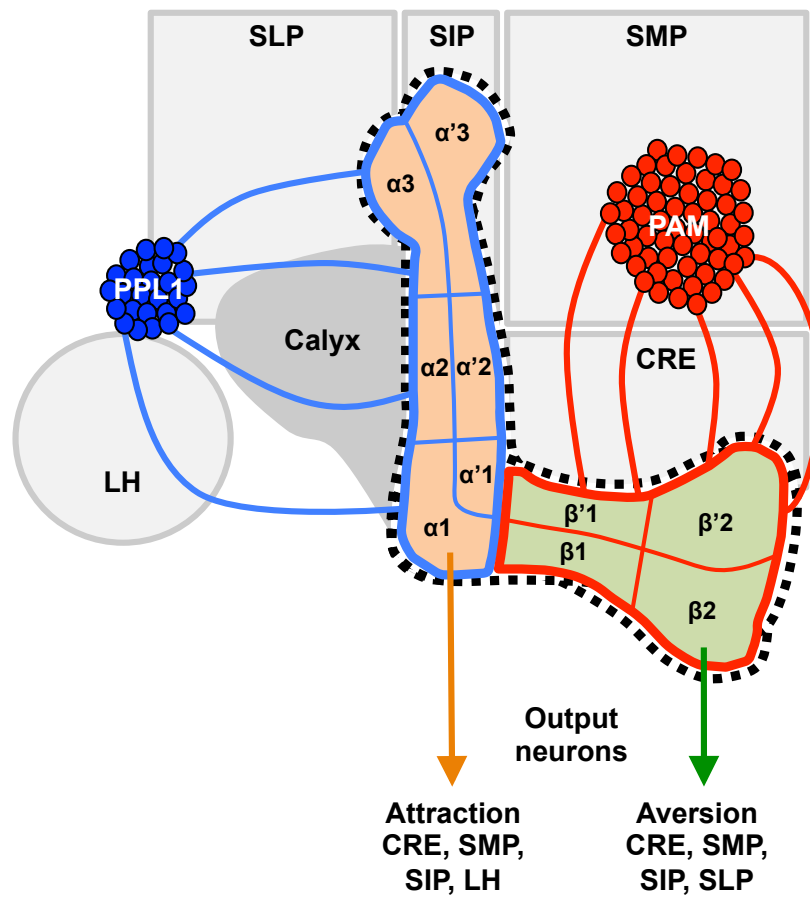
Figure 5. MB lobe input and output circuitry

Schematic representation of the MB on one side of the fly brain. DANs of the PAM (red) and PPL1 (blue) clusters innervate the horizontal lobe (green) and vertical lobe (orange) respectively. MBONs innervating the horizontal lobe drive behavioural aversion and MBONs innervating the vertical lobe drive behavioural attraction. DANs and MBONs have anatomically compartmentalized overlapping innervation patterns that tile the MB lobes (γ lobe not shown). The MB output regions innervated by MBONs from each lobe are represented in grey behind the MB schematic. Crepine (CRE), superior lateral protocerebrum (SLP), superior intermediate protocerebrum (SIP), superior medial protocerebrum (SMP), and lateral horn (LH).

two neuron types there are also populations of octopaminergic and serotonergic neurons which innervate the MB (Aso, Hattori, et al., 2014; Nobuaki K Tanaka et al., 2008). DANs provide neuromodulatory axonal input to the lobes; with the PAM cluster neurons innervating the horizontal lobe and the PPL clusters innervating the vertical lobe (Figure 5). DANs have been extensively studied in the context of learning and memory and have been shown to facilitate the formation of various types of memory in response to diverse sensory stimuli (Huetteroth et al., 2015; Schwaerzel et al., 2003). They have also been shown to respond directly to olfactory and gustatory stimulation and have been implicated in signalling internal state changes such as hunger and thirst (Krashes et al., 2009; S. Lin et al., 2014). Indeed, MB innervating DANs are required for the formation of reward based associative memory whereby starved flies reduce or increase their attraction to an odour paired with sugar reward (Huetteroth et al., 2015; Vogt et al., 2014; Yamagata et al., 2015). PPL1 DANs have also been shown to signal punishment in experiments where electric shock is paired with an odour, increasing the flies' subsequent avoidance response (Aso et al., 2012; Galili et al., 2014).

1.5.4 Mushroom body output neurons (MBON)

DAN presynaptic arbours are constrained to specific compartments of the MB lobes and overlap with MBON innervation, forming anatomical and functional compartments (Figure 5). MBONs output information from the lobes, and so have a reversed input-output polarity relative to DANs (Aso, Sitaraman, et al., 2014). Their dendritic arbours are also constrained to anatomical compartments in the same way as the DANs (Figure 5). MBONs send axonal projections to neuropil regions medial and lateral of the MB vertical lobes: the superior medial protocerebrum (SMP), superior lateral protocerebrum (SLP), superior intermediate protocerebrum (SIP), and the crepine (CRE) (Figure 5). MBONs also innervate the LH and parts of the MB itself. MBONs innervating the horizontal lobe of the MB drive aversion and those innervating the vertical lobe drive attraction. This functional segregation is mirrored by a divergence in the neurotransmitter systems used for downstream signalling. Horizontal lobe MBONs (aversive) are glutamatergic and vertical lobe MBONs (attractive) are cholinergic and GABAergic (Aso, Hattori, et al., 2014; Aso, Sitaraman, et al., 2014). A recent study has shown that the decorrelated and sparse representation of odours at the level of the KCs broadly activates

18

MBONs innervating both MB lobes (Hige, Aso, Rubin, et al., 2015). Thus it can be considered that the KC-MBON synapse may be the point in the fly brain where ascending olfactory information, in which odour identity is largely preserved, is generalized into positive and negative categories that may in turn drive attractive or aversive motor programs depending on the composition of the olfactory sensorium (Hige, Aso, Rubin, et al., 2015).

KC-MBON connectivity alone may allow flies to weigh diverse information from a complex sensory environment and initiate a behavioural response. Modulatory input from DANs in the form of internal state, past experience, and sensory context likely regulates KC-MBON synaptic transmission, thus providing a biologically and environmentally appropriate contextual background for sensory-motor transformation.

1.6 Aversive and attractive odour processing

Many odours elicit behavioural responses in flies, and often those behaviours take the form of attraction or aversion towards or away from an odour source. That is, flies exercise a hedonic preference in response to an innate or learned expectation of what an odour source is. Attractive odours often signal environmental sources of food and water, although some attractive pheromones have the specific purpose of attracting male and female flies during courtship (e.g., C 27 diene) (Bilen et al., 2013; Heimbeck et al., 2001). In general there seems to be a greater number of attractive odours than aversive (Knaden et al., 2012), probably due to the large number of compounds that can be produced by *Drosophila melanogaster's* multiple sources of food and their decomposition. Aversive odours are generally considered to indicate sources of danger (e.g., geosmin, CO_2), although as with attractive odours, some act as pheromone triggers of socially motivated behaviours (e.g., cVA). That odours have hedonic valence at all implies that each odour, or combination of odours, must have a specific representation in the fly's brain whereby detection of an odour triggers a stereotyped behavioural response. Unlike spatial retinotopy in the mammalian visual cortex (Choudhury, 1978), or tonotopy (Ehret & Romand, 1994) in the auditory cortex, olfactory coding has been notoriously difficult to understand due to the absence of a simple mapping of 'chemical space' onto a defined neuroanatomical structure (Johnson & Leon, 2007; Murthy, 2011). Indeed, the MB and

LH of the *Drosophila* olfactory pathway have not easily yielded an explanation of olfactory coding. Despite this lack of an obvious logic to olfactory coding there is some degree of functional anatomical segregation. The glomerular structure of the insect antennal lobe (and mammalian olfactory bulb) is non-uniformly segregated into glomeruli that represent attractive odours and glomeruli that represent aversive odours (Semmelhack & Wang, 2009). In zebrafish it has been observed that odorants with similar physiochemical properties activate distinct regions of the olfactory bulb (Friedrich & Korsching, 1998). Segregation of olfactory attraction and aversion has also been observed in the fly at the level of the lateral horn (LH) (Strutz et al., 2014), and at the level of the mushroom body (MB), where two populations of output neurons each drive either attractive or aversive behaviour (Aso, Sitaraman, et al., 2014). Given that flies are continually exposed to a broad mix of odours with differing hedonic valences an interesting question, and part of the motivation behind the project described in this thesis, becomes apparent. How is conflict between odours of opposing hedonic valence resolved in the fly brain?

1.6.1 Sensory conflict

Sensory conflict is a common occurrence for all animals, and the fly's ecology represents a particularly prominent and experimentally accessible example (Figure 6). The fly's primary habitat and food source is fruit, which releases a vast array of conflicting odour signals over the course of its ripening and eventual decay. While they ripen, climacteric fruit, such as bananas, apples, and melons, release large amounts of CO_2 (de Vries et al., 1996; Silva et al., 2001; Young et al., 1962), a strongly aversive odour for *Drosophila* (Suh et al., 2004). However, as the fruit ripens the emission of CO_2, a product of glucose metabolism, reduces while the attractive volatile products of fermentation and decomposition by yeast and bacteria increase (e.g., linalool, monoterpine, 2-heptanol). Intuitively, this causes flies to be strongly attracted to the fruit. However, as the fruit continues to decompose, the levels of CO_2 emission begin to increase again, meaning the fruit releases both attractive and aversive odours. Despite this increase in aversive CO_2 flies continue to engage in approach behaviour (Bräcker et al., 2013). This behaviour has also been demonstrated in a laboratory setting using a standard two-choice T-maze assay (Tully & Quinn, 1985); hungry flies are able to overcome their strong aversion to CO_2

20

when it is paired with an attractive appetitive stimulus such as vinegar (Bräcker et al., 2013; Faucher et al., 2006). This behaviour represents a clear example of ecologically relevant olfactory conflict (Figure 6), in which a neural circuit mechanism able to contrast multiple sensory stimuli must initiate a singular behavioural output.

An interesting consequence of decision-making also observable in flies is that it takes the insects longer to make a decision when faced with more complex stimuli. For example, when presented with two different but very similar concentrations of the same odour, flies took longer to initiate a behavioural response than when the concentrations were more dissimilar (DasGupta et al., 2014; Parnas et al., 2013). The behaviours demonstrated in these studies are also observable in other mammals, including humans (Drugowitsch et al., 2012).

1.6.2 CO_2 and vinegar as experimental odours

Odours are often used experimentally as motivators of behaviour where the primary question is not necessarily how the olfactory component of the behaviour functions. For example, MCH and octanol are commonly used as conditioned stimuli in learning and memory experiments (C. Liu et al., 2012; Perisse et al., 2013; Préat, 1998),

Figure 6. A fruit fly's olfactory environment is composed of conflicting cues

When deciding on whether or not to approach an area a fly has to weigh the potential gains and losses before choosing a course of action.

pheromones such as cVA and methyl laurate are used to induce courtship related behaviours (Dweck et al., 2015; Kurtovic et al., 2007), ethanol has been used to study the effects of alcohol dependence and withdrawal (Robinson et al., 2012), and vinegar to study olfactory and visual sensory integration (Stewart et al., 2010). The hedonic valence of the odours used in these studies is often of little consequence to the broader question the researchers are trying to elucidate. Therefore it is often the case that specific questions of how olfactory information drives the behaviours in question remain unanswered.

In *Drosophila*, CO_2 and vinegar drive opposing behavioural responses via segregated neural pathways that remain segregated even at the apex of the sensorimotor transformation, the mushroom body (Hige, Aso, Rubin, et al., 2015; Semmelhack & Wang, 2009). This is an important finding as it has previously been shown that CO_2 aversion can be inhibited at the level of the CO_2 sensory neuron by the volatile compounds 1-hexanol and 2,3-butanedione that are released by some fruits (S. L. Turner & Ray, 2009). Importantly, these compounds are not found in vinegar, suggesting the reduction in CO_2 aversion observed by Bräcker et al. was not a result of inhibition of peripheral CO_2 sensation. An additional unique aspect of CO_2 olfaction is that stimulation with CO_2 more strongly inhibits other AL glomeruli, presumably focussing the flies' olfactory system on CO_2 (Hong & Wilson, 2015). It has also been observed that the V-glomerulus, which is the exclusive recipient of innervation from CO_2 sensory neurons in the AL, lacks expression of GABA receptor (J. W. Wang, 2012), providing further support for the hypothesis that vinegar inhibition of CO_2 avoidance behaviour must occur in higher brain regions. These characteristics and experimental foundations make CO_2 and vinegar ideal tools with which to study sensory conflict resolution and decision making in higher brain centres in *Drosophila*.

1.7 Internal states and innate behaviour modulation

Sensory information is essentially an energetic map of the external world, neurally rendered in colour, motion, smell, temperature, sound, and touch. In many cases direct representations of this sensory map can be found in the brain, and the behavioural responses to different portions of this sensory map vary depending on an animal's repertoire of innate behaviours. Innate behaviours in themselves can be interpreted as

22

learned associations formed in the brain's architecture over evolutionary time. Unfortunately for an individual fly, human, or any other animal, evolution only brings about change on the time-scale of entire generations and does not necessarily reflect events as they happen. Consequently, innate responses to sensory stimuli are not always adequate to help an animal best find food or a mate. This places the requirement on nervous systems that they dynamically process sensory information and modulate innate behaviours instantaneously and over time. These modulations are online processes in which past and currently occurring experiences compete to drive behaviour through the excitatory or inhibitory action of neuromodulatory neurons (Cohn et al., 2015; Hige, Aso, Modi, et al., 2015). This processing task needs to take place in the context of prescient biological requirements that can bias the behavioural outcome in one direction or the other and allow the organism maximum flexibility to respond appropriately to its environment.

Drosophila demonstrates a wide variety of behaviours in response to a wide range of stimuli. Often these behaviours are in response to external stimuli, such as a fly's innate avoidance of CO_2 (Suh et al., 2004), the initiation of grooming behaviour due to a build up of foreign material on its carapace (Seeds et al., 2014; Yanagawa et al., 2014), or its avoidance of high temperatures (Rosenzweig et al., 2005). But often these stimuli are filtered based on their relevance to internal biological requirements. For example, a recently sated male fly may approach a piece of fruit also inhabited by other flies (Figure 6). With its requirement for nutrients met, reproductively salient stimuli may dominate its sensory experience leaving it free to pursue female flies and initiate courting behaviour. This behavioural outcome does not result from the fly's nervous system no longer being sensitive to the food odours emitted by the fruit, but rather that the representation of food is actively inhibited in the context of satiety (Krashes et al. 2009). The courting behaviour executed in the absence of competing behavioural drives is itself likely a function of the male fly's recent courting success and the reproductive receptivity of the female flies (McBride et al., 1999; Siegel & Hall, 1979; Yamamoto et al., 1997). All of these behavioural interactions may be overridden by an imminent danger signalled by a different set of sensory conditions and necessitating an immediate escape response. Recent research has shown that the sufficiency of a particular set of sensory information to drive a particular behaviour may be also be dependent on the precise behavioural state of an animal at the time of sensation (Cohn et al., 2015). This implies that execution of a particular behaviour in response to a stimulus depends not only on learned associations,

naïve biases, and internal state, but also on the likelihood that an animal is in an appropriate physical position and has enough time to execute a given behaviour.

There is growing evidence from studies on insects and mammals to suggest that dopaminergic neurons represent internal state and gate the flow of sensory information to pre-motor and motor circuits necessary for behavioural execution (Bargmann, 2012; Cohn et al., 2015; Marder, 2012; Wise, 2004). In *Drosophila* the MB is a critical structure in mediating the modulation of sensory information and therefore allowing the adaption of behaviour within specific chemosensory environments based on biological requirements. It was a major goal of the study presented in this thesis to contribute to our understanding of the specific circuit mechanisms though which dopaminergic neurons in the *Drosophila* brain perform this gating of sensory information flow in the *Drosophila* MB for the immediate adaptation of behaviour.

1.8 Thesis aims

Due to the complexity of chemical environments the fruit fly, *Drosophila melanogaster,* often encounter situations in which it receives multiple conflicting odour stimuli. Within any chemical environment may be found compounds indicative of food, water, other flies, and potential predators. At any one moment a fly is likely inundated with competing signals compelling it to either avoid or approach an area or object (Figure 6). However, flies cannot move in two directions at once making most possible behavioural outputs mutually exclusive; it must choose. The process by which the fly weighs multiple possibly conflicting sensory inputs and initiates behaviour in response to just one of those inputs is the process of decision-making. But the singularity of the behavioural output belies the complexity of the required neural processing. All stimuli, conflicting or otherwise, are sensed, transduced, undergo primary processing, and are eventually integrated in higher brain regions where one or a combination will drive behaviour and associative learning. The *Drosophila* MB is a comparatively simple neural system that integrates complex sensory information to facilitate the execution of a number of behavioural tasks. The aim of the study presented in this thesis was to apply a number of techniques, including behavioural analysis, calcium imaging, and anatomical analysis, to better understand whether and how the sensory integration capabilities of the MB are utilized in resolving

24

immediate olfactory conflict. It has already been established by Bräcker et al. that the MB is required for processing what was traditionally considered an innately processed odour, CO_2, in the context of starvation (Bräcker et al., 2013). These findings suggest a system whereby simple stimuli less relevant to immediate biological requirements more directly drive behaviour, while complex stimuli (e.g., multiple conflicting odours) and single stimuli relevant to biological maintenance, must be integrated by the MB in order for an eventual behavioural output to reflect their cumulative importance to the fly. The MB is a complex structure with a unique anatomy and multiple populations of neurons involved in its processing tasks. Therefore the main focus of this study has been in the identification and description of specific MBONs and DANs and the local circuits they form in order to resolve the sensory conflict represented via simultaneous presentation of the aversive odour, CO_2, and the attractive odour, vinegar.

The aims of this study can be broken down into several key points:

1) Behavioural screening of MB Split-GAL4 lines labelling KCs, MBONs, and neuromodulatory neurons to identify putative MB compartment(s) involved in processing conflicting olfactory stimuli.

2) Identification of specific MB compartment(s) responsible for processing olfactory conflict and description of the MBONs and neuromodulatory neurons innervating them.

3) Application of calcium imaging to ascertain which neuron types represent which odours and describe physiological mechanisms of integration. Here I test the hypothesis that DAN activity suppresses CO_2 aversion.

4) Description of possible circuit mechanisms based on further behavioural analysis and calcium imaging.

2.0 Materials and Methods

2.1 Flies

2.1.1 Fly lines, rearing, and crosses

Drosophila melanogaster fly lines were stored and reared at either 18°C or 25°C and at 60% relative humidity in a 12h/12h light dark cycle. Flies were group housed on standard cornmeal medium and flipped onto fresh food every 2-3 weeks depending on the housing temperature. Crosses were made between 15-20 males and ~70 virgin females and stored at 18°C until hatching. Subsequently collected experimental flies were commonly aged 4-7 days and were stored on fresh food at 25°C prior to experimentation. The Canton-S (CS) fly line was used for wild type experiments, however the majority of experimentation was conducted on transgenic fly lines harbouring genetically functional cassettes introduced via p-element insertion. The Split-GAL4>UAS, GAL4>UAS, and LexA>LexAop expression systems were used to drive expression of thermogenetic, optogenetic, and fluorescence effector and reporter proteins. For experimentation only F_1 progeny of crosses between Split-GAL4, GAL4, and LexA line males and UAS and LexAop virgin females were used.

All Split-GAL4, GAL4, and LexA driver line transgenes were inserted into a w-genetic background, as were all the effector and reporter lines with the exception of *UAS-dTrpA1*, which was inserted into a w+ genetic background. To analyse the functional and anatomical characteristics of MB input, output, and interneurons required during the integration of conflicting olfactory signals we utilized a library of Split-GAL4 lines generated at Janelia Farm Research Campus by Dr. Hiromu Tanimoto, Dr. Yoshinori Aso, and Dr. Gerald Rubin. The Split-GAL4 lines were generated by inserting the GAL4 AD at loci attP2 on the third chromosome, and the DBD at loci attP40 on the second chromosome. In some Split-GAL4 lines the AD and DBD transgenes were recombined on the same chromosome (for a summary of Split-GAL4 line expression see index). For the purposes of the olfactory behavioural screen males of the Split-GAL4 lines were crossed to virgin females of *20XUAS-IVS-Shibire^{ts1}-p10* (Pfeiffer et al., 2012).

For follow up behavioural experiments the Split-GAL4 lines *MB002B-Split-GAL4*, *MB011B-Split-GAL4*, *MB056B-Split-GAL4*, *MB047B-Split-GAL4*, *MB109B-Split-GAL4*, *MB316B-Split-GAL4*, *MB042B-Split-GAL4*, and *MB040B-Split-GAL4* were crossed variously to the effector lines *UAS-Shibire^{ts1}* (Kitamoto, 2001), *UAS-dTrpA1* (Hamada et al., 2008), and *10XUAS-CsChrimson-mVenus (attP18)* (Klapoetke et al., 2014). For further anatomical characterization of MBONs and DANs *MB011B-Split-GAL4* and *MB109B-Split-GAL4* were crossed to *UAS-mcd8::GFP* (Lee & Luo, 1999), and *UAS-DenMark::mCherry; UAS-Syt::GFP* (Nicolai et al., 2010). GRASP analysis (Pech et al., 2013) was carried out using *MB109B-Split-GAL4/CyO, R14C08-LexAp65*, and *R15B01-LexAp65* in attP40, to drive expression of *w-; Bi/CyO; UAS-CD4::spGFP1-10/TM2*, and *w-; LexAop-CD4::spGFP11/CyO; TM2/TM6B*. And for double-labeling experiments the same lines were used to drive expression of *LexAop2-mCD8GFP*, and *10XUAS-IVS-mCD8RFP*. Calcium imaging experiments were carried out exclusively using the driver lines *MB011B-Split-GAL4* and *MB109B-Split-GAL4*, which were crossed to *UAS-GCaMP6f* (Nakai et al., 2001).

2.1.2 Heat shock virgin production

Due to the large number of virgins required throughout screening and subsequent experiments we used virginator versions of the effector lines (*UAS-Shibire^{ts2}* and *UAS-dTrpA1*) and genetic background lines (w- and w+). A virginator line has an additional heat shock inducible *hid* gene on the Y chromosome that causes lethality in male larvae and pupae upon 2-4 hours of heat-shock at 37°C, leaving only virgin females to develop (Venema, 2006).

2.1.3 Starvation

Throughout the study we sought to understand how starvation state affected innate behavioural responses to appetitive (vinegar) and aversive (CO_2) odours. Therefore many experiments were performed simultaneously on fed and starved flies. Starvation was achieved by placing experimental flies in a bottle with tap water moistened tissue paper for 24-42h at 25°C. Flies were starved in the same way for both behavioural and calcium

imaging experiments. Non-starved (fed) flies were stored on fly food until experimentation.

2.2 Behavioural Setups

2.2.1 T-Maze choice assay

To assay olfactory decision-making behaviour we used the simple T-maze olfactory choice assay (Tully & Quinn, 1985) (Figure 7). Approximately 40-80 flies were initially aliquoted into storage tubes containing filter paper moistened with 200μl of tap water. We used a standard non-aspirated T-maze to provide flies with a choice between two stimulus tubes, usually with atmospheric air on one side and an odour on the other. Flies were placed into an elevator at the top of the T-maze (Figure 7, left panels) from where they were inserted into the choice point and allowed to move into one stimulus tube or the other. After one minute the elevator was raised thus blocking flies into whichever stimulus tube they chose. Undecided flies that remained in the elevator were excluded from the analysis. Two T-mazes were always used simultaneously with each having the stimulus tubes placed in the opposite configuration to the other (Figure 7, right panel), thus controlling for unwanted spatial bias. The two tubes from each T-maze were then sealed and the number of flies in each counted. For each experimental group 8-12n was typically collected except during screening when 4n was collected. A preference index was then calculated for each n using the following equation:

$$PI = \frac{\# \, flies \, side \, a - \# \, flies \, side \, b}{total \, \# \, flies}$$

Due to its versatility the T-maze was used for the initial screening of MB Split-GAL4 lines and for a portion of the follow up experiments.

2.2.2 Stimulus tube preparation

Odour stimulus tubes were prepared just prior to experimentation. For appetitive stimulation 40µl of a 10% Balsamic vinegar (Alnatura, Germany) solution, diluted with deionized water, was pipetted onto a small piece of filter paper and placed in the bottom of a stimulus tube. The tube was then sealed with parafilm. For filling stimulus tubes with CO_2 we used a custom built filling setup that utilized two mass flow controllers (MFCs) (Natec sensors, Germany) to regulate the flow of bottled pure CO_2 and pressurized atmospheric air. For most experiments we used a CO_2 concentration of 0.3-0.5%, which is above atmospheric levels and sufficient to cause robust avoidance behaviour, but not high enough to have any anaesthetic effects. Upon leaving the MFCs the two gases converge and mix before being output from the filling setup into a stimulus tube.
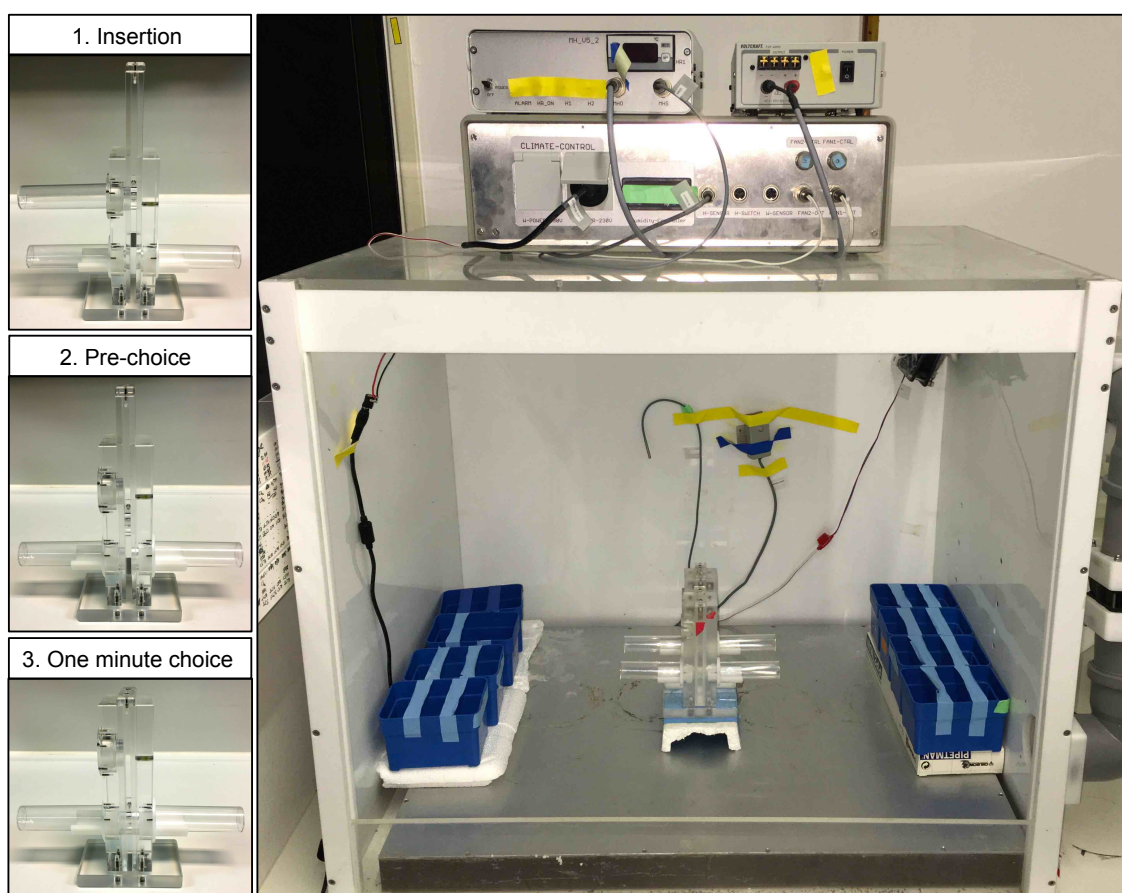
Figure 7. T-maze behavioural assay and climate chamber

The operational procedure of the T-maze assay is represented in the left three panels. The right panel shows the T-maze assays in situ in the climate control chamber. On the top of the chamber is the climate control apparatus. When in use a cover is placed over the front of the chamber. Armholes in the cover allow access. The metal plate at the bottom of the chamber heats up to increase the temperature.

2.2.3 Climate and environmental control

The initial screen and many of the subsequent experiments involved the thermogenetic silencing or activation of MB neurons via the targeted expression of Shibire[ts1] or dTrpA1 respectively. Thus it was necessary that we control the temperature and humidity of the environment in which the T-maze experiments were conducted. To achieve this we used climate control chambers in which T-mazes could be placed and used by an experimenter (Figure 7, right panel). Experiments were carried out at 60% relative humidity and at 32°C, a temperature at which Shibire[ts1] and dTrpA1 silence and activate neurons respectively. Low temperature controls were carried out at 25°C. When using Shibire[ts1] flies were acclimatized for 20 minutes prior to testing to ensure full depletion of synaptic vesicles in the targeted neurons. dTrpA1 expressing flies were acclimatized for 5 minutes prior to testing. Stimulus tubes were also placed in the climate chamber before testing to ensure their temperature was equilibrated to that of the T-maze itself.

2.2.4 Optogenetic arena

To test whether subsets of MBONs and DANs providing output and neuromodulatory input to MB were sufficient to drive attractive or aversive behaviours we used an automated optogenetic arena assay. The assay was built by Dr. Yoshinori Aso at Janelia Farm Research Campus based on a previous olfactometer design (Aso, Sitaraman, et al., 2014; Vet et al., 1983). During experimentation the optogenetic arena was housed in dark conditions at ambient temperature and humidity.

Expression of CsChrimson (Klapoetke et al., 2014) was targeted to MB neurons using the Split-GAL4 driver lines. CsChrimson is a red-shifted channel-rhodopsin that triggers neuronal depolarization upon exposure to red light. 15-20 experimental flies were introduced into the optogenetic arena, which consisted of a 10cm diameter, 3mm high open circular arena segregated beneath the arena level into four equally sized light quadrants (Figure 8, top panel). Each quadrant can be independently illuminated from beneath via arrays of 617nm red LEDs (Red-Orange LUXEON Rebel LED-122 lm), a wavelength sufficiently distant from the peak absorption of endogenous rhodopsins in the fly's eyes, thus leading to negligible phototaxis behaviour. Neuronal activation is therefore

30

triggered only in CsChrimson expressing neurons in flies standing directly above the illuminated quadrants. The patterns of activation of the LED quadrants were computer controlled via an arduino and custom python script. An experimental protocol was designed to incorporate acclimatization and control of spatial bias. The protocol proceeded as follows: fly insertion into setup > 60 seconds acclimatization time > 30 seconds red light stimulation in two diagonally opposite quadrants > 30 seconds no stimulation > 30 seconds red light stimulation in the alternate two diagonally opposite quadrants (Figure 8, top panel). The behaviour of the flies in response to LED illumination was captured via a camera positioned above the arena (Point Grey ROHS 1.3 MP B&W Flea3 USB3.0).
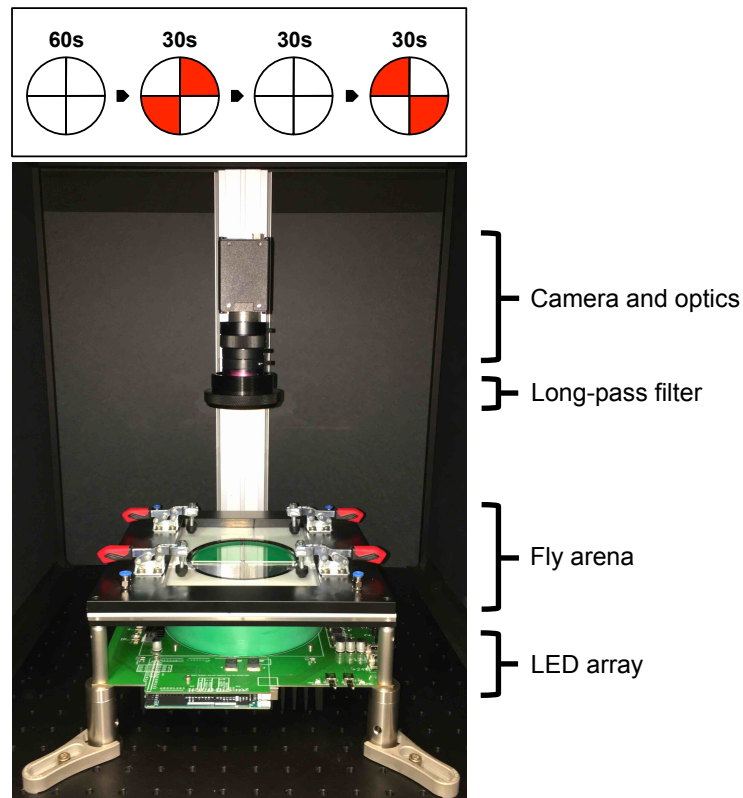
Figure 8. Optogenetic arena behavioural assay

The operational procedure used during optogenetic arena testing is represented in the top panel. The bottom panel depicts the arena, filter, and camera arrangement.

For each experimental group a sample size of 10-16n was used. Video files were analysed using a custom ImageJ plugin. The behavioural responses in the last 5 seconds of each stimulus period were averaged and used to calculate a preference index relative to quadrant illumination using the following formula:

$$PI = \frac{\# \; flies \; quadrants \; a \; and \; c - \# \; flies \; quadrants \; b \; and \; d}{total \; \# \; flies}$$

2.3 T-maze Split-GAL4 screening protocol

To test whether MBONs and DANs were involved in a starvation dependent MB olfactory integration circuit a library of Split-GAL4 lines was crossed to *20XUAS-IVS-Shibire^{ts1}-p10* and screened for olfactory responses in the T-maze assay. The Split-GAL4 library was produced at the JFRC by Dr. Yoshinori Aso. Initially lines were selected from a library of ~7000 GAL4 lines based on their expression in the MB. The Split-GAL4 approach was applied to pairs of these lines to produce ~2500 intersections that were then anatomically screened for strong and sparse expression specifically targeting the MB. This process produced ~400 Split-GAL4 lines, ~80 of which (see table) were selected by Dr. Aso for inclusion in the JFRC MB collaboration.

Males from approximately 5 Split-GAL4 lines were crossed to *20XUAS-IVS-Shibire^{ts1}-p10* virgin females per week. Experimental flies were collected and aged 4-7 days before being starved for 42 hours. The flies were then tested at restrictive temperature (32°C) for CO_2 avoidance, vinegar attraction, and response to a mixture of CO_2 and vinegar. A total of 4n was collected per genotype per stimulus condition and then compared to a pooled control genotype (*Shi/w-*) from across all the screening experiments. Secondary experiments were performed on statistically significant hits from the primary screen and included a larger sample size (8n), parallel GAL4 genetic controls (*+/Split-GAL4*), and low temperature controls (25°C).

2.4 Behavioural protocols for CO_2 conditioning experiments

To test whether CO_2 avoidance can act as a CS in associative learning experiments we developed a test protocol for use with the T-maze. Experimental flies were first trained for 1 minute via exposure to air (procedural control), CO_2 (adaptation control), or CO_2 (CS) plus vinegar (US). Flies were then returned to an odourless environment for 3 minutes after which time their CO_2 avoidance behaviour was tested in a T-maze assay (Figure 7).

To test whether artificial activation of DANs was sufficient to induce CO_2 associated memory we designed a similar protocol. A group of flies expressing dTrpA1 in DANs were acclimatized to 32°C for 2 minutes after which they were placed in a CO_2 environment for a further 2 minutes, thus pairing activation of DANs with exposure to CO_2. Flies were then removed from the CO_2 environment and their CO_2 avoidance responses tested in a T-maze. A second group of flies was tested in parallel at 25°C (non-activating).

2.5 Calcium imaging

in-vivo two-photon calcium imaging was used to establish responsiveness of the MB input and output neurons to the experimental odours and to provide physiological evidence that single populations of MBONs integrate conflicting olfactory information. Experiments were performed on 4-7 day old female flies of the genotypes *MB011B-Split-GAL4;UAS-GCaMP6f* and *MB109B-Split-GAL4;UAS-GCaMP6f* to measure changes in intracellular calcium levels in β'2 innervating MBONs and DANs. Flies were immobilized in a modified pipette tip with the antennae free and the dorsal side of the head carapace sealed with wax against a plastic membrane. A small window was then opened through the plastic membrane and the head carapace to expose the brain neuropil (Figure 9). A reservoir above the plastic membrane was then filled with fly ringer solution (see index for composition). The whole assembly could then be easily placed beneath the microscope objective, leaving clear access to stimulate the fly with olfactory cues from a custom odour delivery setup (Figure 9). To image and excite the GCaMP6f an Olympus FV-1000

microscope system was used in tandem with a mode-locked T:Sapphire MaiTai DeepSee laser.

Throughout the entire experiment a charcoal filtered humidified continuous air stream of 1L/min was delivered by a Syntech stimulus controller to the antennae from a distance of ~10mm away via an 8mm diameter Teflon tube (Figure 9). The odour delivery setup functioned by redirecting ~30% of the continuous airstream for 1 second through an odour vial containing diluted odourant or solvent. For CO_2 stimulation pure CO_2 and pressurized atmospheric air were controlled and mixed by MFCs and then fed into the main airstream. For CO_2 and vinegar combined stimulation both odours were fed simultaneously into the airstream via the activation of solenoid valves.
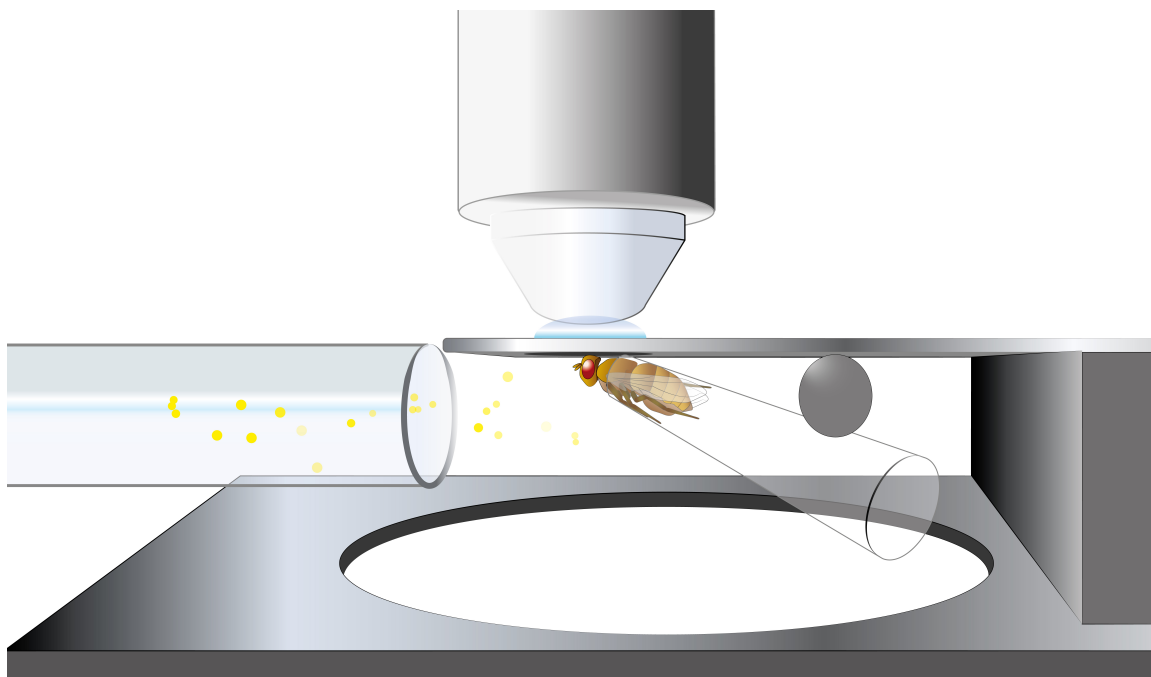
Figure 9. in vivo calcium imaging stimulation preparation

The in vivo preparation allows simultaneous olfactory stimulation of a living fly and measurement of calcium induced changes in the fluorescence signal emitted via the genetically encoded calcium sensor GCaMP.

For the analysis of calcium imaging data the appropriate anatomical regions were specified using ImageJ to define regions of interest and obtain time traces of fluorescence levels. The change in fluorescence intensity as reported by the calcium sensor (GCaMP6f) was calculated via the following formula:

$$\frac{\Delta F}{F} = \frac{100 \, (Fn - Fo)}{Fo}$$

Fn refers to the *n*th frame after stimulation and *Fo* the average basal fluorescence 5 frames prior to stimulation. All data was normalized to the ΔF/F calculated for the background signal measure when the flies were stimulated air alone.

2.6 Statistics

All behavioural data was tabulated and stored using Microsoft Excel and statistically analysed using Graphpad Prism software (Graphpad Inc.). All datasets were tested for normality prior to statistical analysis. Due to the small and variable sample sizes of the initial behavioural screen the statistically stringent Kruskal Wallis non-parametric One-Way ANOVA was used, followed by Dunn's post-hoc test for multiple comparison between pooled control (*shi/w-*), and experimental groups (*shi/Split-GAL4*). For analysis of subsequent data containing more than three experimental groups One-way ANOVA was used followed by planned pairwise Bonferroni's multiple-comparison post-hoc test. Where only two experimental groups were compared, such as for calcium imaging data, p-values were calculated via the student's T-test. The significance threshold (α) was set to 0.05.

2.7 Anatomical analysis

In order to examine whether MBONs and DANs are potential synaptic partners it was first important to determine whether they innervate the same anatomical regions within the fly brain. The targeted expression of fluorescent markers to neuronal subtypes was achieved using the fly lines and expression systems detailed in section 2.1. Flies were

dissected, fixed, and stained using standard methods (Bräcker et al., 2013). Microscopy was performed using an Olympus FV-1000 confocal microscope and image stacks processed using ImageJ and Photoshop. Detailed anatomical analysis of all Split-GAL4 fly lines used in this study can be found in the study published by Aso et al. (Aso, Hattori, et al., 2014).

2.7.1 Antibodies

To provide anatomical background against which to judge neurons of interest neuropil was stained with the nc82 antibody (AB) (represented as magenta in figures). Anti-GFP AB and Dsred AB were used to amplify the fluorescence intensity of expressed GFP and mCherry respectively (Table 1).

Staining	Primary Antibodies	Secondary Antibodies
GFP	α-GFP (rabbit, 1:1000, Invitrogen) (rat, 1:200, Chromotek)	α-rabbit (Alexa Fluor 488, 1:1000, Invitrogen) α-rat (Alexa Fluor 488, 1:250, Invitrogen)
Denmark (mCherry)	α-Dsred (rabbit, 1:200, Clontech)	α-rabbit (Cy3, 1:250, Jackson Immunoresearch)
Synaptotagmin (GFP)	α-GFP 3H9 (rat, 1:200,Chromotek)	α-rat (Alexa Fluor 488, 1:250, Invitrogen)
GRASP (GFP)	α-GFP (mouse, 1:200, NeuroMab clone N86/38)	α-mouse (Alexa 488, 1:250 Invitrogen)
Dopaminergic neurons	α-TH (mouse, 1:100, ImmunoStar)	α-mouse (Alexa 633, 1:250, Invitrogen)
Glutamatergic neurons	α-dvGlut (rabbit, 1:1000, gift of DiAntonio)	α-rabbit (Cy3, 1:250, Jackson Immunoresearch)
nc82 neuropil	α-nc82 (mouse, 1:50, DSHB)	α-rabbit (Cy3, 1:250, Jackson Immunoresearch) α-mouse (Alexa 633, 1:250, Invitrogen)

Table 1. Primary and secondary antibodies

Antibodies used to stain genetically encoded markers or endogenously expressed proteins for anatomical characterization.

2.7.2 MBON and DAN cell polarity

The input and output regions of MBONs and DANs were analysed using the Split-GAL4 driver lines *MB002B-Split-GAL4*, *MB011B-Split-GAL4*, and *MB109B-Split-GAL4* to drive expression of *UAS-DenMark::mCherry; UAS-Syt::GFP*. Expression of DenMark::mCherry was therefore restricted to the dendritic input regions (red in the figures), and Synaptotagmin::GFP to the axonal output regions (green in the figures).

2.7.3 Double labeling experiments

To establish whether MBONs and DANs had anatomically overlapping fields of innervation we first recombined 1) *MB109B-Split-GAL4/CyO* (DAN) and *R14C08-LexAp65* (MBON), and 2) *MB109B-Split-GAL4/CyO* (DAN) and *R15B01-LexAp65* in attP40 (MBON). *R14C08-LexAp65* and *R15B01-LexAp65* in attP40 both label MBONs targeting the β'2 MB lobe region. These lines were then used to drive expression of *LexAop2-mCD8GFP*, and *10XUAS-IVS-mCD8RFP*. This allowed us to simultaneously visualize MBONs and DANs, expressing GFP and RFP respectively, in a single fly brain.

2.7.4 GRASP (GFP reconstitution across synaptic partners)

GRASP analysis was carried out using *MB109B-Split-GAL4/CyO*, *R14C08-LexAp65*, and *R15B01-LexAp65* in attP40, to drive expression of *w-; Bi/CyO; UAS-CD4::spGFP1-10/TM2*, and *w-; LexAop-CD4::spGFP11/CyO; TM2/TM6B*. When two neurons come into close contact, and each expresses half of a split GFP, functional GFP is reconstituted and fluorescence restored. A fluorescence signal can therefore be taken as indicative of two neurons being synaptic partners.

3.0 Results

3.1 Establishing the behavioural basis for olfactory conflict resolution

Bräcker et al. (Bräcker et al., 2013) previously demonstrated that starved flies can overcome their aversion to CO_2 to approach appetitive vinegar odour. In order to determine the types of responses I would observe throughout experimentation I initially tested the effect of blocking transmission of either vinegar or CO_2 olfactory information to the MB on the behavioural responses to vinegar, CO_2, and the conflict mixture of both

Genotype		Shi/w-	+	+	+					
		Shi/GH146				+	+			
		Shi/Gr63a							+	+
Stimulus		Vinegar	+			+				
		CO2		+					+	
		Conflict			+		+			+
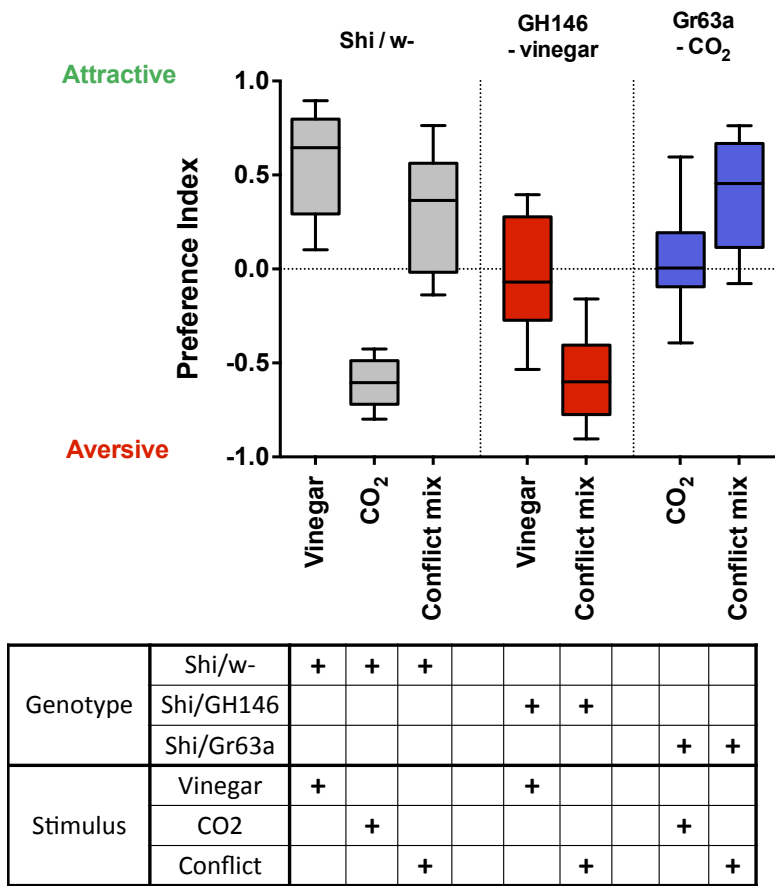
Figure 10. Food odour inhibits aversive behaviour

Negative PI value denotes aversion, positive PI value denotes attraction.
The grey bars represent control flies capable of exhibiting wild type like behaviour. The red bars represent flies' responses to vinegar and conflict stimulus upon silencing of vinegar representing PNs. The blue bars represent flies' responses to CO_2 and conflict stimulus upon silencing of the Gr63a OSNs. n=16-20. The upper and lower extents of the box plots represent the interquartile range, the bisecting line the median value, and the whiskers the 10th and 90th percentiles.

odours. As expected I observed that 42 hour starved flies are innately attracted to vinegar and innately averse to CO_2 (Figure 10, grey bars). When exposed to the conflict odour, starved flies are capable of overcoming their aversion to CO_2 to approach the vinegar odour (Figure 10, grey bars). This behaviour can be examined and dissected via the use of the T-maze behavioural assay and by blocking neurons critical to the sensation and execution of behavioural responses to these olfactory stimuli. GH146-GAL4 labels a subset of PNs required for vinegar attraction but does not include those PNs required to process CO_2 aversion. When GH146 is used to drive expression of the temperature sensitive dominant negative allele of dynamin, Shibire[ts1], vinegar attraction is completely abrogated at the non-permissive temperature of 32°C (Figure 10, red bars). Upon stimulus with the conflict mixture of CO_2 and vinegar flies are unable to properly process vinegar sensation and so avoid the CO_2 (Figure 10, red bars) and instead choose the air-side of the T-maze. If the CO_2 sensitive Gr63a OSNs are likewise blocked by expression of Shibire[ts1], flies are unable to sense CO_2 and in response to the conflict stimulus approach the conflict stimulus vinegar component (Figure 10, blue bars). Through these simple experiments it is possible to show that selective silencing of populations of neurons in the fly brain restricts the sensory channels available to the fly for decision making and behavioural modulation. Throughout the study presented here I leverage this behavioural technique to analyse higher-level neural circuits mediating olfactory conflict resolution.

3.2 Olfactory choice T-maze behavioural screen of MB neurons

In order to examine the higher brain regions responsible for integrating conflicting stimuli and resolving sensory conflict for the purpose of singular behavioural output, I conducted a T-maze behavioural screen on a library of 79 Split-GAL4 lines specifically labelling nearly all MB associated neurons (see appendix tables 6, 7, 8, and 9). For the purposes of experimentation I took vinegar attraction, CO_2 aversion, and a mix of the two, to be representative of generalised attraction, aversion and sensory conflict resolution respectively. Split-GAL4 lines labelling KC subpopulations, MBONs, DANs, and some additional MB innervating neurons were crossed to *20XUAS-IVS-Shibire[ts1]-p10*, and the F_1 generation collected and starved for 42 hours prior to experimentation. No fed flies were tested for the primary screen as Bräcker et al. (Bräcker et al., 2013) had previously shown that the MB was only required under starvation conditions. Each *Split-GAL4 ; 20XUAS-*

IVS-Shibire[ts1]*-p10* line was tested at non-permissive temperature (32°C) against a vinegar concentration of 10% (v/v), and a CO_2 concentration of ~0.1%. For the conflict stimulus the same concentrations of vinegar and CO_2 were used and combined in one stimulus tube. The expression patterns of lines will be described where necessary. For those lines not directly referred to, details of expression pattern and level and promoter region can be found in the appendix (Tables 7-10).

The following sections will describe the behavioural screening results of the four distinct populations of neurons. Namely the KCs, MBONs, DANs, and other MB innervating neurons.

3.2.1 KC interneuron blockade

3.2.1.1 α'/β' KC play dominant role in CO_2 avoidance

A primary purpose of the screen was to elaborate on the findings of Bräcker et al. (Bräcker et al., 2013) by identifying with a higher degree of precision which KC subsets are involved in processing CO_2 and to test whether there was any specificity for the vinegar and mixed stimuli. Bräcker et al. showed that silencing the α'/β' KCs caused the largest reduction in CO_2 avoidance, while silencing the α/β KCs didn't produce a phenotype. The strongest phenotype was expressed upon silencing of all KCs, suggesting the γ KCs may play a role. However, in the context of the primary screen presented here, silencing γ KCs had no significant affect on CO_2 avoidance (Figure 11, blue bars). In support of the findings from Bräcker et al. a significant reduction in CO_2 avoidance was observed upon blockade in two of five Split-GAL4 lines labelling α'/β' KCs: MB370B and MB461B (Figure 11, green bars). These lines both label α'/β' KCs although there is some difference in terms of expression level (Table 2). With the exception of MB418B, which only labels α'/β'm KCs, the α'/β' labelling lines express in all α'/β' KC subsets (a, p, and m). Interestingly, a phenotype was observed upon blockade in line MB371B, which labels only a subset of α/β KCs, namely α/βp KCs (Figure 11, orange bars). This incongruence with the observations presented by Bräcker et al. – that the α/β KCs play little or no role in processing CO_2 avoidance – could be explained by their usage of a different driver line (R67B04) in targeting α/β KCs that perhaps had lower expression

40

levels in the α/βp subset of α/β KCs. A statistically significant CO_2 avoidance phenotype was also observed upon silencing of all KCs using the driver line MB152B (Figure 11, grey bars), which has strong expression in α'/β' KCs, but not in other broadly expressing lines (Table 2). This irregularity of phenotype in lines that in principle should produce strong phenotypes may be due to uncontrollable changes in fly rearing conditions leading to a false negative results. This is certainly a possibility given that the sample size of most experimental groups in the primary screen was 4n, making the experiment susceptible to variability. In addition, the statistical test used to identify positive hits in the screen (Kruskal-Wallis ranked analysis of variance) was particularly stringent to avoid the possibility of false positive results. These results confirmed the findings of Bräcker et al. in suggesting a dominant role for α'/β' KCs in processing innate CO_2 aversion. They also suggest a possible, if more limited role for α/βp but not γ KCs.

Figure 11. CO_2 avoidance response upon silencing of subsets of KC neurons

Negative PI value denotes aversion, positive PI value denotes attraction.
CO_2 response at non-permissive temperature. Control is *Shi/w-*. The upper and lower extents of the box plots represent the interquartile range, the bisecting line the median value, and the whiskers the 10th and 90th percentiles. The grey box spanning the length of the plot represents the control interquartile range. Experimental groups comprise 4-8n, control value pooled across 32n. (Kruskal-Wallis ANOVA and Dunn's post-hoc test, ns $p>0.05$, *$p<0.05$, **$p<0.01$).

3.2.1.2 Vinegar response upon KC blockade

Given that vinegar is a complex food odour activating 6 AL glomeruli (Semmelhack & Wang, 2009), one would expect there to be a larger number of redundant pathways by which it can affect behavioural output. Indeed, upon inactivation of populations of KCs under starvation conditions, very few statistically significant vinegar attraction phenotypes were observed, although there were several non-significant reductions in attraction (Figure 12). The lines in which phenotypes were observed, MB185B and MB131B (Figure 12), labelled α/βs and γ KC interneurons respectively (Table 2). Further, the magnitude of vinegar attraction phenotypes upon γ KC blockade was generally higher than CO_2 aversion phenotypes (Figures 11 and 12). That blockade of γ KCs (MB horizontal lobe) causes phenotypes in vinegar attraction but not CO_2 aversion is perhaps intuitive given that γ KCs have been implicated in appetitive reward learning (Huetteroth et al., 2015). This implies that γ KCs may perhaps play a greater role in representing appetitive stimuli than aversive stimuli.

	Broad				γ					α'/β'					α/β			
	MB010B	MB152B	MB364B	MB417B	MB028B	MB419B	MB355B	MB009B	MB131B	MB005B	MB461B	MB463B	MB370B	MB418B	MB371B	MB008B	MB185B	MB477B
KC γd	▓	▓	■		░	▓	▓	▓	░									
KC γmain	▓	▓	■				░	░	▓									
KC α'/β'ap	■	■		■						▓	■	■	░					
KC α'/β'm	■	■		■						▓	▓	░	▓	▓				
KC α/βp	■	░	▓	■											▓	■		
KC α/βs	■	▓	■	■												■	▓	▓
KC α/βc	■	░	■	░												■		
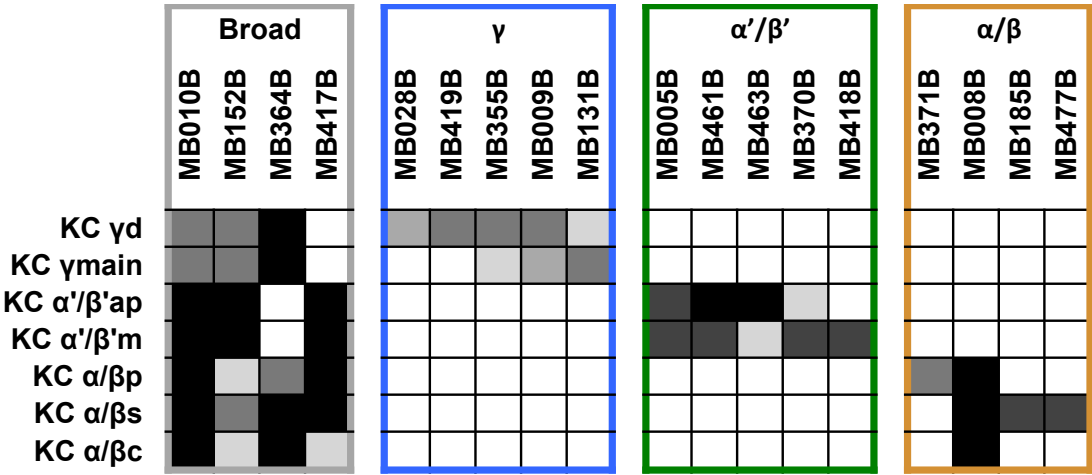
Table 2. KC Split-GAL4 line expression patterns and levels

Each fly line (MBxxxB) targets expression to cell types as indicated by greyscale rectangles. Black corresponds to strongest expression and light grey to weakest expression. Neuron designations are indicated on the far left. These anatomical and expression analysis were carried out by Aso et al. (Aso, Hattori, et al., 2014).
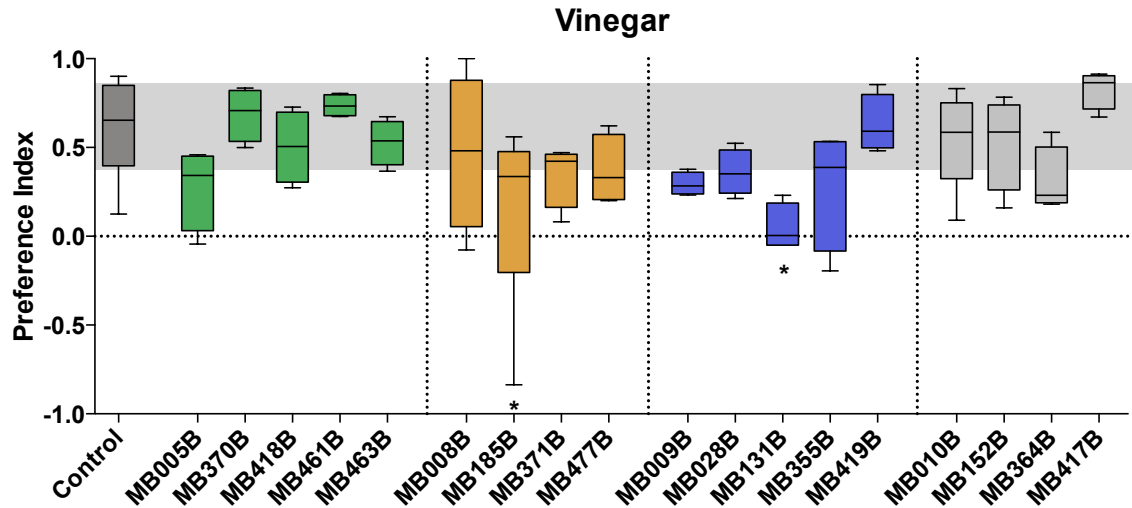
Figure 12. Vinegar attraction response upon silencing of subsets of KC neurons

Negative PI value denotes aversion, positive PI value denotes attraction.
Vinegar response at non-permissive temperature. Control is *Shi/w-*. The upper and lower extents of the box plots represent the interquartile range, the bisecting line the median value, and the whiskers the 10th and 90th percentiles. The grey box spanning the length of the plot represents the control interquartile range. Experimental groups comprise 4-8n, control value pooled across 32n. (Kruskal-Wallis ANOVA and Dunn's post-hoc test, ns p>0.05, *p<0.05, **p<0.01).

3.2.1.3 Mixed CO₂ and Vinegar conflict stimulus upon KC blockade.

From behavioural analysis alone there was no clear way to distinguish whether a reduced or increased attraction to the conflict mix was a result of reduced attraction to vinegar (resulting in an increased aversion to CO_2), a reduced aversion to CO_2 (resulting in an increased attraction to vinegar), or a sensory integration phenotype indistinguishable from the single odour phenotypes. One possible way of interpreting the data was to see whether a phenotypic behavioural response to the conflict stimulus had a corresponding phenotype in the single odour tests. For example, the line *MB370B-Split-GAL4 ; 20XUAS-IVS-Shibire^{ts1}-p10*, which targets α'/β' KCs exhibited a strongly reduced CO_2 response (Figure 11, green bars), and correspondingly, its attraction to the mixture of CO_2 and vinegar was stronger than the control value (Figure 13, green bars). Thus, the line's intact attraction pathway drove the behavioural response to the conflict stimulus. The situation is similar, although inverted, for the line MB005B, which also targets expression to α'/β' KCs (Table 2). Unlike MB370B its CO_2 avoidance was not strongly reduced (Figure 11, green bars). Instead, when driving the expression of Shibire^{ts1}, it exhibited a non-

significant reduction in vinegar attraction (Figure 12, green bars), and in response to the mixed odour conflict stimulus it was also less attracted (Figure 13, green bars). This suggests the line's reduced attraction to vinegar caused its behaviour in response to the mixed odour stimulus to be dominated by its intact CO_2 avoidance. Silencing γ KCs and stimulating the flies with the conflict odour produced significant phenotypes in three lines (MB009B, MB028B, and MB131B), with the flies exhibiting aversion rather than attraction (Figure 13, blue bars). This makes intuitive sense given that the same lines displayed more strongly reduced vinegar attraction upon silencing than they did reduced CO_2 aversion (Figure 12 and 11, blue bars). Thus, their intact aversion pathway may have driven their aversive behavioural response. Lines targeting expression to α/β KCs followed the same general pattern. MB371B, which sparsely targets α/βp KCs (Table 2), exhibited a strong CO_2 avoidance phenotype, a small non-significant reduction in vinegar attraction, and a non-significant increase in attraction to the conflict stimulus (Figure 11, 12, and 13, orange bars). Here, the same logic applies. The line's reduced aversive response leads to it's increased attraction in the context of the conflict stimulus. Line MB185B, which labels only α/βs KCs (Table 2), displayed an almost normal aversive

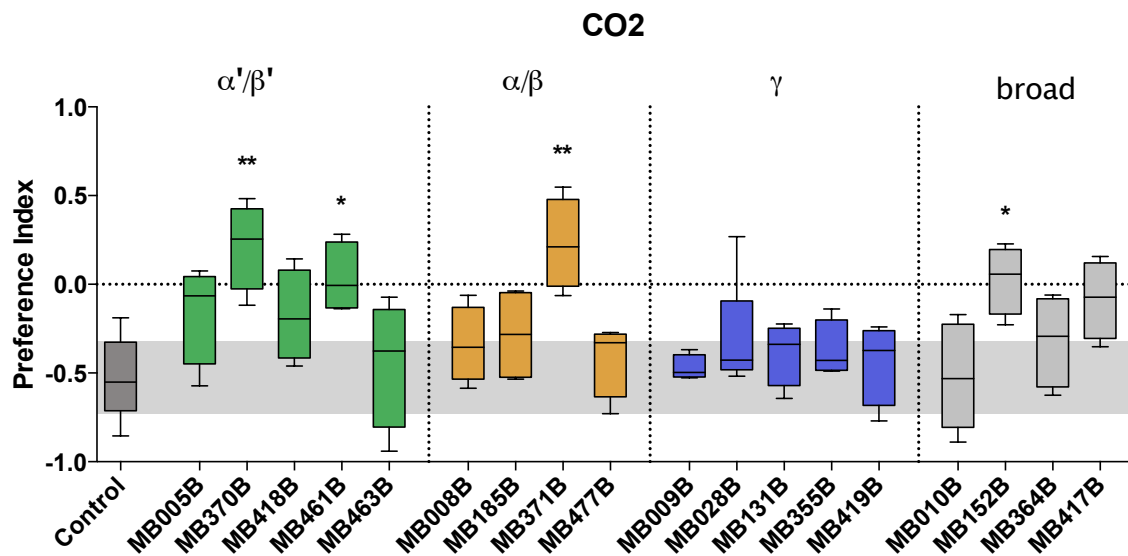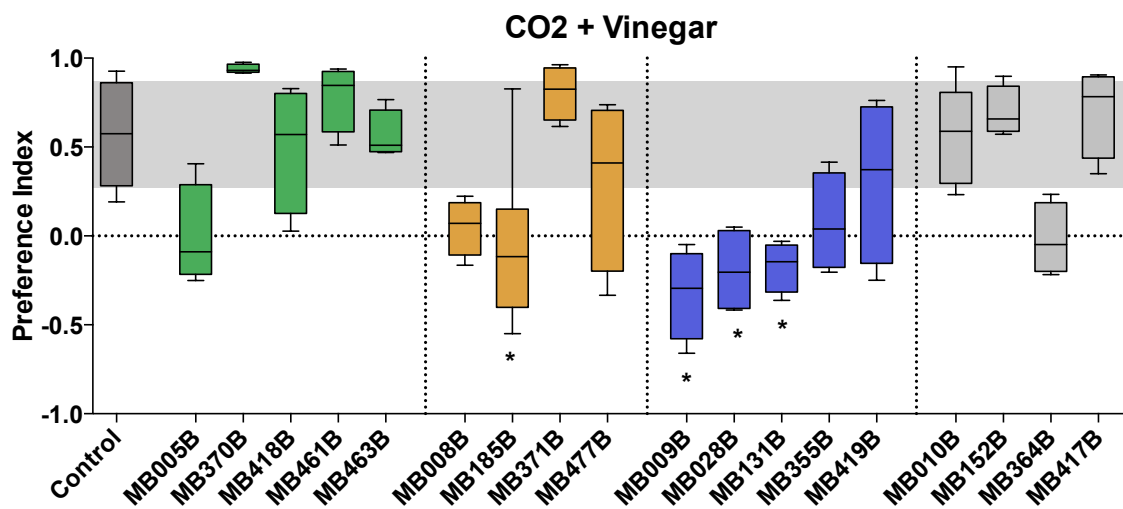**Figure 13. Mixed odour conflict response upon silencing of subsets of KC neurons**

Negative PI value denotes aversion, positive PI value denotes attraction.
Mixed odour conflict response at non-permissive temperature. Control is *Shi/w-*. The upper and lower extents of the box plots represent the interquartile range, the bisecting line the median value, and the whiskers the 10th and 90th percentiles. The grey box spanning the length of the plot represents the control interquartile range. Experimental groups comprise 4-8n, control value pooled across 32n. (Kruskal-Wallis ANOVA and Dunn's post-hoc test, ns $p > 0.05$, *$p < 0.05$, **$p < 0.01$).

response to CO_2, a significantly reduced attraction to vinegar, and correspondingly, a significantly reduced ability to overcome CO_2 aversion in the context of the conflict stimulus (Figure 11, 12, and 13, orange bars).

From these data a general observation can be made, that if a line displayed a reduction in aversion, it is more likely to be more attracted to the conflict stimulus. If the neuronal inactivation elicits a reduction in attraction, it will be more likely to be averse to the conflict stimulus:

$$behaviour\ valence = odourA\ (\pm x) + odourB\ (\pm x)$$

Where x describes the valence and strength of representation of the given odour.

While this observation may explain the relationships between single lines across different stimulus conditions, it doesn't explain why the odour responses are different across several lines that target the same KC subpopulations. One reason for these differences may be that the differing expression levels between the lines lead to what amounts to a slightly different KC odour representation, capable of driving attractive and aversive behaviours with differing strengths. Given that 1) the α'/β' and α/β KCs both innervate the vertical and horizontal MB lobes, and that 2) the vertical lobe drives attractive behaviour and the horizontal lobe aversive, differing expression levels in different KC populations may differentially drive attractive or aversive behaviour in response to what remains of the odour representation after neuronal silencing. This hypothesis makes sense in the context of recent research that demonstrated different thresholds for activation of aversive and attractive behaviours via horizontal lobe and vertical lobe MBONs. That blockade of the γ KCs seems to have more of an affect on vinegar attraction than CO_2 aversion is somewhat confusing given that γ KCs are likely synaptically connected to MBONs driving both attractive and aversive behaviours. The reason for this should become clear once the nature of the synaptic connectivity between the KCs, MBONs, and DANs is better understood.

3.2.2 Mushroom body output neuron blockade

3.2.2.1 Horizontal lobe β'2 mushroom body output neurons drive aversive CO_2 output

MBONs innervate specific anatomical compartments of the MB lobes and are post-synaptic to the KCs. The olfactory information they receive is gated by DAN modulation of the KC presynapse. Included in the behavioural screen were 25 Split-GAL4 lines labelling MBONs innervating both the horizontal and vertical MB lobes. Upon neuronal inactivation only four statistically significant phenotypes were obtained (MB011B, MB074C, MB434B, and MB399B) for CO_2 avoidance behaviour (Figure 14, green bars). Three of the four phenotypes were produced by lines almost exclusively labelling MBONs innervating the β'2 region of the MB horizontal lobe (MB011B, MB074C, and MB399B) (Table 3) indicating a possibly dominant role for the horizontal lobe in processing CO_2 aversive behaviour. The line MB011B exhibited the strongest CO_2 aversion phenotype and labels four MBONs that together cover the entire β'2 region of the MB (Table 3). Notably, these neurons have very little innervation in the adjacent γ lobe, which based on the KC silencing data, may represent vinegar. These data corroborate the findings published by Bräcker et al. and also fit with the KC silencing phenotypes in which the α'/β' KCs were identified as dominantly representing CO_2 aversion.

Figure 14. CO_2 avoidance response upon silencing of subsets of MBONs

Negative PI value denotes aversion, positive PI value denotes attraction.
CO_2 response at non-permissive temperature. Control is *Shi/w-*. The upper and lower extents of the box plots represent the interquartile range, the bisecting line the median value, and the whiskers the 10th and 90th percentiles. The grey box spanning the length of the plot represents the control interquartile range. Experimental groups comprise 4-8n, control value pooled across 40n. (Kruskal-Wallis ANOVA and Dunn's post-hoc test, ns $p > 0.05$, *$p < 0.05$, **$p < 0.01$).

3.2.2.2 Vertical lobe mushroom body output neurons dominantly represent vinegar attraction

Upon silencing of MBONs and stimulation with vinegar odour, it was observed that fly lines labelling vertical lobe outputs elicited stronger reductions in attraction than did horizontal lobe outputs (Figure 15). This observation is corroborated by the findings of Aso et al (Aso, Sitaraman, et al., 2014) which demonstrate that when activated, vertical lobe MBONs drive attractive behaviour. The strongest phenotype was exhibited by the line MB112C which labels a MB recurrent GABAergic MBON (MBON-γ1pedc>α/β) innervating multiple compartments of the vertical and horizontal lobes (Figure 15, blue bars, and Table 2). Despite this, it's activation triggers attractive behaviour (Aso, Sitaraman, et al., 2014). Upon silencing, horizontal lobe MBONs did not display statistically significant reductions in attraction behaviour (Figure 15, blue bars). Analysis

	Horizontal lobe											Vertical lobe													
	MB298B	MB434B	MB433B	MB011B	MB210B	MB002B	MB074C	MB399B	MB310C	MB083C	MB057B	MB112C	MB051B	MB018B	MB093C	MB082C	MB052B	MB552B	MB543B	MB542B	MB027B	MB050B	MB549C	MB080C	MB242A
MBON-γ4>γ1γ2																									
MBON-β1>α (MB-MV2)																									
MBON-γ5β'2a (MB-M6)																									
MBON-β'2mp (MB-M4)																									
MBON-β'2mp_bilateral																									
MBON-β2β'2a																									
MBON-α1																									
MBON-γ3																									
MBON-γ3β'1																									
MBON-β'1																									
MBON-γ1pedc>α/β (MB-MVP2)																									
MBON-γ2α'1																									
MBON-α'2 (MB-V4)																									
MBON-α3 (MB-V3)																									
MBON-α'1																									
MBON-α2sc (MB-V2α)																									
MBON-α2p3p																									
MBON-α'3ap (MB-V2α'3)																									
MBON-α'3m (MB-V2α'3)																									
MBON-calyx (MB-CP1)																									

Table 3. MBON Split-GAL4 line expression patterns and levels

Each fly line (MBxxxB) targets expression to cell types as indicated by greyscale rectangles. Black corresponds to strongest expression and light grey to weakest expression. Neuron designations are indicated on the far left. These anatomical and expression analysis were carried out by Aso et al. (Aso, Hattori, et al., 2014). The names of MBONs used as part of the old system of MB neuron nomenclature are indicated in brackets.

of these data indicates a functional divergence between the representation of the attractive and aversive odours, vinegar and CO_2, between the vertical and horizontal lobes respectively. These data are somewhat incongruent with the γ KC silencing data that suggest that the γ lobe may also represent vinegar (Figure 12, blue bars), indicating a strong divergence in function between the sub-lobes of the MB horizontal lobe, and that attraction and aversion may be differentially represented in terms of amount of input required to initiate the respective behaviour.

3.2.2.3 Vertical lobe and horizontal lobe MBON conflict odour response

As with the KC data, I looked to see if a reduction or increase in behavioural response to the mix of CO_2 and vinegar could be explained by deficits in processing of the single odour response. Line MB083C, for example, exhibited a strong avoidance (Figure 16, green bars), and although only small in magnitude, it had a relatively strong reduction in vinegar attraction compared to other lines targeting horizontal lobe MBONs (Figure 15, green bars). A larger proportion of the vertical lobe innervating MBONs exhibited conflict odour response phenotypes (Figure 16, blue bars). This is likely due to the overall larger number of single odour vinegar attraction phenotypes observed upon silencing of the same
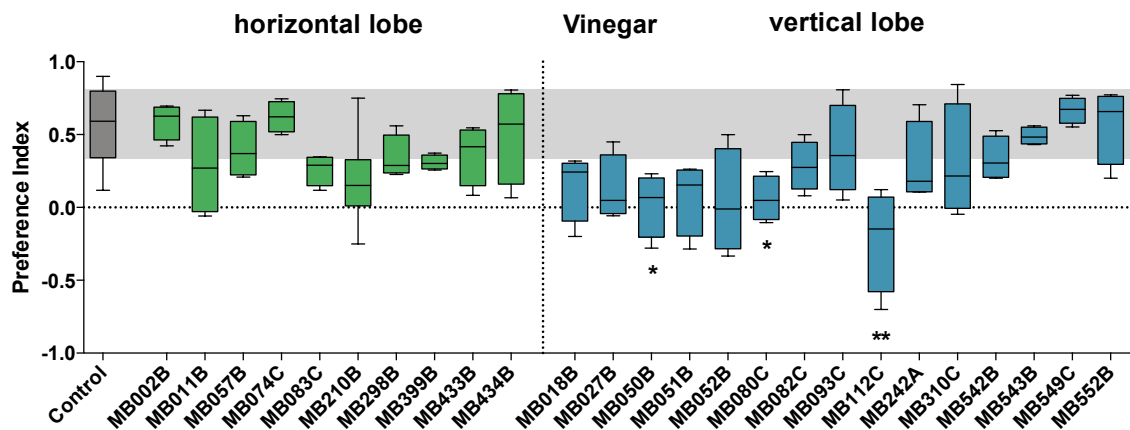
Figure 15. Vinegar response upon silencing of subsets of MBONs

Negative PI value denotes aversion, positive PI value denotes attraction.
Vinegar response at non-permissive temperature. Control is *Shi/w-*. The upper and lower extents of the box plots represent the interquartile range, the bisecting line the median value, and the whiskers the 10th and 90th percentiles. The grey box spanning the length of the plot represents the control interquartile range. Experimental groups comprise 4-8n, control value pooled across 46-48n. (Kruskal-Wallis ANOVA and Dunn's post-hoc test, ns p>0.05, *p<0.05, **p<0.01).

neurons (Figure 15, blue bars). Line MB112C, for example, exhibits a largely normal CO_2 avoidance (Figure 14, blue bars), a strongly reduced vinegar attraction (Figure 15, blue bars), and an aversive conflict odour response (Figure 16, blue bars), suggesting it strongly represents vinegar. Importantly the lines labelling MBONs that innervate the β'2 region (MB011B, MB074C, and MB399B) did not exhibit phenotypes, which one would expect given their reduction in CO_2 aversion.

The MBON screening data, like the KC data, recapitulate the findings of Bräcker et al. (Bräcker et al., 2013) that the α'/β' KCs dominantly represent CO_2, and implicate the β'2 MBONs as the downstream postsynaptic neurons that mediate CO_2 avoidance behaviour. They exhibit strong reductions in CO_2 aversion (Figure 14, green bars), but not in conflict response (Figure 16, green bars), and did not display reductions in vinegar attraction suggesting they may be specific for aversive odours. Correspondingly, silencing of the vertical lobe MBONs elicited vinegar attraction but not CO_2 phenotypes (Figures 14 and 15), a finding supported by the recent study by Aso et al. (Aso, Sitaraman, et al., 2014). These data, along with findings from Lin et al. point to the possibility of the horizontal lobe playing a greater role in the processing of innate behavioural responses (S. Lin et al., 2014).
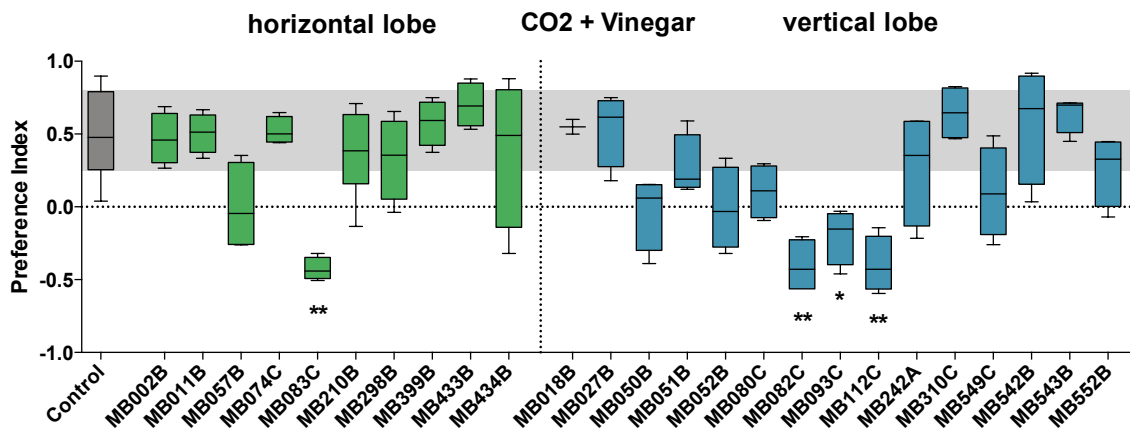
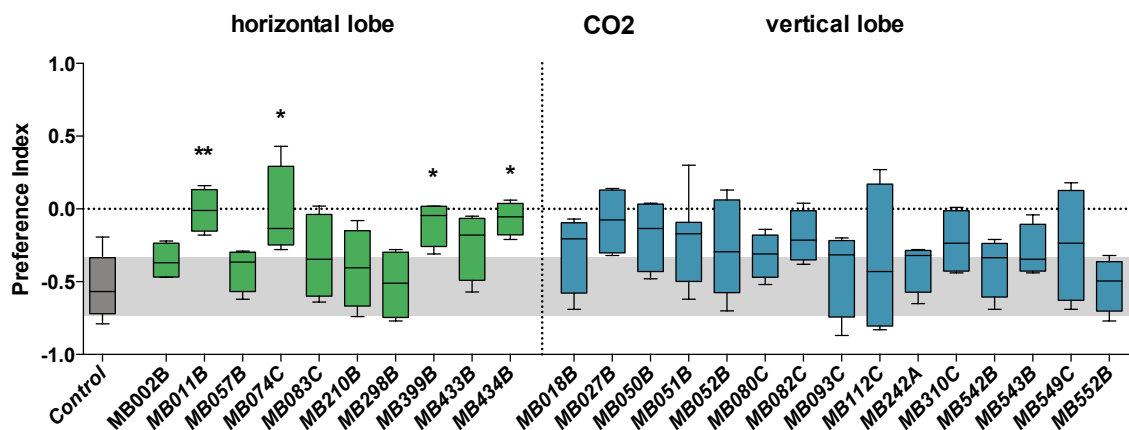**Figure 16. CO_2 and Vinegar conflict response upon silencing of subsets of MBONs**

Negative PI value denotes aversion, positive PI value denotes attraction.
Conflict response at non-permissive temperature. Control is *Shi/w-*. The upper and lower extents of the box plots represent the interquartile range, the bisecting line the median value, and the whiskers the 10th and 90th percentiles. The grey box spanning the length of the plot represents the control interquartile range. Experimental groups comprise 4-8n, control value pooled across 46-48n. (Kruskal-Wallis ANOVA and Dunn's post-hoc test, ns p>0.05, *p<0.05, **p<0.01).

3.2.3 PAM and PPL1 cluster dopaminergic neuron blockade

3.2.3.1 PAM cluster neurons modulate both aversive and attractive responses

Given that the screening data for the MBONs seemed to indicate that the vertical lobe plays a dominant role in mediating attractive olfactory responses and the horizontal lobe a role in aversive responses, I expected the populations of dopaminergic neurons innervating the lobes to functionally segregate in a similar fashion. Indeed, DANs of the PAM cluster that project axonal terminals to the horizontal lobe (aversion mediating) cause reductions in CO_2 aversion upon silencing (Figure 17A), while the statistically significant phenotypes observed upon silencing neurons of the PPL1 cluster that innervate the vertical lobe (attraction mediating) are found in response to vinegar but not CO_2 (Figure 18). I also observed that silencing PAM neurons causes vinegar attraction phenotypes (Figure 17B). This could possibly be explained in relation to the γ lobe KC vinegar stimulus data, which suggests that the γ KCs may represent attractive vinegar odour (Figure 12, blue bars). Many of the PAM neurons also directly innervate the γ lobe (Table 4) and so may be responsible for modulating horizontal lobe mediated vinegar attraction as well as aversion.

Given that the MBON silencing data presented above implicated the β'2 horizontal lobe region in processing CO_2 aversion one would expect that the DANs innervating this same region may generate CO_2 response phonotypes upon silencing. However, in the screening data presented here, lines labelling DANs innervating the β'2 region (Table 4) did not produce consistent or readily interpretable results.

Figure 17. CO_2 and Vinegar single odour responses upon silencing of subsets of PAMs

Negative PI value denotes aversion, positive PI value denotes attraction.

PAM cluster neurons innervate the MB horizontal lobe. CO_2 and vinegar single odour responses at non-permissive temperature. Control is *Shi/w-*. The upper and lower extents of the box plots represent the interquartile range, the bisecting line the median value, and the whiskers the 10th and 90th percentiles. The grey box spanning the length of the plot represents the control interquartile range. Experimental groups comprise 4-8n, control value pooled across 46-48n. (Kruskal-Wallis ANOVA and Dunn's post-hoc test, ns $p > 0.05$, *$p < 0.05$, **$p < 0.01$).

Only one line (MB042B) expressing in β'2 innervating PAM DANs produced a significant reduction in CO_2 avoidance (Figure 17A, blue bars). However, due to its broad expression (Table 4) it is not possible to say with any certainty that it was indeed the β'2 PAM DANs that caused the phenotype. Several other lines did produce non-significant CO_2 phenotypes but not in a manner consistent with the data obtained from the silencing of MBONs innervating the same MB compartments (Figure 14). Interestingly some of the DAN labelling lines produced vinegar attraction phenotypes upon silencing. For example line MB087C, which targets expression to PAM-β'2a, exhibited a significant reduction in vinegar attraction (Figure 17B). This was contradictory to my initial expectation that these neurons represent vinegar in order to suppress CO_2 avoidance, and that therefore their activity is not necessarily required for attraction to vinegar. Alternatively, if PAM DAN activity is required to inhibit aversive behaviour, and therefore drive attractive behaviour, it may also be logical that their silencing reduces attractive behaviours.

The most likely explanation for the lack of an obvious pattern in PAM DAN function across the lines tested here is that within the cluster of ~200 PAM neurons there is significant functional redundancy. The existence of multiple PAM DAN neurons that perform the same or similar tasks may effectively reduce the magnitude of a phenotype caused by blocking only one neuron. Given this redundancy and that DANs may allow complex internal state information to positively or negatively impinge on the transformation of olfactory information into behaviour (Cohn et al., 2015; Owald et al., 2015b) it is likely that behaviour is modulated dynamically by the entire ensemble. Thus, interpretation of the effect of silencing an individual or arbitrary population of neurons is very difficult without detailed understanding of the DAN representation of internal state. This situation does not apply in the same way to behavioural analysis of MBON function due to their much reduced ensemble size and therefore level of redundancy.

Another possible interpretation of the PAM DAN lack of valence specificity is that they often innervate lobes also innervated by KCs that seemingly represent both attractive and aversive odours (Figures 11 and 12). Indeed, in comparison to the PAM DAN findings presented here, synaptic silencing of the vertical lobe innervating PPL1 DANs appeared to cause clearly different effects in behavioural responses to vinegar and to CO_2 (Figure 18); I observed significant reductions in vinegar attraction (lines MB058B, MB065B, and MB304B) (Figure 18B), but not in CO_2 avoidance (Figure 18A). These may reflect the

52

findings presented by Aso et al. (Aso, Sitaraman, et al., 2014) in which all MBONs innervating the vertical lobe seem to drive attractive behaviour upon optogenetic activation. In addition, the vertical lobe consists of only two sub-lobes (α and α') to the horizontal lobe's three (β, β', and γ), and appears to have a more consistent appetitive representation across these two sub-lobes whereas the horizontal lobe may have opposing representations between the γ (appetitive) and β / β' (aversive) sub-lobes (Figures 11-16), effectively making the PAM DAN modulations more complex than those of the PPL1 DANs.

Taken together, these PAM DAN and PPL1 DAN data may reflect the relative complexity of the processing tasks performed by the two MB lobes. The PAM DAN ensemble may modulate outputs from sub-lobes representing both attractive and aversive stimuli, whereas the PPL1 DAN neurons may only modulate the KC representation of attractive odours. It is not clear from these data whether the β'2 MBONs are modulated by PAMs also innervating this region. However, this will be elaborated upon in later sections.

PPL1 cluster DANs: MB060B, MB065B, MB504B, MB438B, MB439B, MB502B, MB308B, MB058B, MB296B, MB304B

PAM cluster DANs: MB315C, MB109B, MB087C, MB301B, MB213B, MB299B, MB056B, MB312B, MB043B, MB188B, MB195B, MB025B, MB042B, MB040B, MB196B, MB032B, MB047B, MB194B, MB316B

Neuron designations (far left rows):
PPL1-γ1pedc (MB-MP1)
PPL1-γ2α'1 (MB-MV1)
PPL1-α'2α2 (MB-V1)
PPL1-α3
PPL1-α'3
PPL1-γ1
PAM-γ5
PAM-β'2a
PAM-β2β'2a
PAM-β2
PAM-β'2m
PAM-β'2p
PAM-γ4<γ1γ2
PAM-γ4
PAM-β1(MVP1)
PAM-β1ped
PAM-α1
PAM-γ3
PAM-β'1ap
PAM-β'1m

Table 4. DAN Split-GAL4 line expression patterns and levels

Each fly line (MBxxxB) targets expression to cell types as indicated by greyscale rectangles. Black corresponds to strongest expression and light grey to weakest expression. Neuron designations are indicated on the far left. These anatomical and expression analysis were carried out by Aso et al. (Aso, Hattori, et al., 2014). The names of DANs used as part of the old system of MB neuron nomenclature are indicated in brackets.
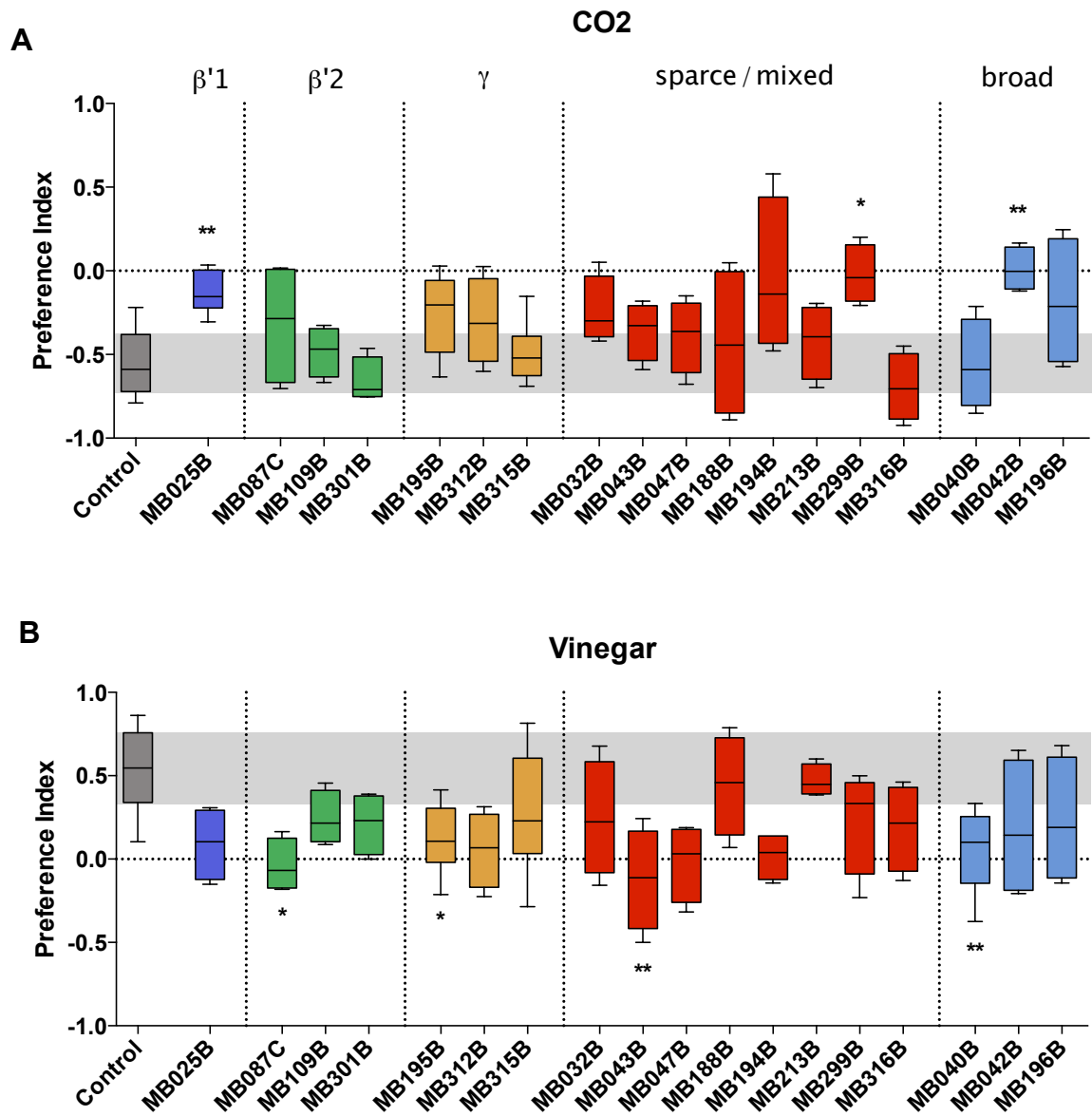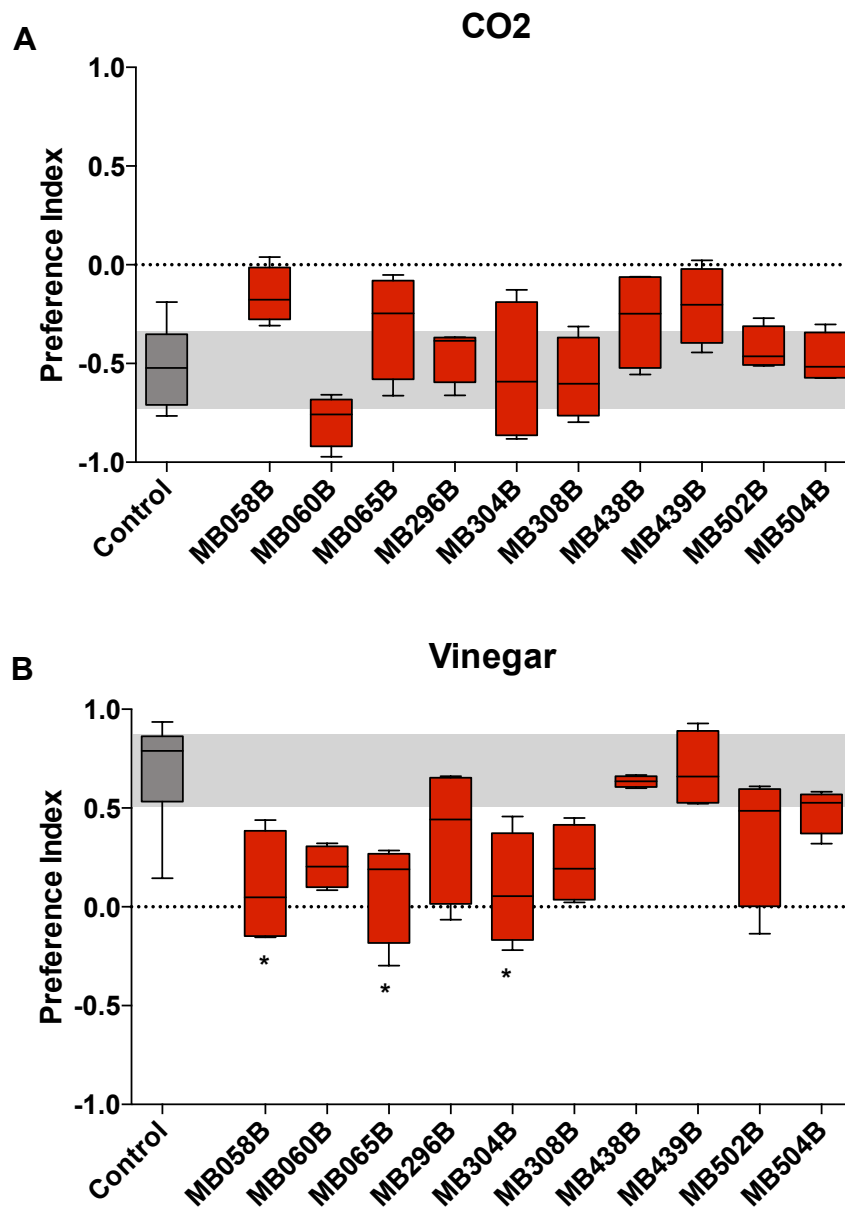
Figure 18. CO$_2$ and Vinegar single odour responses upon silencing of subsets of PPL1s

Negative PI value denotes aversion, positive PI value denotes attraction.
PPL1 cluster neurons innervate the MB vertical lobe. CO$_2$ **(A)** and vinegar **(B)** single odour responses at non-permissive temperature. Control is *Shi/w-*. The upper and lower extents of the box plots represent the interquartile range, the bisecting line the median value, and the whiskers the 10th and 90th percentiles. The grey box spanning the length of the plot represents the control interquartile range. Experimental groups comprise 4-8n, control value pooled across 46-48n. (Kruskal-Wallis ANOVA and Dunn's post-hoc test, ns p>0.05, *p<0.05, **p<0.01).

3.2.3.2 PAM and PPL1 DAN conflict odour response

In response to blockade of subsets of DANs and simultaneous presentation with a choice between conflict odour and air, flies generally exhibited a reduction in attraction relative to controls (Figure 19). This can possibly be explained by the fact that vinegar attraction phenotypes were observed in both the PAM and PPL1 clusters of DANs leaving intact avoidance pathways to drive CO_2 aversion behaviour. Line MB299B labels PAM neurons innervating both the vertical lobe (PAM-α1) and horizontal lobe (PAM-β1, PAM- β2) (Table 4) and demonstrated a significant phenotype in CO_2 avoidance (Figure 17A, red bars), a non-significant phenotype in vinegar attraction (Figure 17B, red bars), but no phenotype in conflict stimulus response (Figure 19, red bars), indicating that both attractive and aversive behaviours may have been suppressed leading to a normal response to the mixed attractive and aversive stimulus. This interpretation is corroborated by findings from several recent studies. Aso et al. (Aso, Sitaraman, et al., 2014) demonstrated that simultaneous activation of aversive and attractive MBONs leads to behavioural responses at neither extreme; neither strong attraction nor strong aversion. It has additionally been shown that DAN input to the KC-MBON synapse can either depress or potentiate MBON output. Taken together with these findings, my screening data seems to indicate that the fly's response to the conflict stimulus is a summation of attractive and aversive drives.
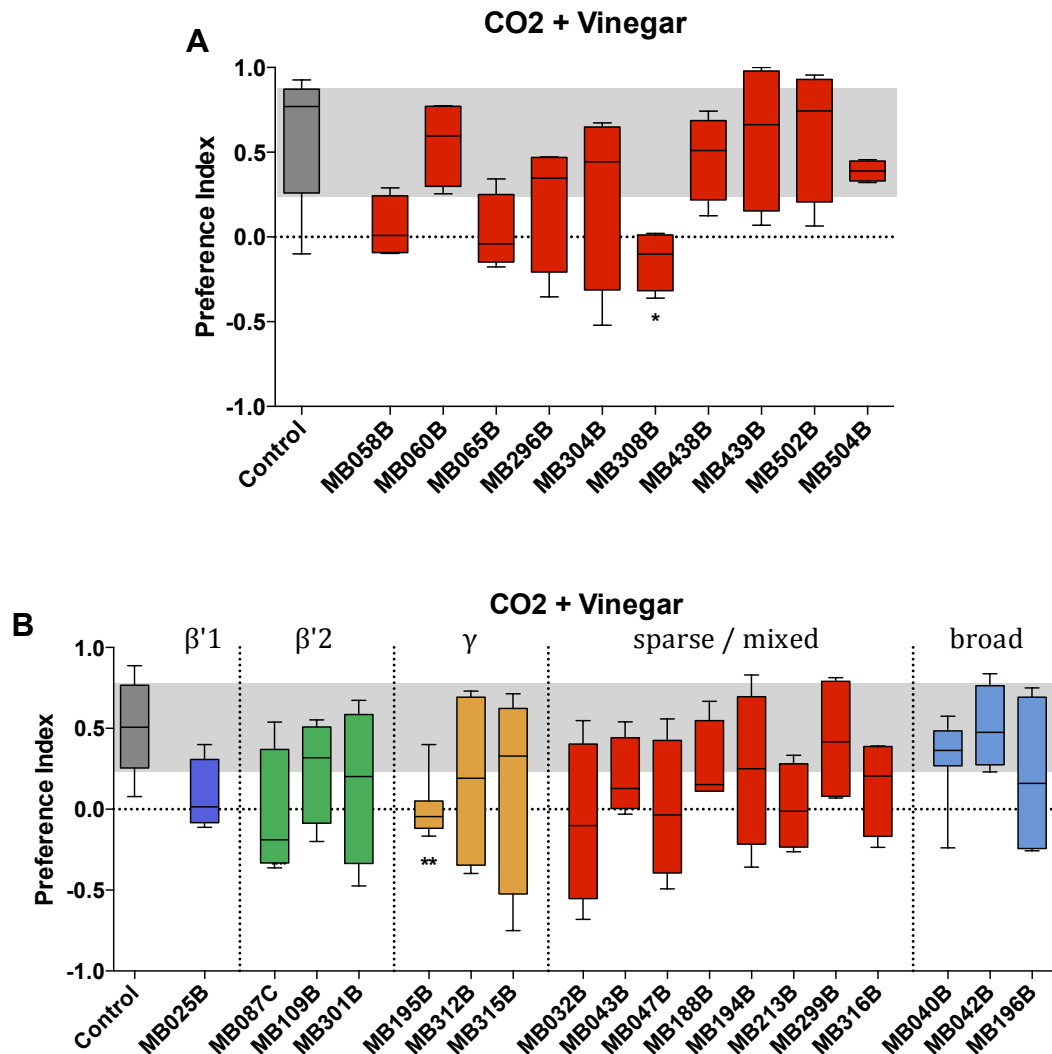
Figure 19. Conflict odour responses upon silencing of subsets of PPL1 and PAM DANs

Negative PI value denotes aversion, positive PI value denotes attraction.
(A) PPL1 cluster neurons innervate the MB vertical lobe. **(B)** PAM cluster neurons innervate the horizontal MB lobe. Conflict odour responses at non-permissive temperature. Control is *Shi/w-*. The upper and lower extents of the box plots represent the interquartile range, the bisecting line the median value, and the whiskers the 10th and 90th percentiles. The grey box spanning the length of the plot represents the control interquartile range. Experimental groups comprise 4-8n, control value pooled across 46-48n. (Kruskal-Wallis ANOVA and Dunn's post-hoc test, ns $p>0.05$, *$p<0.05$, **$p<0.01$).

3.2.4 Blockade of octopaminergic neuromodulatory input

Until recently it was though that in insects octopamine (OA) was the primary signalling molecule for reward (Hammer, 1993; Mizunami & Matsumoto, 2010; Schroll et al., 2006; Schwaerzel et al., 2003) and that dopamine mediated aversive reinforcement (Aso et al., 2010; Claridge-Chang et al., 2009). However, it is now understood that dopamine signals both appetitive and aversive reinforcement to the MB lobes and that octopamine has a more limited role in representing appetitive motivation (Burke et al., 2012; C. Liu et al., 2012). To test whether octopamine is required for innate olfactory behaviour or in resolving olfactory conflict I included three lines (MB021B, MB022B, and MB113C) labelling octopaminergic neurons in the behavioural screen. The lines labelled two neurons, OA-VPM3 and OA-VPM4 (Table 5), which both innervate the MB (Busch et al., 2009). Upon synaptic inactivation via Shibire[ts] expression none of the lines exhibited CO_2 avoidance phenotypes but did display non-significant reductions in vinegar attraction and significant reductions in conflict stimulus attraction (Figure 20). These findings are consistent with previous observations that octopaminergic neurons do not encode aversive information (Schwaerzel et al., 2003).
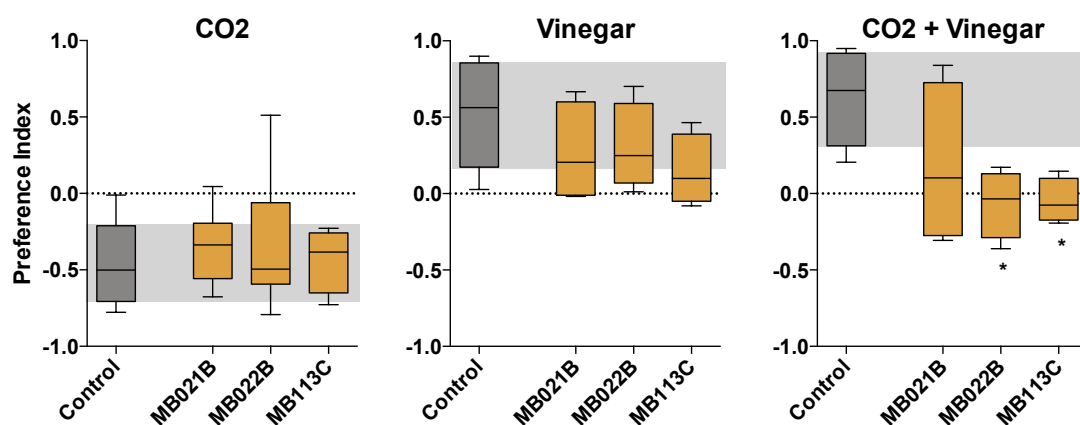
Figure 20. CO_2, vinegar, and conflict odour responses upon silencing of MB innervating octopaminergic neurons

Negative PI value denotes aversion, positive PI value denotes attraction.
Control is *Shi/w-*. The upper and lower extents of the box plots represent the interquartile range, the bisecting line the median value, and the whiskers the 10th and 90th percentiles. The grey box spanning the length of the plot represents the control interquartile range. Experimental groups comprise 4-8n, control value pooled across 46-48n. (Kruskal-Wallis ANOVA and Dunn's post-hoc test, ns p>0.05, *p<0.05, **p<0.01).

3.2.5 Blockade of additional mushroom body extrinsic neurons

As well as neuromodulatory input neurons and output neurons there are other cell types that innervate various parts of the MB. Four lines in the Spli-GAL4 library I had access to sparsely labelled neurons innervating broadly across the superior protocerebrum and part of the MB (Table 5). Line MB013B targeted expression to a SIFamide secreting neuron that innervates both the MB calyx and lobes (Aso, Hattori, et al., 2014; Verleyen et al., 2004). Not a lot is understood about the function of SIFamide except that it may play a role in sexual behaviour (Terhzaz et al., 2007) and the promotion of sleep (Park et al., 2014). Silencing of synaptic transmission of MB innervating SIFamide neurons elicited no CO_2 aversion phenotypes but did cause a significant reduction in vinegar attraction and a corresponding non-significant reduction in attraction to the conflict stimulus (Figure 21). Line MB380B targeted expression to the GABAergic MB-C1 neurons, which innervate both the LH and the MB calyx (Aso, Hattori, et al., 2014; Nobuaki K Tanaka et al., 2008) and are postulated to sparsen the KC odour representation. In the context of the behavioural screen blockade of the MB-C1 neurons produced significant reductions in vinegar attraction and conflict odour attraction but only a slight non-significant reduction
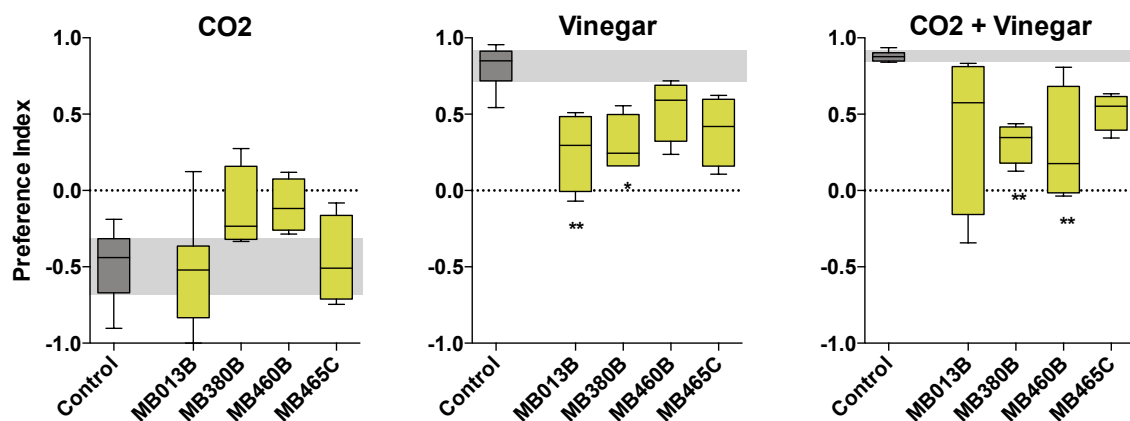
Figure 21. CO$_2$, vinegar, and conflict odour responses upon silencing of MB innervating neurons

Negative PI value denotes aversion, positive PI value denotes attraction.
Control is *Shi/w-*. The upper and lower extents of the box plots represent the interquartile range, the bisecting line the median value, and the whiskers the 10th and 90th percentiles. The grey box spanning the length of the plot represents the control interquartile range. Experimental groups comprise 4-8n, control value pooled across 46-48n. (Kruskal-Wallis ANOVA and Dunn's post-hoc test, ns p>0.05, *p<0.05, **p<0.01).

in CO_2 aversion (Figure 21). In later confirmation experiments no CO_2 aversion phenotype was observable but the vinegar phenotype remained robust. This selectivity for an appetitive odour may be due to the MB-C1 neuron's spatially restricted innervation of the LH, which also makes the neuron a potential candidate for altering KC odour representation based on internal state changes. Line MB460B selectively labels the bilateral dorsal giant interneurons (DGI) of the dorsal anteriolateral cluster (DAL). Upon blockade the DGIs displayed a non-significant reduction in CO_2 aversion and significant reductions in vinegar and conflict stimulus attraction (Figure 21). The reduction in CO_2 aversion was not observed in subsequent confirmation experiments, although the vinegar attraction phenotype remained. These neurons have been previously implicated in starvation dependent inhibition of dopaminergic input to the MB horizontal lobe (Krashes et al., 2009) and are, like the MB-C1 neurons, good candidates for providing a modulatory hunger signal that can, via the DANs, alter MB olfactory output. Finally, MB465C labels a contralaterally projecting, serotonin immunoreactive, deutocerebral (CSD) neuron (Aso, Hattori, et al., 2014; Dacks et al., 2009; Kent et al., 1987).

Table 5. Octopaminergic and other neuromodulatory neuron expression patterns and levels

OA denotes octopamine. Each fly line (MBxxxB) targets expression to cell types as indicated by greyscale rectangles. Black corresponds to strongest expression and light grey to weakest expression. Neuron designations are indicated on the far left. These anatomical and expression analysis were carried out by Aso et al. (Aso, Hattori, et al., 2014).

Based on work in the hawkmoth *Manduca sexta* it has been suggested that this neuron may modulate AL activity based on mechanosensory stimuli from air movement, and therefore may gate olfactory input to the MB in situations when olfaction is required. Upon synaptic silencing MB465C did not exhibit any phenotypes significantly different from the control (Figure 21).

3.2.6 Summary of screening data

From the screening data it is possible to postulate relationships between the behavioural phenotypes observed in response to attractive and aversive single odours and corresponding phenotypes in response to the mixed conflict stimulus in the context of starvation. However, it is not possible from the screening data alone to establish the specific relationships between the phenotypes observed for the MBONs and DANs and whether they are representative of olfactory conflict resolution. It generally seems that the MB vertical lobe innervating neurons (α, and α ' KCs, PPL1 DANs, and vertical lobe MBONs) generate more phenotypes in response to vinegar upon silencing than they do to CO_2 (Table 6).

		CO_2	Vinegar
KCs	γ	-	+
	α'/β'	+	+
	α/β	+	+
MBONs	Horizontal lobe (γ + β + β' + β' KCs)	+	-
	Vertical lobe (α + α' KCs)	-	+
DANs	PAM (Horizontal lobe)	+	+
	PPL1 (Vertical lobe)	-	+

Table 6. Summary of dominant phenotypes per MB anatomy

Non-quantitative summary of phenotypes across all lines representing various subsections of MB anatomy. (-) represents the absence of a strong phenotype and (+) represents the presence of significant or non-significant phenotypes.

Blockade of horizontal lobe innervating neurons (β, β', and γ KCs, PAM DANs, and horizontal lobe MBONs) causes phenotypes in response to both vinegar and CO_2. Considering the occurrence of vinegar phenotypes upon blockade of γ KCs (horizontal lobe) but not horizontal lobe MBONs, it is possible the horizontal lobe vinegar attraction phenotypes are caused by disruption of the γ lobe. This latter observation fits with the KC silencing screening data in which the horizontal lobe specific γ KCs give strong vinegar but not CO_2 phenotypes, while the α/β and α'/β' KCs gave phenotypes for both stimuli. It is difficult to establish from these data alone what role the horizontal lobe may play in processing vinegar attraction. The horizontal lobe β'2 region innervating MBONs exhibited only weak, non-significant, reductions in vinegar attraction, while some of the PAM neurons innervating the same regions as α'/β' KCs displayed significant reductions in vinegar attraction despite not innervating the γ lobe (e.g., PAM-β'2a, MB087C) (Figure 17B, green bars). These screening data allow me to 1) Identify the horizontal lobe β'2 region as a candidate for representing the aversive odour CO_2 (Figure 22), and 2) identify the horizontal lobe β'2 region MBONs as good candidates for driving CO_2 aversive behaviour (Figure 22). However, it did not identify a DAN candidate for the modulation of aversive output from the β'2 region.
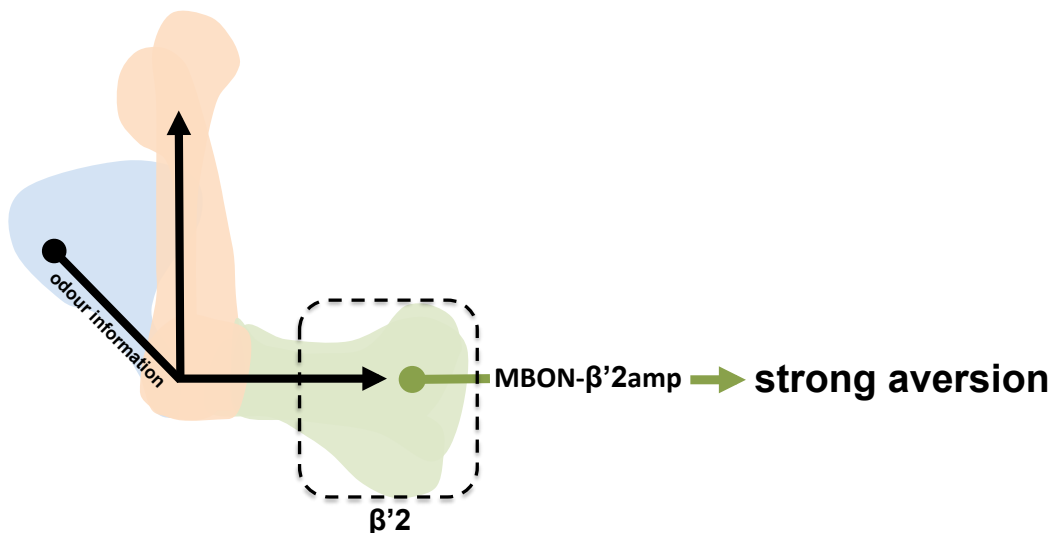
Figure 22. β'2 region MBONs dominantly required for CO_2 aversion

Behaviour screening data implicates MBONs innervating the β'2 region of the MB horizontal lobe (dashed line) as being specifically required for mediating CO_2 aversion behaviour. The lines identified in the screen innervate across all anatomical β'2 subregions (a, m, and p).

3.3 β'2 MBON characterisation

3.3.1 β'2 region MBONs are necessary for CO$_2$ aversion

The β'2 region of the medial tip of the MB horizontal lobe was identified during the screen as being a candidate region for the processing of CO$_2$ aversion (Figure 22). Due to experimental constraints not all necessary controls were performed during screening, therefore it was necessary to confirm important hits from the screen alongside the
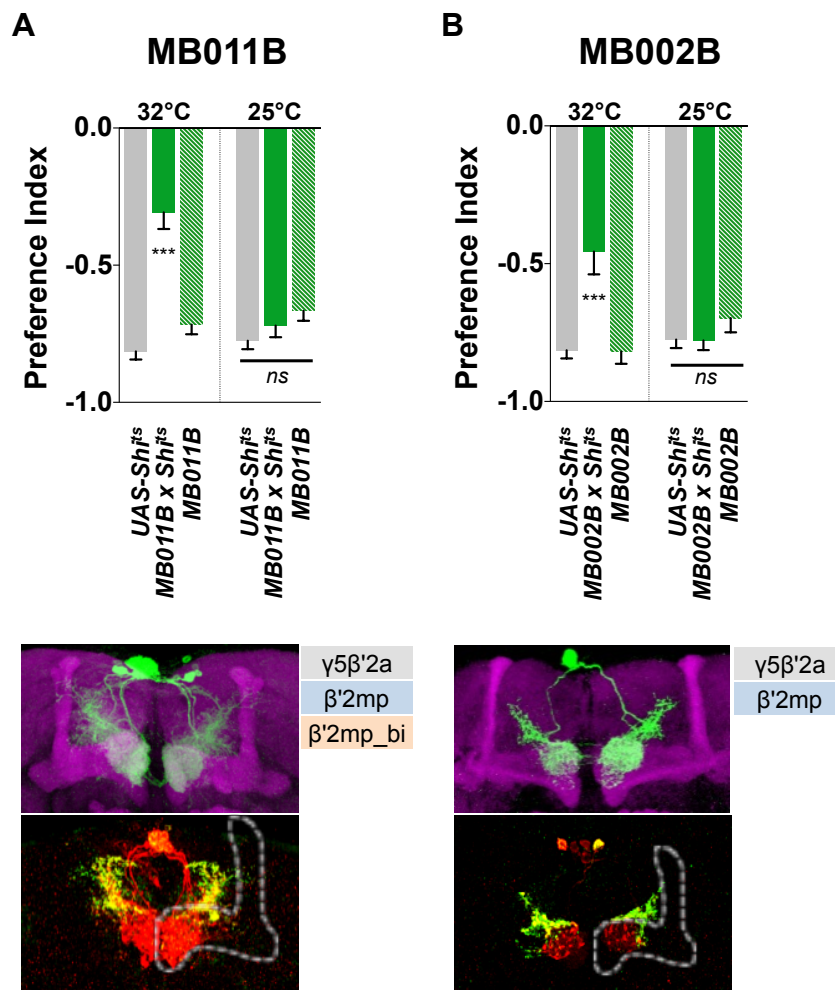
Figure 23. Confirmation of β'2 MBON hits

(A) Top figure shows reduction of CO$_2$ aversion in T-maze assay upon synaptic silencing of MBONs in line MB011B. Top anatomy panel represents MBON morphology through expression of *UAS-mCD8-GFP* (green). Neuropil stained with nc82 (magenta). Bottom anatomy panel shows presynaptic boutons (green), and postsynaptic regions (red) through the expression of *UAS-Synaptotagmin* and *UAS-DenMark* respectively. **(B)** Represents the same as in **(A)** except for line MB002B. PIs are averaged across 10-12n; +/- SEM. P-values calculated via one-way ANOVA and Bonferroni multiple comparison post-hoc test, ns p>0.05, *p<0.05, **p<0.01, ***p<0.001.

appropriate genetic and procedural controls. To this end MB011B and MB002B were selected as representative of β'2 MBONs to confirm the screen data (Figure 23). MB011B targets three neurons, MBON-β'2mp_bilateral, MBON-β'2mp, and MBON-γ5β'2a. MB002B targets only MBON-β'2mp, and MBON-γ5β'2a (Table 3). Both lines demonstrated strongly reduced CO_2 avoidance responses compared to both genetic and low-temperature (permissive) controls. In addition to the behavioural experiments anatomical analysis was conducted using the same Split-GAL4 lines to drive expression of the reporters mCD8-GFP and DenMark / Synaptotagmin to visualise the polarity of the MBONs (Figure 23). The MBONs have dendritic fields within the MB lobes and send axonal projections into the SMP. MB011B and MB002B are redundant for one another and both innervate the entirety of the β'2 region.
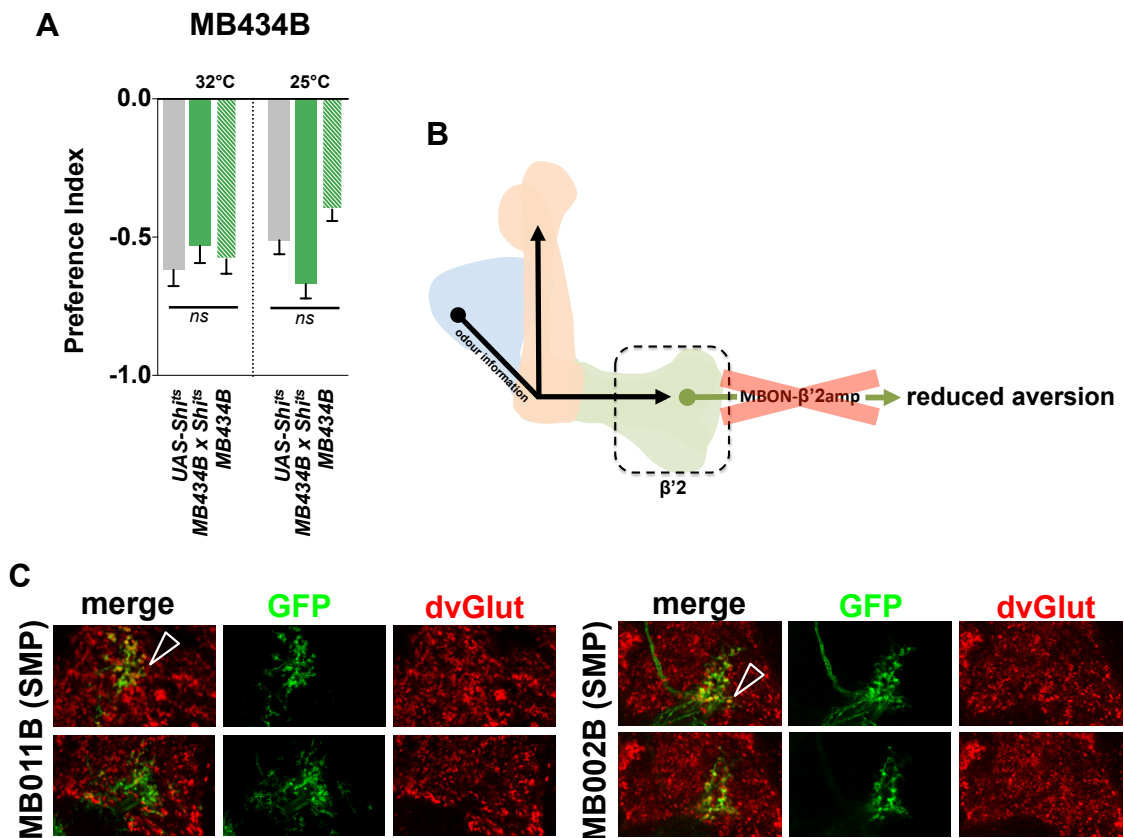
Figure 24. Odour specificity for different horizontal lobe MBONs

(A) Neurons targeted by line MB434B not necessary for CO_2 aversion. **(B)** Schematic of the MB depicting the β'2 region MBONs necessary for CO_2 aversion. **(C)** *Drosophila* vesicular glutamate transporter (dvGlut, red) stainings identify MBONs labelled by MB011B and MB002B (green) as glutamatergic neurons (arrow heads). PIs are averaged across 10-12n; +/- SEM. P-values calculated via one-way ANOVA and Bonferroni multiple comparison post-hoc test, ns p>0.05, *p<0.05, **p<0.01, ***p<0.001.

To ensure that these MBONs were indeed excitatory both lines were used to drive expression of mCD8-GFP and were stained using anti-dvGlut antibody. When imaged, the GFP signal and anti-dvGlut colocalised to the output synapses of the MBONs, confirming them as glutamatergic (Figure 24 C).

Taken together with the screening data these behavioural and anatomical experiments convincingly establish the β'2 region as part of a pathway necessary for outputting aversive olfactory information from the MB (Figure 24B). However, the screen also identified other possible MB regions that may be involved in processing CO_2 avoidance. Upon synaptic silencing line MB434B, which labels two MBONs (MBON-γ4>γ1 and MBON-β1> α), appeared to elicit a reduction in CO_2 aversion. To test whether these neurons were indeed involved in processing CO_2 aversion I performed confirmation experiments alongside appropriate controls and with an increased sample size. Upon re-testing the line MB434B did not exhibit a reduced CO_2 aversion (Figure 24A), thus eliminating this neuron as necessary for CO_2 aversion.
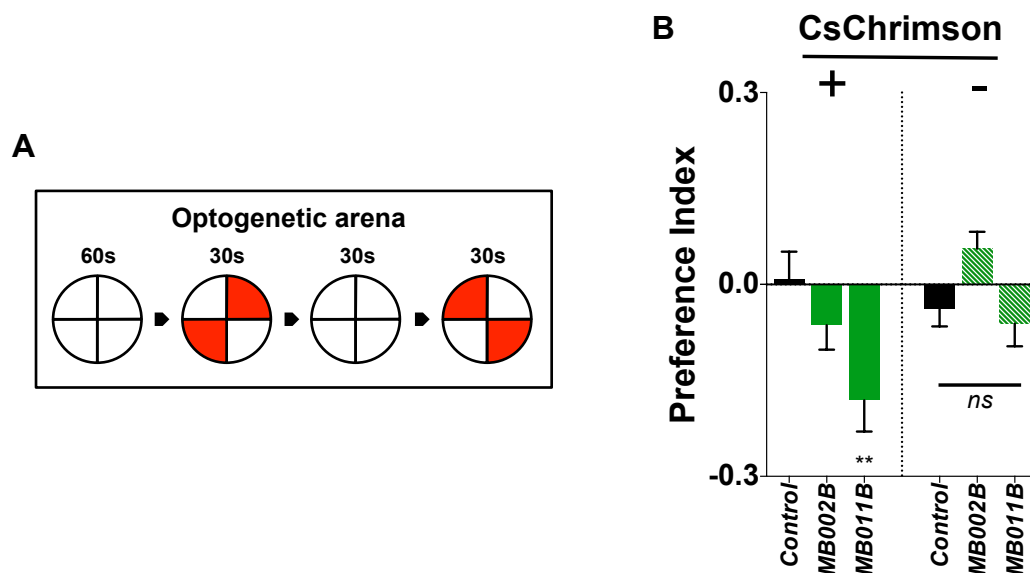
Figure 25. β'2 region MBONs are sufficient to drive aversion behaviour

(A) Schematic representation of optogenetic experimental protocol and arena. **(B)** Optogenetic arena avoidance light avoidance responses of MBON lines crossed to *UAS*-CSChrimson (left bars) or *w-* (right bars). The control genotype is the empty driver, *pBDPGAL4U* in attP2 / *UAS-CSChrimson* or *w-*. PIs are averaged across 10-12n; +/- SEM. P-values calculated via one-way ANOVA and Bonferroni multiple comparison post-hoc test, ns p>0.05, *p<0.05, **p<0.01.

3.3.2 β'2 region MBONs are sufficient to drive aversive behaviour

It is increasingly apparent that the MB is near the apex of the sensory-motor loop. In a recent study it was suggested that the precise point at which processed sensory information can be said to drive motor output is the KC to MBON synapse (Hige, Aso, Rubin, et al., 2015). To test whether the β'2 region MBONs are sufficient to drive aversive behaviours we used a custom-built behavioural arena in which flies are able to freely move in response to optogenetic stimulation via red LEDs positioned under the arena floor (Figure 8 and Figure 25A). Starved flies expressing CSChrimson, a red-shifted channel rhodopsin, in the β'2 region MBONs consistently avoided the red light (Figure 25B).

When taken together with the silencing data it is apparent that these MBONs are both necessary and sufficient to drive CO_2 aversive behaviour. That these MBONs are sufficient to drive aversion in starved flies indicates that they are perhaps directly upstream of premotor circuits, or at least provide a behavioural valence to subsequent downstream processing.

3.4 β'2 PAM neuron characterisation

3.4.1 β'2 region innervating PAM DANs are sufficient to reduce CO_2 aversion

The data described above establishes the β'2 region innervating MBONs as the neurons responsible for driving MB (starvation) dependent CO_2 aversion. The obvious candidates for representing the other half of the conflict stimulus (vinegar), and providing inhibition to the aversive MB output, are the neuromodulatory dopaminergic PAM neurons also innervating the horizontal lobe (Table 4, red box). However, as mentioned previously, no clear candidates were identified in the primary screen so I decided to retest two of the sparser lines innervating the β'2 region. I searched the Split-GAL4 library for candidate lines and found two that between them provided complete coverage of the β'2 region. MB109B labels PAM-β'2a, and MB056B (not included in the original screen) labels PAM-β'2m, and PAM β'2p (Table 4). I confirmed that these neurons were indeed dopaminergic via staining for tyrosine hydroxylase (TH) (Figure 27A). From a superficial assessment of their anatomy (Figure 26, top anatomy panels), and polarity (Figure 26,

bottom anatomy panels) it appears that the axonal arborisations of these neurons in the MB lobes overlap with the dendritic fields of the β'2 MBONs. In the context of a neural circuit it appears these PAM neurons receive input from the SMP region of the fly brain, between the MB vertical lobes, and inputs it to compartments of the MB horizontal lobes. Various studies have suggested that dopaminergic neurons innervating the MB lobes modulate the KC-MBON synapse via the release of dopamine. However, the precise form of the modulation is not well understood. It is also not known which neuronal populations provide input to the DANs. To test whether these β'2 innervating PAM neurons are
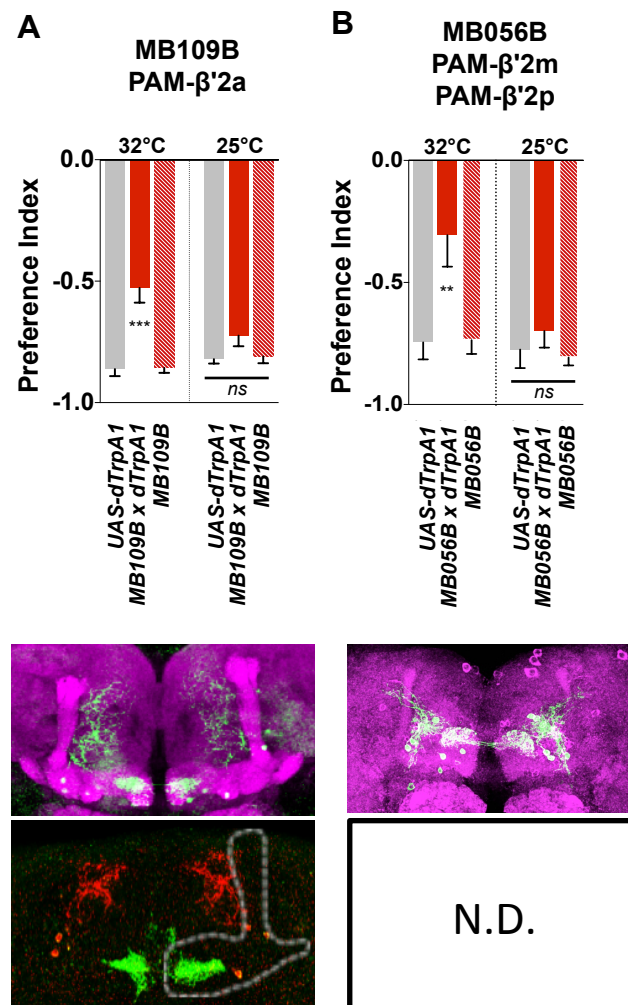
Figure 26. β'2 region innervating PAM neuron activation phenotypes and anatomy

(A) Top figure shows reduction of CO_2 aversion in T-maze assay upon neuronal activation of PAMs in line MB109B. Top anatomy panel represents MBON morphology through expression of *UAS-mCD8-GFP* (green). Neuropil stained with nc82 (magenta). Bottom anatomy panel shows presynaptic boutons (green), and postsynaptic regions (red) through the expression of *UAS-Synaptotagmin* and *UAS-DenMark* respectively. **(B)** Represents the same as in **(A)** except for line MB056B. PIs are averaged across 10-12n; +/- SEM. P-values calculated via one-way ANOVA and Bonferroni multiple comparison post-hoc test, ns p>0.05, *p<0.05, **p<0.01, ***p<0.001.

66

sufficient to suppress CO_2 aversion behaviour I used the lines MB109B and MB056B to drive the expression of UAS-dTrpA1. Testing at 32°C strongly reduced CO_2 aversion (Figure 26), suggesting that whatever this dopaminergic signal represents is sufficient to inhibit the MBON aversive output from the MB horizontal lobe. However, this observation is only meaningful if the β'2 PAMs respond to vinegar and not CO_2. To this end I collaborated with Dr. Siju Purayil who used in vivo two-photon calcium imaging (Figure 9) to measure the activity of these neurons in response to stimulation with vinegar and CO_2. The Split-GAL4 line MB109B (Table 4) was used to drive expression of the calcium sensor GCaMP6f in PAM-β'2a with imaging performed at the level of the MB lobe (Figure 27B). Upon stimulation with 1% vinegar a significant increase in fluorescence was observed compared to stimulation with humidified air (Figure 27C). Importantly, the same neuron does not respond upon stimulation with CO_2 (Figure 27D), indicating that it may specifically confer appetitive contextual information to the MB aversive output region in order to dampen an innate aversive behaviour. It was also observed that the β'2 PAM neurons responded more strongly when the flies were starved than when fed (Figure 27C), indicating that starvation information may modulate PAM
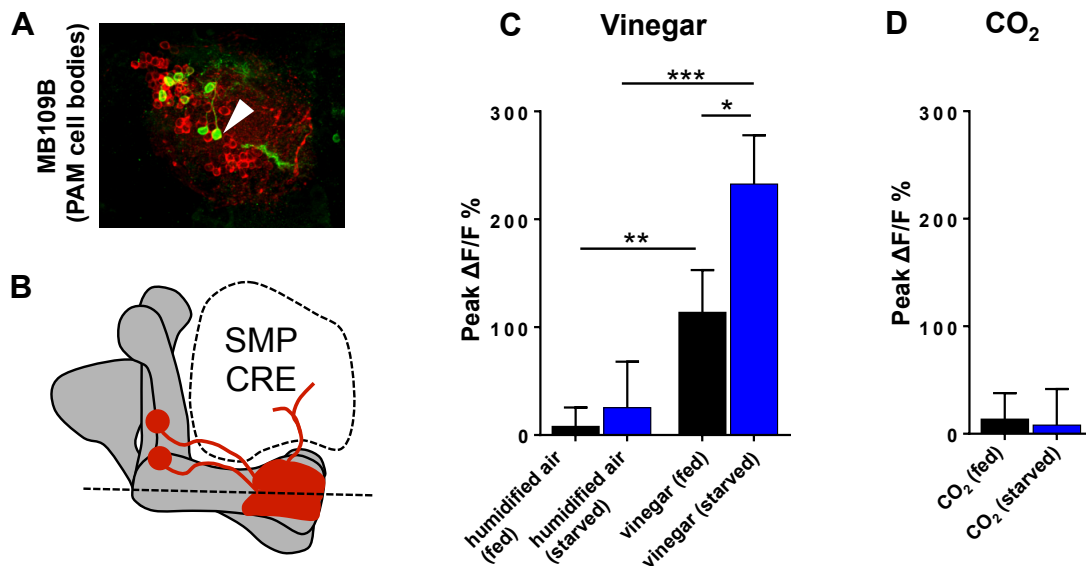
Figure 27. β'2 PAM neuron responds to vinegar but not CO_2

(A) MB109B-Split-GAL4 driving expression of mCD8GFP (green), anti-TH antibody (red) stains MB109B labelled cell bodies (yellow, arrow head). **(B)** Schematic representation of PAM-β'2a MB lobe innervation pattern. **(C)** Peak MB109B-GCaMP6f intensity change after stimulation with vinegar in starved and fed flies. **(D)** Fluorescence intensity change after stimulation with CO_2 in fed and starved flies. 10n; +/- SEM. P-values calculated via one-way ANOVA and Bonferroni multiple comparison post-hoc test, ns $p>0.05$, *$p<0.05$, **$p<0.01$, ***$p<0.001$. p-values calculated via paired Mann Whitney or Wilcoxon matched-pair single rank test. Calcium imaging experiments performed by Siju Purayil, stainings by Anja Friedrich.

neuron activity somewhere upstream of their input to the MB. PAM neurons are known to convey diverse sensory information from multiple sensory modalities to the MB in order to facilitate associative learning (Krashes et al., 2009; S. Lin et al., 2014; Vogt et al., 2014). To establish whether β'2 innervating PAM neurons specifically represent attractive odours the responses of PAM-β'2a to a small panel of attractive and appetitive odours were tested, including acetoin acetate, an appetitive odour produced during yeast fermentation, isoamyl acetate, an appetitive banana associated odour, and benzaldehyde, an odour aversive to *Drosophila*. Stimulation with acetoin acetate, but not isoamyl acetate elicited a fluorescence increase in PAM-β'2a suggesting PAM neurons may be tuned to specific food related odours (Figure 28). It was also observed that the acetoin acetate response was larger in starved flies than it was in fed flies, providing further evidence that starvation state may impinge on PAM neuron activity (Figure 28). Interestingly the neurons did not respond to the aversive odour benzyladehyde, which may suggest that PAM-β'2a is specific for appetitive odours and not aversive (Figure 28). If this were shown to be true for all PAM neurons innervating MB regions outputting aversive information it would represent a satisfying functionally and ecologically meaningful asymmetry in the relationship between MB lobe input and output neurons.
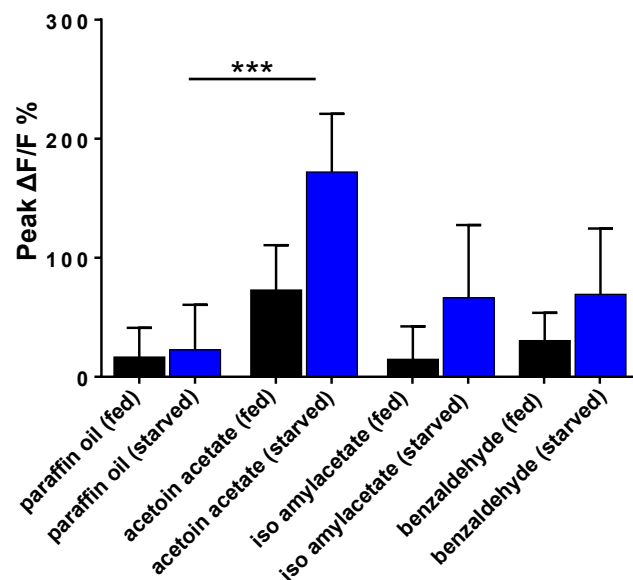
Figure 28. β'2 PAM respond selectively to food odours and not to aversive odours

Peak MB109B-GCaMP6f intensity change after stimulation of starved and fed flies with solvent paraffin oil, acetoin acetate, isoamyl acetate, and benzaldehyde. 10n; +/- SEM. ns p>0.05, *p<0.05, **p<0.01, ***p<0.001. p-values calculated via paired Mann Whitney or Wilcoxon matched-pair single rank test. Experiments performed by Siju Purayil.

3.5 β'2 region MBONs and PAMs are functionally connected

3.5.1 β'2 region innervating PAMs and MBONs are anatomically colocalised and synaptically connected

Taken together, the data presented so far specifically implicate MBONs innervating the medial β'2 tip of the MB horizontal lobe as necessary and sufficient for driving CO_2 aversive behaviour in starved flies. Additionally, a vinegar responsive PAM cluster DAN innervates the same MB region and upon activation causes a reduction in CO_2 aversion. It is important to establish that these two populations of neurons are indeed synaptically connected. In order to visualise both populations of neurons in the same brain double labelling experiments were performed. The driver components of two expression systems labelling the PAM-β'2a neurons and β'2 MBONs, MB109B-Split-GAL4 and R14C08-LexAp65 respectively were genetically inserted into a single fly line and then
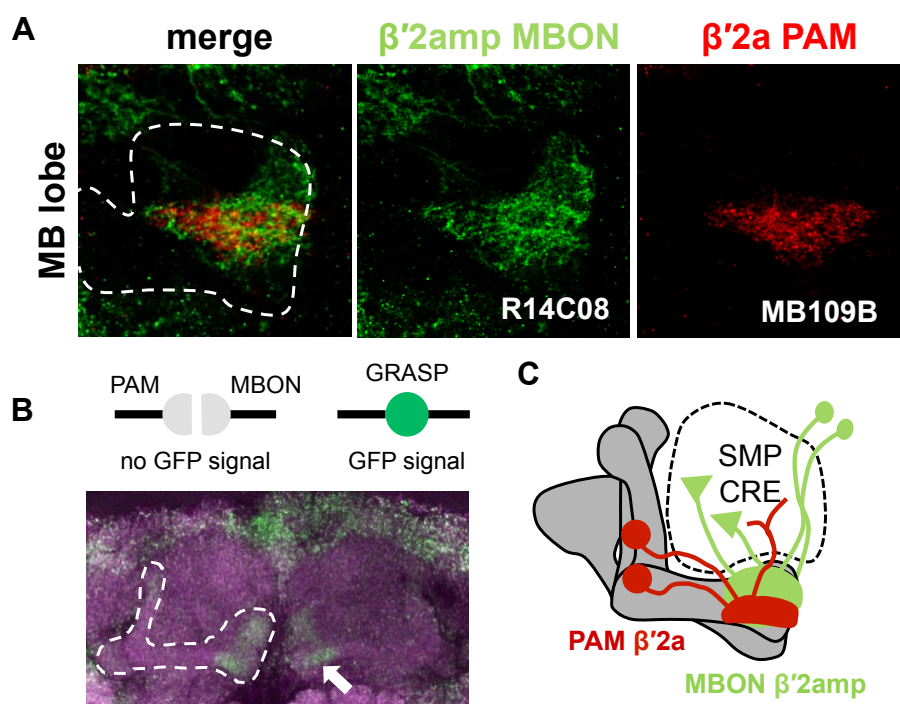
Figure 29. β'2 innervating PAM and MBONs show overlapping innervation and synaptic connectivity

(A) β'2 MBONs labelled by R14C08-LexAp65 driving expression of LexAop2-mCD8GFP (green). β'2a PAM neuron labelled by MB109B-Split-GAL4 driving expression of 10UAS-IVS-mCD8RFP (red). The dotted line represents the MB lobe. **(B)** GRASP using R14C08 to label β'2 MBONs and MB109B to label β'2a PAM neurons. Large arrow indicates reconstituted GFP signal at level of β'2 MB lobe region (green). Brain neuropil stained with nc82 (magenta). The dotted line represents the MB lobe. **(C)** Schematic representation of PAM and MBON innervation in β'2 MB region. Staining and imaging performed by Anja Friedrich.

used which was then used to drive the expression of LexAop2-mCD8GFP (green) and 10xUAS-IVS-mCD8RFP (red) in a single fly. β'2 MBONs and PAMs display overlapping innervation in the MB horizontal lobe indicating the possibility of connectivity (Figure 29A). To strengthen the evidence for connectivity the 'GFP reconstitution across synaptic partners' (GRASP) method was used. The same driver lines as in the double labelling experiments were used to drive expression of two halves of the split-GFP in order to establish possible connectivity between the PAMs and MBONs (Figure 29C). A strong signal was observed at the level of the horizontal MB lobes at the innervation sites of the two neuron types (Figure 29B). As neurons often come into close contact, a GRASP signal does not guarantee synaptic connectivity, but taken together these two lines of evidence provide a strong case for connectivity between β'2 MBONs and PAMs.

3.5.2 PAMs and MBONs are functionally connected

Despite the evidence for synaptic connectivity provided by the double labelling and GRASP data, the possibility remains that the two populations of neurons are not functionally connected. To clarify whether β'2 MBONs and PAMs are indeed synaptic partners calcium imaging experiments were performed in collaboration with Dr. Siju
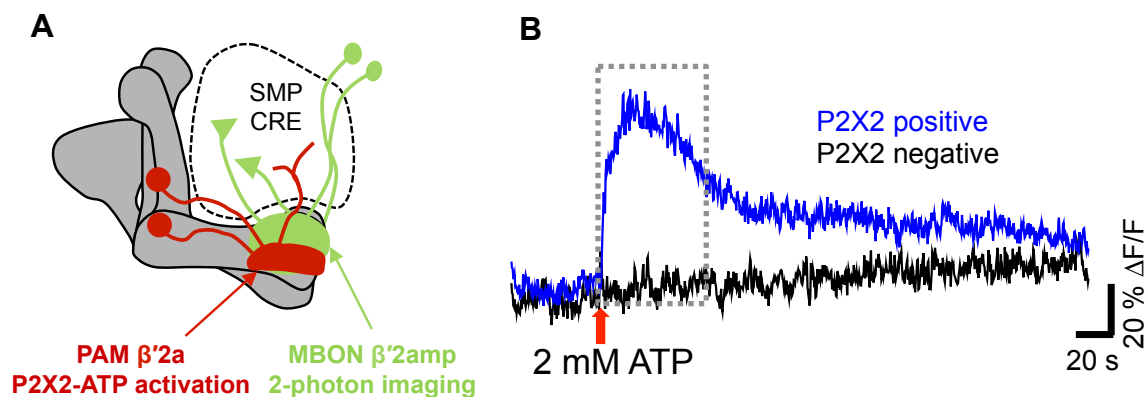
Figure 30. β'2 innervating PAM and MBONs show functional synaptic connectivity

 (A) Schematic representation of P2X2 experiment. β'2 MBONs labelled by R14C08-LexAp65 driving expression of LexAop2-GcAMP6f (green). β'2a PAM neuron labelled by MB109B-Split-GAL4 driving expression of UAS-P2X2 (red). **(B)** The blue curve represents the fluorescence response of GcAMP6f in the MBONs upon bath application of ATP. The black curve is a P2X2 negative control in which P2X2 is not expressed in the PAM neurons. Experiments performed by Siju Purayil.

Purayil. Transgenic flies were generated in which *UAS-P2X2*, an ATP responsive ion channel, was expressed under the control of the broad R58E02 PAM neuron labelling promoter, while expression of the calcium sensor GcAMP6f was driven in β'2 region MBONs using the MB011C promoter (Figure 30A). 2mM ATP was bath applied to the fly brain during the experiment and evoked activity in the MBONs observed via changes in the GcAMP6f fluorescence. Upon ATP application a strong increase in MBON activity was observed (Figure 30B) providing conclusive evidence of direct or indirect synaptic connectivity between the PAM neurons and MBONs innervating the β'2 region.

Despite these data providing convincing evidence of functional connectivity between PAM neuromodulatory dopaminergic MB input neurons and MB output neurons, we would have expected to see a suppression of MBON activity to below baseline. The data so far suggests that the vinegar responsive PAM neurons suppress the innate aversive output of the β'2 region MBONs. However, the P2X2 data demonstrates an increase in MBON activity upon artificial stimulation of the PAM neurons. Either this is an artefact of the artificial activation, or we provided only a partial input to the circuit required for suppression. The P2X2 experiments we performed were done so in the absence of an olfactory stimulus such as CO_2, which means the MBONs were presumably less active or inactive prior to stimulation of the PAMs via ATP application. It is possible that if the MBONs had received aversive olfactory input from the α'/β' KCs then the simultaneous activation of PAM neurons would result in a reduction in MBON activity. Were this hypothesis correct, it would reveal part of the mechanism by which olfactory information is transformed into motor output by these three populations of neurons (KCs, DANs, and MBONs), and would give some idea of the organisation of the synaptic connectivity between them.

3.6 The role of β'2 PAM neurons in modulating MBONs

3.6.1 PAM cluster neuron activation is sufficient to drive attraction behaviour

The β'2 PAM neuron response to appetitive vinegar stimulus and sufficiency to reduce CO_2 aversion (Figure 31B) predict that these neurons should be sufficient to drive the attractive behaviour observed in starved wild type flies as they overcome their CO_2

aversion to approach vinegar. To test this hypothesis we crossed four sparse Split-GAL4 lines (MB056B, MB047B, MB109B, and MB316B) labelling β'2 PAM neurons and two broad Split-GAL4 lines labelling populations of PAM neurons with innervation across the horizontal lobe (MB042B and MB040B) (Table 4), to *UAS-CSChrimson* and tested progeny for their optogenetic behavioural response. In support of our hypothesis all tested genotypes exhibited attraction behaviour to the illuminated quadrants of the arena (Figure 31A). Interestingly, there was no divergence in the behavioural valence elicited by the various lines. When taken together with the horizontal lobe MBON data presented here and by Aso et al. (Aso, Sitaraman, et al., 2014) an inhibitory role for DANs presents itself as the most likely method by which neuromodulation occurs at the KC / MBON synapse. Indeed, a recent study has demonstrated electrophysiologically that dopaminergic input to MB compartments is sufficient to suppress MBON response to KC odour representation (Hige, Aso, Modi, et al., 2015). Hige et al. focussed on regions of the MB best know for facilitating appetitive learning and so didn't specifically study the β'2 region.
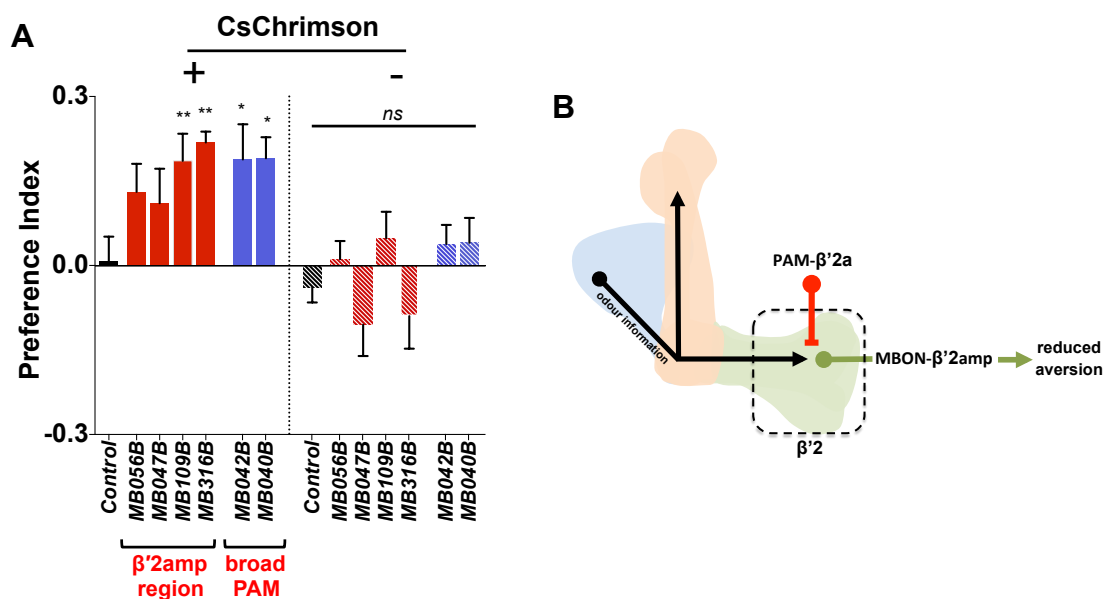
Figure 31. β'2 innervating PAM neuron activation is sufficient to drive behavioural attraction

(A) Optogenetic attraction of Split-GAL4 lines specifically labelling PAM neurons innervating the β'2 MB region (red bars) and broader populations of horizontal lobe innervating PAM neurons (blue bars) drive expression of *UAS-CSChrimson* (left bars) or *w-* (right bars). All genotypes were attracted to the illuminated area quadrants. The control genotype is the empty driver, *pBDPGAL4U* in attP2 / *UAS-CSChrimson* or *w-*. **(B)** Schematic representation of PAM DAN impingement on KC-MBON synapse. For line anatomy see Table 4. PIs are averaged across 10-12n; +/- SEM. P-values calculated via one-way ANOVA and Bonferroni multiple comparison post-hoc test, ns $p > 0.05$, $*p < 0.05$, $**p < 0.01$.

However given our findings, it is likely the mechanism is the same, although perhaps with a differing level of PAM activation required to supress MBON output.

3.6.2 Vinegar odour is sufficient to suppress β'2 MBON CO_2 response

Starved wild type flies are motivated to overcome their aversion to CO_2 in order to approach an appetitive odour source such as vinegar. I have demonstrated that β'2 MBONs are necessary and sufficient for CO_2 avoidance in starved flies, and that functionally connected dopaminergic neurons of the PAM cluster respond strongly to vinegar but not CO_2. The same β'2 innervating PAM neurons are sufficient to strongly reduce CO_2 aversion and drive behavioural attraction (Figures 26 and 31B). To clearly show that MBON aversive output is suppressed in the context of a conflicting appetitive odour we expressed the calcium sensor GcAMP6f in β'2 MBONs under the control of the MB011B-Split-GAL4 driver, and stimulated flies with CO_2, vinegar, and a mixture of CO_2 and vinegar (conflict stimulus) (Figure 32A). The β'2 MBONs responded strongly to
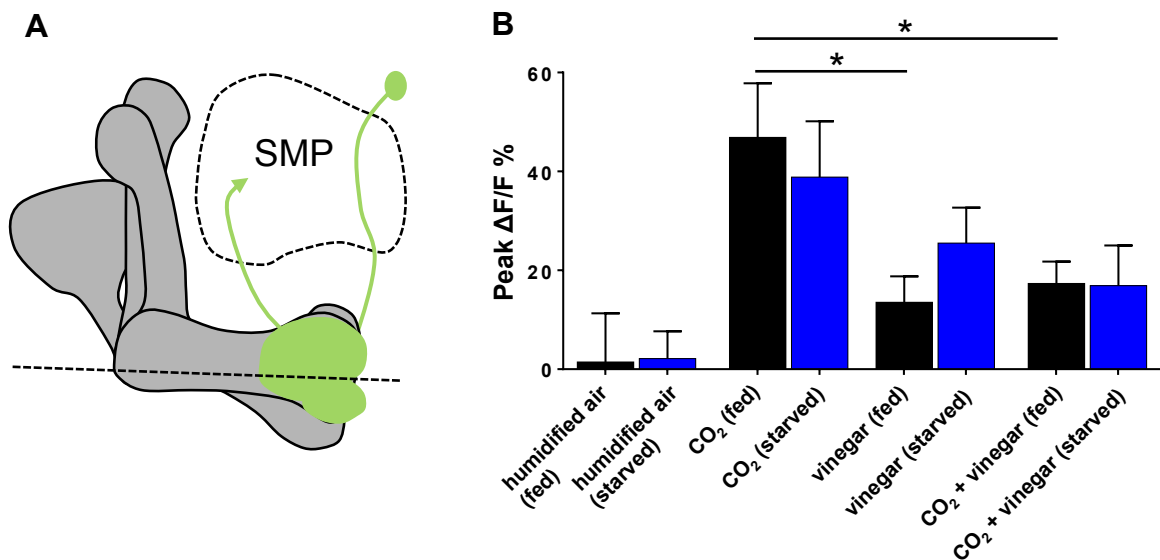
Figure 32. Vinegar reduces aversive β'2 MBON CO_2 output

(A) Schematic representation of β'2 MBONs and experimental imaging plane (dotted line). β'2 MBONs (green) labelled by MB011B-Split-GAL4 driving expression of UAS-GcAMP6f. **(B)** Starved and fed flies were stimulated with humidified air (control), CO_2, vinegar, and conflict odour mix (CO_2 + vinegar). β'2 MBONs respond strongly to CO_2 alone. The Conflict stimulus evokes the same level of MBON response as vinegar alone. 10n; +/- SEM. ns $p>0.05$, *$p<0.05$, **$p<0.01$, ***$p<0.001$. p-values calculated via paired students T-test. Experiments performed by Dr. Siju Purayil.

stimulation with CO_2 alone. They also responded to vinegar alone, albeit with a significant reduction compared to the CO_2 elicited activity (Figure 32B). Importantly, when stimulated with the conflict stimulus, the evoked activity was of the same magnitude as when the fly was stimulated with vinegar alone (Figure 32B). This clearly indicates that the CO_2 induced activity is suppressed in the context of vinegar. Interestingly, in the context of these experiments starvation state elicited no discernable effect on the MBON representation of these odours. Responses to both CO_2 and vinegar were observed at similar levels regardless of starvation state (Figure 32B). Given that the findings of Bräcker et al. (Bräcker et al., 2013) indicate that the KC representation of CO_2 is starvation dependent, it is possible that these MBONs receive CO_2 input from another population of neurons. Taken together the data described thus far and in combination with the findings presented by Bräcker et al., represent a convincing model for how a fly is able to process coincident conflicting stimuli and execute a behavioural program based on nutritional requirements. The precise connectivity between the KCs and MBONs is not well understood. Nor is it known how the DANs modulate the functional relationship between these neurons. There is however a great deal of work currently being conducted to elucidate the form and physiology of these synapses, so an answer to these questions is likely imminent.

3.6.3 β'2 PAM neurons are not sufficient for CO_2 memory formation

Much of the description of MB physiology and function is focussed on its role in learning and memory. β'2 MBONs and PAM have themselves been implicated in memory formation and retrieval (Owald et al., 2015a). However, our data and those from other studies have identified a possible role for the MB in non-learning related instantaneous modulation of behaviour. Therefore we were motivated to test whether 1) vinegar attraction can be used as an unconditioned stimulus (US) to condition a reduction in CO_2 aversion (Figure 33A), and 2) whether pairing of dTrpA1 activation of the vinegar responsive PAM-β'2a labelled by line MB109B with CO_2 exposure is sufficient to artificially condition a lasting (3 minute) reduction in CO_2 aversion (Figure 33C). It was not possible to use innate vinegar attraction in starved flies as a US to condition a lasting reduction in CO_2 (CS) avoidance (Figure 33B). Nevertheless, to be sure that the MB β'2 local circuit was not sufficient to facilitate memory formation we paired artificial

74

activation of PAM-β'2a with 2 minutes of CO_2 exposure and tested flies' CO_2 avoidance response 3 minutes after the end of conditioning. No reduction in CO_2 aversion was observed indicating that these neurons are not sufficient to support memory formation (Figure 33D). In light of these data it is possible that the β'2 region of the MB is dedicated to modulating innate behaviours. That the MB might subserve dedicated functions other than learning is an interesting finding that demands a re-evaluation of the mechanisms by which the MB processes sensory information and drives behaviour. In particular it would be interesting to better understand how learned associations and immediately processed sensory information interact, and which one is prioritised.
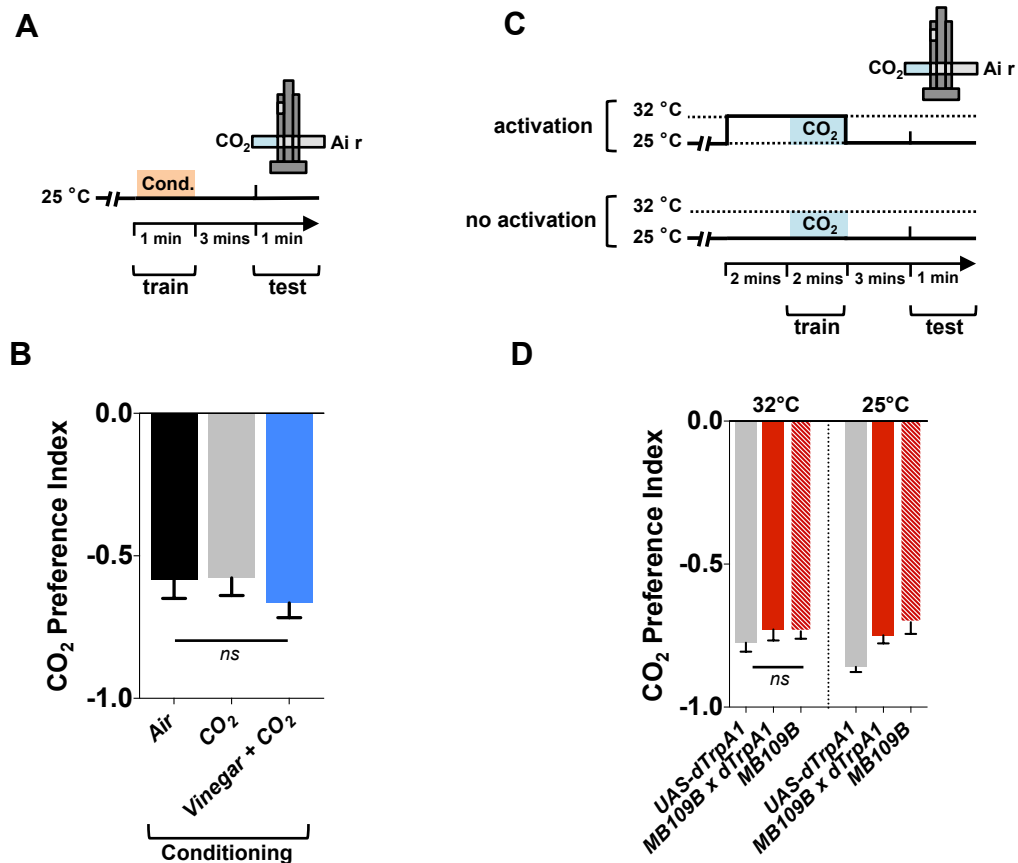
Figure 33. CO_2 avoidance cannot be conditioned

(A) Schematic representation of CO_2 / vinegar T-maze conditioning and testing protocol in wild type flies (CantonS). (B) CantonS flies conditioned and tested using the protocol described in (A). (C) Schematic representation of conditioning and testing protocol whereby CO_2 exposure is paired with dTrpA1 activation of PAM-β'2a (MB109B). (D) *MB109B; UAS-dTrpA1* flies tested using the protocol described in (C). 10-12n; +/- SEM. ns p>0.05, *p<0.05, **p<0.01, ***p<0.001. p-values calculated via one-way ANOVA and the Bonferroni post-hoc test.

3.7 KC starvation dependence not strictly recapitulated in MBONs and PAMs.

The MB is not required for CO_2 aversive behaviour in fed flies. Bräcker et al., however, showed that when flies are hungry a MB dependent pathway is necessary for CO_2 aversion (Bräcker et al., 2013). This was achieved via thermogenetic silencing of subsets of MB KCs. Despite the KCs providing odour representation to the MB lobes there was the possibility of PAM / MBON local circuits still playing a role in KC independent pathways necessary for facilitating motor output from the putative LH MB independent pathway. To test this I repeated β'2 MBON silencing and PAM activation behavioural experiments in fed flies instead of starved. I expected to observe normal CO_2 avoidance in recapitulation of the data presented by Bräcker et al. Surprisingly there were reductions in avoidance upon both silencing of β'2 MBONs and activation of β'2 PAMs (Figure 34A_a – C_a), indicating that the β'2 MB compartment performs a role independent of starvation state. Importantly, the reductions in CO_2 avoidance were significantly smaller than those observed in starved flies (Figure 34A_b – C_b) , suggesting that increased hunger is still represented in the strength of MBON output.
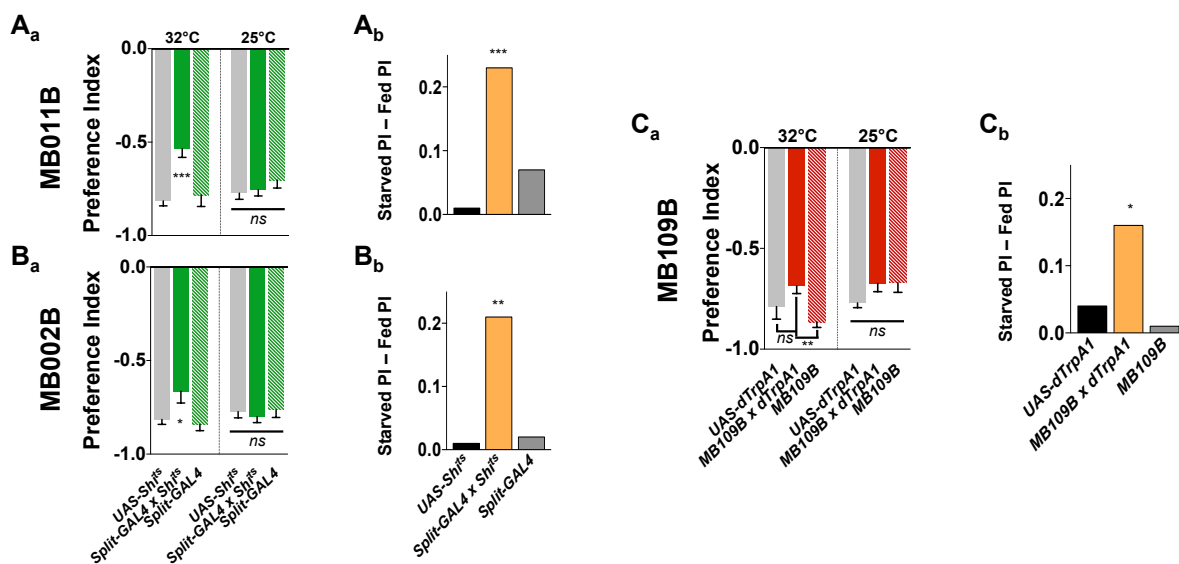
Figure 34. β'2 MBONs and PAM neurons function in fed flies

(A_a - B_a) T-maze CO_2 aversion response of β'2 MBON lines MB011B, and MB002B upon neuronal silencing. **(C_a).** T-maze CO_2 aversion response of line β'2 PAM labelling line MB109B upon neuronal silencing. **(A_b – C_b)** Plots represent the deltas calculated via the starved PIs shown in (Figure 21 and 24A) and the fed PIs shown here. Asterisks represent statistical significance calculated between the starved and fed PI for each delta. 10-12n; +/- SEM. ns $p>0.05$, *$p<0.05$, **$p<0.01$, ***$p<0.001$. p-values calculated via one-way ANOVA and the Bonferroni post-hoc test.

4.0 Discussion

4.1 Summary of results

Using a combination of new genetic tools, behavioural genetics, and two-photon calcium imaging, we have demonstrated that flies' ability to contrast two conflicting olfactory stimuli and resolve the conflict into one behavioural output, is facilitated by a local circuit of the MB horizontal lobe β'2 compartment. An olfactory response behavioural screen in which subsets of MB intrinsic and extrinsic neurons were thermogenetically silenced confirmed and built upon previous work by Bräcker et al. that implicated the MB in starvation-dependent innate CO_2 aversion (Bräcker et al., 2013). The screen confirmed that α'/β' KCs are dominantly involved in CO_2 aversion and that
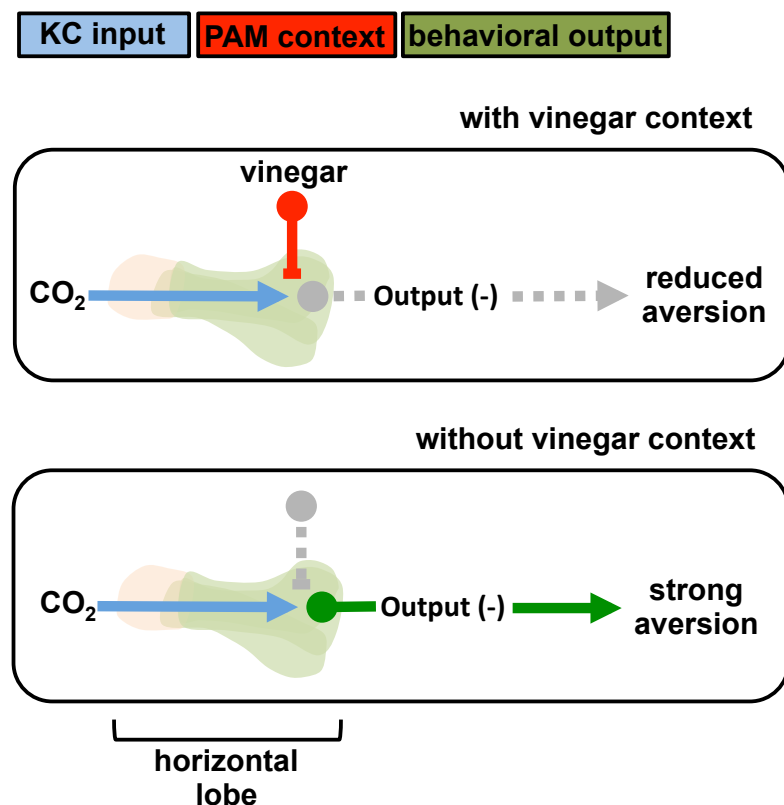
Figure 35. β'2 MBONs and PAM conflict resolution model

In response to CO_2 stimulation alone β'2 MBON are able to mediate normal CO_2 avoidance. In the context of vinegar, β'2 innervating PAM neurons inhibit the avoidance mediating MBONs, thus reducing CO_2 avoidance and allowing the fly to approach the vinegar.

downstream β'2 region MBONs are required for flies to execute aversive behavioural responses (Figure 14). Subsequent experimentation confirmed that β'2 MBONs are CO_2 responsive (Figure 32) and are necessary and sufficient for CO_2 aversion behaviour in starved flies (Figure 23 and Figure 25). This finding is consistent with recent literature that identifies a functional divergence between the MB horizontal and vertical lobes for aversive and attractive behaviour respectively (Aso, Sitaraman, et al., 2014). We also found that vinegar responsive neurons belonging to the PAM cluster subset of MB innervating DANs, which also innervate the β'2 compartment (Figure 26), are sufficient to suppress the aversive output of their canonical MBONs (Figure 26). These two populations of neurons, differentially responsive to one of a pair of conflicting odours, represent a neural substrate for internal state dependent decision-making in the fly brain. In an ecological setting these circuits allow flies to determine whether their degree of hunger is sufficient for them to approach a food source. The neural substrates described here are likely candidates for facilitating this important behaviour. This study adds significantly to a fledgling but growing literature that examines roles for the insect MB beyond learning and memory (DasGupta et al., 2014; S. Lin et al., 2014) and contributes to our growing understanding of how neural circuits subserve sensory processing and behavioural execution. Furthermore, I have identified additional types of neurons that appear to contribute to the behaviours in question. These results open the way to understanding neural circuits underpinning decision-making outside of the KC-MBON-DAN circuit.

4.2 Different KC sub-types dominantly represent vinegar and CO_2

4.2.1 Deciphering KC olfactory representation from behavioural output

In *Drosophila* the MB's ~2000 KCs represent olfactory information projected from the AL via ~200 PNs. This significant divergence in connectivity allows odours to be sparsely represented by the activity of distributed subsets of KCs (Campbell et al., 2013). Different odours activate different subsets of KCs that differ between individual flies based on developmental experience dependent synaptic plasticity (Campbell et al., 2013). All KC subsets, α/β, α'/β', and γ KCs, co-innervate MB regions with populations of MBONs driving both attractive and aversive behaviour (Aso, Sitaraman, et al., 2014),

therefore silencing of their synaptic output would be expected to produce behavioural phenotypes that depend on 1) the strength of the attraction and aversion mediating synapses (post-synaptic MBONs) being blocked relative to those that remain active, 2) the strength of the representation of a given odour by the KCs, and 3) the strength of expression of Shibire[ts1] by the driver. Given these factors, one can only make general observations of KC function, as it is difficult to assess how redundancy within the system manifests in the phenotypes and to quantify the different representation strengths of different odours.

4.2.2 KC lobes differentially represent attractive and aversive olfactory drive

Despite the limitations mentioned above some general features emerge from analysis of the KC screening data. It is clear that γ KCs don't drive CO_2 aversion behaviour (Figure 11, blue bars), but do play a role in attraction to vinegar (Figure 12, blue bars). This may be due to the relative proportions of attractive and aversive MBONs downstream of γ KCs: 2 aversive and 4 attractive (Aso, Hattori, et al., 2014). Silencing of γ KCs may therefore have a larger affect on attractive behavioural drive than it does on aversive. Both α/β and α'/β' KC populations led to some non-significant and significant reductions in CO_2 aversion and vinegar attraction upon silencing (Figures 11 and 12). This isn't surprising given that both populations also have overlapping innervation with both attractive and aversive MBONs. However, α'/β' KC blockade produced no significant reductions in vinegar attraction but did cause strong significant reductions in CO_2 aversion (Figures 11 and 12) suggesting that CO_2 aversion is driven more strongly by these KCs than is vinegar attraction. The functional basis for the differential representation of odours between KC subsets is not yet fully understood, although it has long been suggested that different KC ensembles might represent different olfactory channels based on the behavioural significance of an odour (G. C. Turner et al., 2008; Yao Yang et al., 1995), or represent information from other sensory systems. For example, recent studies have shown that certain subsets of KCs respond to visual stimuli (Vogt et al., 2014).

The data presented here indicate a possible functional divergence between attraction and aversion at the level of the KCs that may be also be represented in the tuning of MBONs post-synaptic to the KCs. When considering olfactory ecology intuition

would suggest that not all odours be represented equally by the KCs, nor that all odours be equally sufficient to drive behaviour. A recent study by Hige et al. confirms this idea (Hige, Aso, Rubin, et al., 2015). They have shown that although most MBONs are generally broadly tuned to many odours regardless of valence, the representation of CO_2 and vinegar is almost always segregated, providing labelled line like channels by which these odours can drive behaviour. This means that upon stimulation with the CO_2 and vinegar conflict stimulus, two segregated ensembles of KCs represent each of the two odours. It may also be possible that individual KCs represent odour mixes, nevertheless the data from my behavioural screen indicate that the aversive CO_2 component of the conflict mix is represented dominantly by the α'/β' KCs and that vinegar is represented mainly by γ KCs. If the two odours are essentially summed by MBONs then removing the primary channel for one of the two odours should allow the remaining odour to drive behaviour, and indeed some of my olfactory screen data supports this hypothesis. When the γ KCs are silenced flies mostly exhibited a strong avoidance of the conflict stimulus, suggesting the vinegar representation was compromised and an intact CO_2 avoidance response dominated (Figure 13, blue bars). In the case of α'/β' KC blockade the responses were harder to observe as the attraction of the control to the conflict stimulus was already very high, not leaving much room for the observation of an increased attraction. However, upon blockade of α'/β' KCs some lines exhibited an observable increase in attraction to the conflict stimulus relative to the control (MB461B and MB470B) (Figure 13, green bars), while the other lines gave behavioural responses similar to the control. Only one line exhibited a reduction in attraction (non-significant) to the stimulus.

Taken together, these data and the findings of Hige et al. (Hige, Aso, Rubin, et al., 2015) support a model of MB olfactory representation whereby odours of greater ecological significance, such as CO_2 and vinegar, elicit more robust KC representations that in turn more reliably activate specific subsets of MBONs to drive innate aversion or attraction. Despite what the behavioural data presented here indicates, there is as yet no electrophysiological or imaging data to suggest that CO_2 and vinegar are represented any differently by the KCs than other odours lacking segregated representation at the level of the MBONs. It may be that, for the purposes of CO_2 and vinegar response behaviour, the KC odour code is already sufficiently sparse, and that additional sparsening is only required at the level of MBONs. However, it is also possible that the sensation of certain ecologically important odours such as vinegar may be able to sparsen KC olfactory

representation via neurons such as MB-C1 which when blocked elicits strong reductions in vinegar attraction. It can also be said that CO_2 and vinegar are not likely integrated by the KCs, although this is hard to demonstrate behaviourally as there are no driver lines that label KCs on a single cell basis, thus it is currently difficult to block the KC representation of a single odour.

Despite these KC silencing data providing an indication of defined attraction and aversion pathways within the MB, further experimentation would be required in which a larger sample size was used along with appropriate controls and a broader panel of attractive and aversive odours. Additionally, it would be advisable to calibrate the conflict stimulus odour concentrations such that the control attraction was lower, allowing for better observation of increased attraction in behavioural experiments. Finally, these behavioural data would benefit from supporting neuronal physiological data showing the segregation more directly.

4.3 MBONs function downstream of KCs in a DAN dependent manner

4.3.1 β'2 and γ MBON silencing phenocopies α'/β' and γ KC blockade

I showed that aversion mediating MB horizontal lobe β'2 MBONs generate the strongest CO_2 avoidance phenotypes upon silencing (Figure 14, green bars, Figure 23), whereas no significant vinegar response phenotypes were observed (Figure 14, blue bars). Interestingly, attraction-mediating MBONs innervating the vertical lobe gave the strongest vinegar attraction phenotypes in response to silencing (Figure 15, blue bars). The strongest vinegar phenotypes were elicited in lines labelling MBONs innervating MB compartments also innervated by γ KCs (MB112C and MB051B), or in lines specifically or strongly labelling MBON-α2sc (MB50B and MB080C), which has been shown in other studies to be a strong driver of attractive behaviour (Aso, Sitaraman, et al., 2014; Hige, Aso, Modi, et al., 2015). These MBON data corroborate the KC data; both α'/β' KCs and β'2 MBONs elicited CO_2 avoidance phenotypes upon silencing, while γ KCs and γ innervating MBONs both elicited vinegar attraction phenotypes. These observations are also in line with the findings presented by Hige et al. (Hige, Aso, Rubin, et al., 2015), in which vinegar and CO_2 representation is segregated at the level of the MBONs. A consequence

of these findings is that if I had used attractive and aversive odours other than vinegar and CO_2 then I may have only observed odour specific behavioural phenotypes in lines labelling KCs, which maintain segregated odour representations, but not in lines labelling MBONs, which only have segregated representations for vinegar and CO_2 and not for other odours. In the same study Hige et al. (Hige, Aso, Rubin, et al., 2015) show that MBONs don't sample information from every KC fibre that passes through their anatomical compartment. It is possible therefore that a larger degree of synaptic connectivity might be found between KCs and MBONs more strongly representing CO_2 and vinegar which might contribute to their sparser representation.

4.3.2 Are naïve and learned behaviours mediated via the same MBONs?

MBONs innervating all lobes of the MB have been implicated in facilitating memory formation and recall (Aso, Sitaraman, et al., 2014). It is now clear that at least some MBONs are also responsible for processing innate behaviours (S. Lin et al., 2014) that may possibly relate to the fulfilment of important biological requirements (this thesis; Lewis et al. 2015). Taken together these findings raise questions about the extent to which these two processes are separable. My data suggests a role for β'2 MBONs in the naïve processing of the food related odours, CO_2 and vinegar, which despite being of opposing valences and eliciting strong behavioural responses, are not associable in a standard learning paradigm (Figure 33). I also showed that β'2 innervating PAM neurons are not sufficient to induce an appetitive association with CO_2 in spite of their sufficiency in instantaneous suppression of CO_2 avoidance (Figure 33s and 26). The MB is therefore necessary for the processing of at least some odours independent of the formation of learned associations. Other studies also demonstrate roles for the β'2 region in temperature response and naïve water vapour attraction in thirsty flies (S. Lin et al., 2014; Tomchik, 2013). Lin et al. found that two different DANs were responsible for naïve water attraction and for thirst motivated odour learning, providing further evidence of a possible functional segregation between MBONs responsible for outputting associative information and those responsible for outputting innate behavioural drives. However, while this segregation between naïve odour response modulation and associative learning is a possibility, is also possible that there is very little functional difference between MBONs beyond behavioural output valence, and that they simply serve as integrators of biologically relevant

82

contextual information (thirst, hunger, food and water odours) from the DANs, and raw olfactory information from the KCs. It may be the case that every MBON is capable of outputting both modulated responses in naïve flies and also learned responses. Further, it is also likely that, given the limited number of MBON output channels (32 neurons in 15 compartments), MBON outputs are a summation of both learned and naïve odour representations. This would provide the fly with the capability of affecting a behavioural response based on immediate internal state and external sensory environment, and learned responses. Any apparent segregation observed to date may simply be representative of experiments performed with a limited number of olfactory and other stimuli. Moreover, it makes sense that an immediate value-based decision may trigger a long-lasting representation in the brain, and that the same circuit elements subserve both of these functions. Whether or not a lasting association is formed may depend on the context represented by the value-encoding DANs. Such a system allows maximum flexibility of behavioural output depending on environmental and biological context.

The recent elegant study by Aso et al. (Aso, Sitaraman, et al., 2014) aimed at a broad characterisation of MBON function and focussed on learning and memory related behaviours. While they described the role of MBONs in the formation of distinct forms of learned association (e.g., visual, olfactory, gustatory), they did not account for MBONs' possible role in processing basic olfactory drives that may be a prerequisite for learning. The data presented here (Figure 33) and as part of other studies (S. Lin et al., 2014) suggest that there may be specific MBONs responsible for memory formation and MBONs responsible for processing naïve odour responses. In the Aso et al. study there were often single MBONs identified as being involved in learned responses that has also been implicated in naïve odour processing in other studies. For example, Aso et al. showed that MBONs of the β'2 region are involved in 2 hour appetitive olfactory memory, appetitive odour-ethanol intoxication memory, and visual appetitive memory (Aso, Sitaraman, et al., 2014). The same study also showed that β'2 MBONs are wake promoting when activated. They were, however, not required for thirst motivated water memory (S. Lin et al., 2014) and elicited very strong phenotypes in naïve odour avoidance (Figure 23).

Given the degree of feedback between MBONs and DANs (Cohn et al., 2015; Ichinose et al., 2015) and the experimental similarity between naïve and learned

behaviours (attraction or aversion), it may be difficult to precisely distinguish whether observed phenotypes are indeed learning phenotypes, or whether they result from evoked deficits in the fly's ability to respond naïvely to stimuli during the training, retention, and expression phases of learning behavioural paradigms. Thus, the learning phenotypes observed by Aso et al. could in principle derive from deficits in basic naïve stimulus processing observed by Lin et al. and by me. Furthermore, despite the MBON>DAN feedback demonstrated by Ichinose et al. (Ichinose et al., 2015) and Cohn et al. (Cohn et al., 2015), Hige et al. showed that learning may not be dependent on spiking activity in MBONs (Hige, Aso, Modi, et al., 2015). So the question remains whether MBONs are simply downstream conduits for the DAN modulated olfactory information, or whether they play an active role in naïve odour processing and the formation of learned associations. It is likely that both accounts are true and that MBONs are differentially recruited depending on the specific processing task at hand. It is clear that more work is required in order to fully understand the differing functional states of the MB lobe circuitry.

4.3.3 Experimental approaches to dissect naïve and learned mushroom body output neuron mediated behavioural responses

Based on our current understanding it is not easy to distinguish MB neurons or modes of function related to naïve odour processing from those related to learning. The differences between these two functions of the MBONs are likely very subtle and continuous with one another. In order to elucidate the precise roles of specific MBONs they will have to be fully behaviourally and physiologically characterised under multi-modal stimulus conditions, and in the varying biological contexts (hunger, thirst, pregnant, sick, etc.) represented by DANs. Moreover, due to redundancy and feedback within the MB circuits it may be insufficient to perform single blocks or activations of populations of neurons. Carefully designed perturbations must be made in which some components of the circuitry are silenced while others are activated. For example, it would be very informative to see the effect on naïve and learned odour behavioural responses while the entire ensemble of either aversion mediating or attraction mediating MBONs are blocked while the remaining MBONs are artificially activated. It would be ideal for this simultaneous silencing and activation to be carried out on every combination permutation of pairs and

ensembles of MBONs. Under such perturbation conditions it might be possible to expose the how the state of the DAN-KC synapses (e.g. learning biased or naïve) and the artificial perturbations combine to drive the eventual behavioural output. In order for such an experiment to be meaningful the odour tuning of individual MBONs would have to be known prior to perturbation so that a naïve response can be distinguished from a learned response. Such an experiment would build significantly on my MBON activation data (Figure 25) and the findings of Aso et al. (Aso, Sitaraman, et al., 2014) in which it was demonstrated that activation of horizontal lobe MBONs drive aversion and vertical lobe MBONs drive attraction, and that when both aversive and attractive MBONs are activated the behavioural response falls somewhere between the responses upon single MBON activation, thus indicating summation of outputs downstream of the MBONs.

Experiments such as these would allow the highly detailed dissection of relationships between pairs and groups of neurons, and could reveal a possible segregation between naïve and learned behavioural output between different MBON populations. Alternatively it might be revealed that naïve and learned output is mediated across all MBONs but one or the other dominates during different internal and external sensory contexts and biological states. It may also be necessary to take a similar approach with DAN populations. Given that DANs appear to modulate the KC-MBON synapse to instantaneously adapt behaviour and skew the synaptic weighting for the purpose of learning, it may be impossible to correctly elucidate downstream MBON function without a detailed understanding of the nature of DAN modulation.

Previously it would have been impossible to target expression of effectors to neurons with the precision required to perform such experiments. However, due to the recent advances in intersectional expression systems, such as the Split-GAL4 system employed in this thesis, precision of expression is no longer a barrier.

4.4 DAN representation and modulation

4.4.1 DANs encode biologically meaningful internal and external sensory information

In functional terms the MB serves as a coincidence detector. Largely unfiltered odour information is represented by the KCs (CS in learning experiments), which in naïve flies drive aversive and attractive behaviour via specific sets of MBONs (Lewis et al., 2015; Owald et al., 2015b). Two primary clusters of DANs provide valence specific axonal input to the MB and encode the US in learning experiments. The PAM cluster innervates the horizontal lobe and the PPL1 cluster innervates the vertical lobe, and they each modulate the KC>MBON synapse, over time in the case of learning or instantaneously, to shift the balance between behavioural attraction and aversion. Traditionally, in the context of memory formation, PAM cluster neurons have been understood to signal reward stimuli such as a sugar meal (S. Lin et al., 2014; C. Liu et al., 2012; Vogt et al., 2014), water consumption (S. Lin et al., 2014), nutrient value (Huetteroth et al., 2015), and possibly stimuli related to courtship (M a Joiner & Griffith, 2000; Mei-ling a. Joiner & Griffith, 1999; McBride et al., 1999; Neckameyer, 1998). PPL1 cluster DANs signal aversive stimuli such as cold (Tomchik, 2013) and electric shock (Aso, Sitaraman, et al., 2014; Qin et al., 2012; Vogt et al., 2014). These stimuli all convey information relevant to the health and survival of the fly in some respect, whether they represent potential danger or sources of food. Most studies have sought to understand how biologically relevant stimuli can be associated with other environmental odours to facilitate useful learning. However, it is also the case that flies must make instantaneous decisions based on the convergence of internal and external biologically relevant stimuli without necessarily having to form associative memories. It is therefore intuitive that DANs represent appetitive and aversive stimuli other than those commonly used to drive associative learning. In this study it is demonstrated via 2-photon calcium imaging that PAM neurons innervating the CO_2 aversion mediating β'2 region respond strongly to stimulation with vinegar in a starvation-dependent manner (Figure 27), and that the activation of these PAM neurons is sufficient to reduce CO_2 aversive behaviour and to drive attractive behaviour (Figure 26 and Figure 31). This integration is effectively the fly making a value-motivated decision whether to obey the CO_2 or the vinegar signal. The calcium imaging data also showed that the same PAM neurons were strongly responsive to acetoin acetate but much less to isoamyl acetate (Figure 28), both of which are

appetitive food related odours, suggesting that there may be odour tuning at the level of the DANs. The same neurons were not responsive to the aversive odours CO_2 or benzaldehyde (Figure 28) which accords with the common understanding of PAM neurons as representing positive or rewarding stimuli. Hige et al. (Hige, Aso, Rubin, et al., 2015) showed that, with the exception of some biologically relevant attractive and aversive stimuli, there is limited segregation of odour representation at the level of the MBONs. Perhaps one explanation for this broad tuning is that the DANs represent a second more segregated and biologically relevant odour code that impinges on the KC-MBON synapse to filter environmental olfactory information for the execution of attractive or aversive behaviour. The generally broad tuning of the MBONs allows most of the odours represented by the KCs to be paired, either for learning or instantaneous decision making, with internal state and sensory information represented by the PAM DANs. The odours which maintain a segregated representation at the level of the MBONs (e.g., CO_2 and vinegar) may still be able to be paired with other stimuli (as my data has shown), but might, due to their importance to the animal, have an additional channel through which they can drive behaviour. Thus, future experimentation might find that odours with more segregated representations are more able to override learned or innate responses to odours lacking non-segregated MBON representation.

My findings are consistent with those from the learning and memory field except that they relate to behavioural response upon the initial integration of the biologically relevant contextual information (vinegar) with the environmental odour (CO_2), rather than a subsequent expression of a learned association. Thus, they demonstrate that the MB is important for behavioural flexibility independent of learning or memory. During the training phase of classical conditioning paradigms commonly used in *Drosophila* learning and memory research, flies are not given the option to behave, nor is behaviour measured. It is not standard practice to employ operant conditioning procedures in which the training session constitutes an active decision-making process where the behavioural outcome is measured and recorded. Were learning experiments to be conducted in this fashion any deficits observed in the initial training / decision-making phase of the paradigm may explain phenotypes resulting from the silencing of MBONs. Acquisition of data and perturbation during both training and testing phases may allow a better distinction to be made between phenotypes that relate to the disruption of naïve olfactory processing and those that relate directly to learning. However, this depends on the extent to which naïve

and learned representations interact. If it can be demonstrated that under certain internal and external stimulus conditions an MBON only drives naïve behaviour, then any phenotypes observed upon their manipulation could be excluded from subsequent analysis. Furthermore, the detailed characteristics of behavioural execution during the training phase of a learning paradigm might affect how memory is formed. If there are MBONs specific for processing naïve behavioural responses, then they may be able to modulate memory formation indirectly via the modulation of behavioural execution during memory acquisition.

4.4.2 DANs modulate MBON activity

If DANs are to directly modulate the KC-MBON synapse they must possess axonal projections overlapping with the MBON dendritic field located in the MB lobes. Via double-labelling experiments and GRASP we identified a set of β'2 PAM DANs that have overlapping innervation with β'2 MBONs (Figure 29). In collaboration with Dr. Siju Purayil I showed that activation of β'2 PAM neurons reduces CO_2 avoidance (Figure 26) and that upon stimulation with a combination of CO_2 and vinegar β'2 MBONs respond more weakly than they do to CO_2 alone (Figure 32B). These data explain how the aversive behavioural drive to CO_2 is reduced upon presentation with the conflict stimulus. Interestingly, the aversive β'2 MBONs also responded to vinegar alone (Figure 32B), and
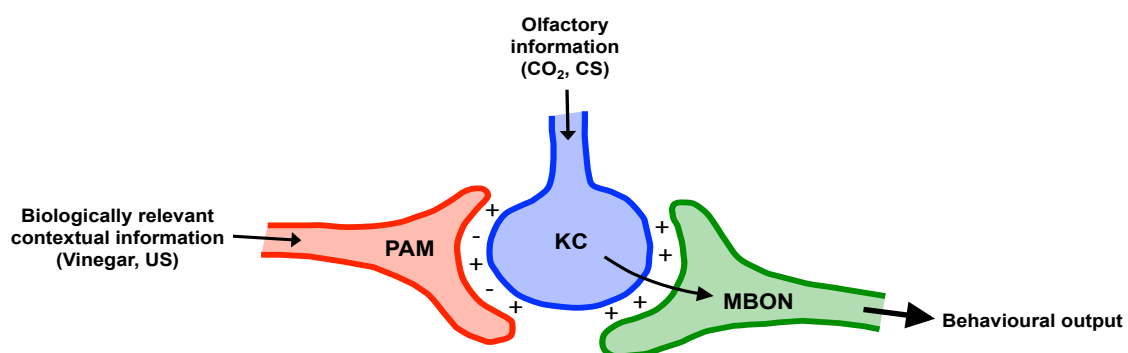
Figure 36. KC DAN MBON synapse

In the naïve state olfactory information represented by the KCs drives behaviour via the MBONs. In the context of biologically relevant information the PAM neurons (or PPL1) either suppress or excite the KC to either inhibit or reinforce MBON output.

88

it was observed that the reduction in activity in response to the conflict stimulus was to the level of the vinegar response. A possible explanation for this is that one of the MBONs innervating the β'2 region (MBON-γ5β'2a) also innervates the γ5 region of the γ lobe, which my data suggests is vinegar responsive (Figure 12 and Figure 13). Recent work by Hige et al. examined the physiological basis for PPL1 (vertical lobe innervating) DAN modulation of MBONs in the context of learning, and also showed that direct activation of PPL1 neurons physiologically suppresses MBON activity. The molecular mechanism by which this suppression is achieved is not yet understood; indeed there are contradictory accounts of DAN modulation. Some recently published research suggests that dopamine receptor (DopR1) expression is required in α/β KCs for the normal formation of long-term memory (Ichinose et al., 2015). Dopamine can elicit both excitatory and inhibitory effects on post-synaptic neurons depending on the receptor expression profile (Keeler et al., 2015). Ichinose et al. suggest that a recurrent circuit consisting of an MBON that feeds back onto itself via a PAM neuron and its input KC is required for memory consolidation. Even though they don't provide physiological data it is likely that in this case the PAM neuron excites the KC>MBON synaptic partners. Our data corroborate these findings; we showed that activation of PAM neurons excites β'2 MBONs (Figure 30B) despite expectations of observing suppression. It is possible that DANs either excite (Cohn et al., 2015; Ichinose et al., 2015; Owald et al., 2015b) or suppress (Cohn et al., 2015; Hige, Aso, Modi, et al., 2015; Owald et al., 2015b) MBONs depending on the particular KC odour representation or the type of internal stimulus. This would suggest a highly dynamic system whereby biologically relevant olfactory information represented by the DANs modulates the KC activation of MBONs depending on KC activity. If the KCs are inactive and the PAMs active, the PAMs may excite MBONs via the KC synapse, however if KCs are actively representing a competing odour then the PAM representation may suppress that of the KCs (Figure 36). Indeed Cohn et al. (Cohn et al., 2015) have elegantly demonstrated precisely this relationship. They showed that KC-MBON signalling is depressed when PAM neuron activation is temporally paired with KC activation, and that when the activity in these two neuron types in unpaired KC-MBON signalling is potentiated. However, further experimentation is required to resolve the precise processing capabilities of the KC-DAN-MBON synapse and whether it operates in different functional modes depending on different types of input from the KCs and DANs. A greater understanding of the MBON-DAN recurrence observed by Ichinose et al. will also

be required to understand to what degree MB output results from feedback from its lobes and how this ultimately impinges on behavioural drive.

4.4.3 PAM DAN integration of internal state and internal state relevant odours

Changes in internal state elicit dramatic effects on the metabolism and physiology of all animals (Rolls, 2015; Root et al., 2011; Schloegl et al., 2011; Siju et al., 2010). A possible mechanism for the modification of behaviour based on changes in internal state is one in which specific internal state information, for example hunger, is integrated with external sensory information relevant to hunger, i.e. food odours. The hungry state of the fly may lead to an increased representation of the food odour in DAN neurons innervating appropriate MB compartments and capable of modulating behavioural output, e.g., suppress CO_2 aversive output via the MBONs. Given that *Drosophila* olfactory sensitivity and behaviour appears to be concentration dependent (Semmelhack & Wang, 2009; J. W. Wang et al., 2003) it may be that behavioural valence and magnitude derive from the
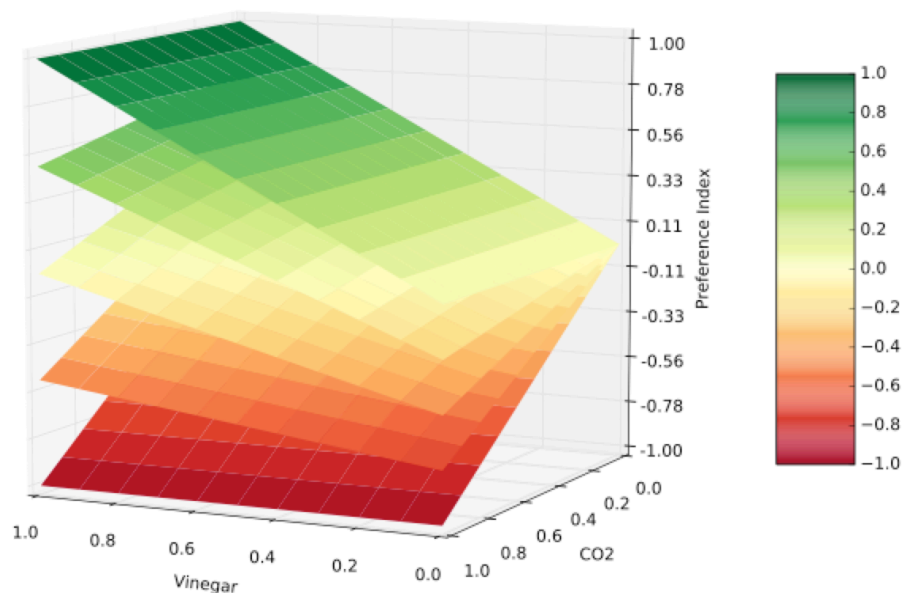
Figure 37. Idealised model of interaction between CO_2 and vinegar concentration and starvation time

Green represents behavioural attraction and red behavioural aversion. Odour concentrations on the x and z axes are percentages. The bottom surface represents the behavioural response at starvation time 0 and the top surface after 20 hours of starvation. At t=0 CO_2 aversion dominates, but as starvation time increases vinegar attraction dominates. When both CO_2 and vinegar concentrations are 0 the behavioural preference is also 0.

relative salience of the odours between which the fly has to decide plus the magnitude of its hunger (Figure 37). Thus, in the case of vinegar and CO_2, a strong starvation dependent PAM DAN vinegar representation would be needed in order to overcome a strong CO_2 representation (Figure 37). Indeed, my data shows that β'2 PAM neuron responses to the food odours vinegar and acetoin acetate are significantly higher in starved flies than in fed (Figure 27C and Figure 28), and presumably increase the PAM suppression of aversive MBON output. There is also evidence from another study that has shown that neurons releasing *Drosophila* neuropeptide F (dNPF), the *Drosophila* homologue of human NPY and a regulator of satiety, regulate MB innervating DANs (Krashes et al., 2009). The dNPF neurons therefore provide a satiety internal state signal to the DANs, which in turn suppress MB MBON output. On the basis of these findings it would be informative to conduct calcium-imaging experiments to see whether PAM neuron vinegar representation is modulated via dNPF. Further, a GABAergic neuron (DGI/DAL, line MB460B) in the same cluster as the Krashes et al. dNPF neuron was identified in my MB behavioural screen as eliciting a strong reduction in vinegar attraction upon silencing (Figure 21), meaning it may also provide a basic starvation dependent drive in response to vinegar stimulation. It may be that MB innervating DANs act as coincidence detectors between internal state conditions and external sensory information, allowing them to effectively filter sensory information in order to then direct which olfactory information is able flow from KCs to MBONs and drive behaviour. It would be interesting to see if the DGI/DAL neuron mentioned above is capable of modulating DANs in the case of naïve behavioural execution.

4.4.4 Putative PAM olfactory input pathways

A significant unknown in the MB field is how information reaches the DANs. More specifically, it is not yet understood how the olfactory vinegar signal and hunger information reach the PAM neurons. DAN dendritic input regions are in roughly the same brain region as the MBON output regions, namely the CRE, SMP, SIP, and SLP (Figure 23 and Figure 26). It is clear from the data presented in this study that DANs are responsive to olfactory stimulation, and they are likely also responsive to gustatory input (Burke & Waddell, 2011; Colomb et al., 2009). As mentioned, it is likely that DANs represent internal state filtered multimodal information rather than a raw sensory code.

This is illustrated by the fact that certain forms of learning and memory execution are entirely dependent on starvation state. It is already known that the two primary populations of DANs that innervate the MB, the PAM and PPL1 clusters, represent a segregation of rewarding and punishing signals. However, the question remains, what are the inputs to the DANs? They seem to integrate external sensory information with internal state information, and then present this internal / external abstraction to relevant regions of the MB for comparison with current olfactory information from the KCs. Therefore, they must receive at least two primary sources of input. I have already postulated one possible input for starvation state (DGI/DAL neuron), but as yet there are no strong candidates for providing other forms of internal state information such as reproductive state, thirst, sickness, temperature, etc. The same is true of olfactory and gustatory inputs to the DANs. Despite this lack of concrete evidence for DAN input candidates there are three main possibilities based on anatomical and functional constraints (Figure 38). First, DANs receive olfactory input directly from the AL. Lin et al (H.-H. Lin et al., 2013) identified a PN (PN$_v$-2) labelled by the GAL4 line E0044 that directly innervates the SMP and possibly has overlapping innervation with DANs and MBONs innervating the MB. This
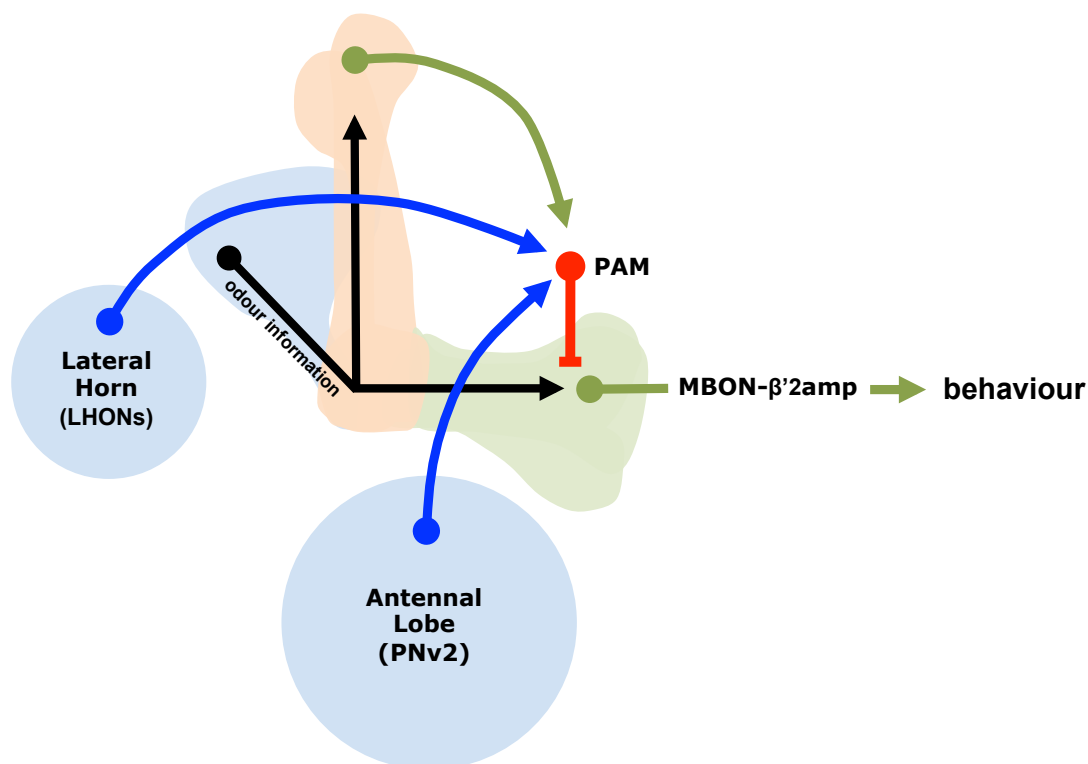
Figure 38. Putative sources of PAM neuron olfactory inputs

Possible sources of PAM neuron olfactory input are the LH via LH output neurons (LHONs), the antennal lobe via PNs, and from the MB lobes by way of MBONs.

PN, and others like it, should they exist, could potentially synapse onto the DAN dendritic fields and provide direct olfactory input. Second, DANs receive segregated olfactory input from LH output neurons. The LH receives olfactory information from the majority of olfactory PNs and outputs information across the protocerebrum (H.-H. Lin et al., 2013; Nobuaki K Tanaka et al., 2004). It is possible that LH output neurons project to the DAN MBON input output regions and synapse with DANs. This is also an intriguing possibility as the LH has been shown to filter olfactory information based on attractive and aversive odour characteristics (Strutz et al., 2014). If the LH output neurons provide channel-based input to the DANs it may explain why they appear to be tuned to specific odours. It might also explain why certain aversive and attractive odours (CO_2 and vinegar) have been observed to maintain segregated representation at the level of the MBONs despite most MBONs exhibiting broad odour tuning (Hige, Aso, Rubin, et al., 2015), i.e. DAN input to the MBONs may slightly sparsen the broad MBON odour code for innately aversive and attractive sensory information. Third, DANs may receive olfactory information via the MBONs. If the limited segregation of the MBON odour code into a central broad odour tuning and aversive and attractive extrema is mediated by the MBONs themselves then the putative DAN odour selectivity could result from MBON input. It has been demonstrated that MBONs likely synapse with DANs outside of the MB lobes (Cohn et al., 2015; Ichinose et al., 2015), and the MBONs do respond to olfactory stimulation (Figure 32), therefore they are possible candidates for providing olfactory input to the DANs. A likely situation is that all three of these possibilities are to some extent true, and that each ensemble of candidate neurons plays some regulatory role on the system as a whole. However, I think the LH is the best candidate for providing olfactory input to the DANs. This would allow the system to encode a second olfactory representation based on a different set of filter properties than those imposed at the level of the KCs. The convergence of these two olfactory representations at the level of the DAN KC MBON synapse would maximise the processing space available to impose internal biological requirements on the processing of immediate and learned olfactory information.

4.5 How meaningful is the idea of 'hard-wired' sensory information processing?

The observation that fundamental, and regularly occurring, internal state changes modulate innate behaviours challenges the idea of innate behavioural responses to odours being 'hard-wired' and therefore inflexible. The concept goes hand-in-hand with the functional neuroanatomical idea of labelled lines, in which sensory information, rather than being processed or modulated, is simply transmitted from the peripheral sensory organs to a brain region where it triggers a stereotyped behavioural or homeostatic response. That innate behaviours can be modulated at all implies that there is no such 'hard-wired' system whereby a stimulus will always evoke a characteristic response. It is reasonable to assume that all organisms are at times hungry, thirsty, sated, or exposed to sensory information with conflicting valences. When there are so many factors that require a 'hard-wired' system to be flexible, the notion of the system being 'hard-wired' at all is called into question. The findings of this study illustrate this clearly and implicate a neural substrate traditionally associated with learning and memory in modulation of innate behaviour. Behavioural responses previously though of as being 'hard-wired', such as CO_2 aversion, were only though of as such because no one had yet observed a circumstance in which innate CO_2 response behaviour needed to be modulated by higher brain regions – it has been shown that CO_2 sensation can be inhibited at the periphery by the antagonistic action of the odorants 1-hexanol and 2,3-butanedione (S. L. Turner & Ray, 2009). It is important to distinguish between closed sensory-motor loops such as the *Drosophila* optomotor response, and seemingly inflexible sensory responses, yet people often fail to make this distinction. In any case, no neural network is independent of modulation, for example, under certain conditions the optomotor response is modulated (M. Barth et al., 2010; S. M. Wasserman et al., 2015). There is likely always a set of conditions under which a so-called reflexive action will be modulated. This is certainly true of sensory processing pathways, which many neurobiologists still insist can sometimes be considered 'hard-wired'. There has to be recognition that a cognitive tool for understanding and discussing neural processes has limits when applied as an actual model for neural function. Otherwise our interpretation of experimental data may become biased without our knowing it, and long-lasting damage done to fields of study in which researchers are often not privy to each other's interpretive processes.

4.6 Behavioural flexibility and the mushroom body in an evolutionary context

Across insect species MB morphology, circuitry, and function varies depending on the sensory processing tasks specific to an insect's ecology. Despite this variability different evolutionary iterations of the MB neuropil all allow the comparison of past and on-going multi-modal sensory information (Haehnel & Menzel, 2012; Mizunami, Weibrecht, et al., 1998; Owald et al., 2015b). Complex MB structures seem to evolve more often in generalist insects, such as *Drosophila* (Lachaise et al., 1988), *Hymenoptera*, and *Periplaneta* (Bell et al., 2007) that feed from diverse food sources and in diverse environments, thus demanding the construction of more salient (i.e., multimodal) representations of sensory objects. This additional functionality afforded MB possessing insects may come at the cost of higher energy requirements, which may explain why insect species living in more limited ecological niches secondarily lose their MBs (Chittka & Niven, 2009; Niven & Laughlin, 2008; Strausfeld et al., 1998). It is also likely that more complex brains are a requirement of complex social behaviours (Farris, 2013).

In mammals various structures have been identified as critical for sensory integration and memory formation including the hippocampus (Basu et al., 2016; Bekinschtein et al., 2010), and amygdala (Yiu et al., 2014). It has recently been suggested that the insect mushroom body and vertebrate pallium, the most highly developed portion of the vertebrate forebrain, share a common evolutionary origin (Tomer et al., 2010) in a bilaterian ancestor. Specifically the older hippocampus and dentate gyrus, but not the neopallium, may share a genetic heritage with the mushroom body (Tomer et al., 2010). Obviously in ~600 million years a significant amount of divergent evolution has taken place, driven by the diversity of habitats in which subsequent bilaterians have found themselves. The apparent utility of the ancestral structure from which both the MB and the pallium developed makes it clear that an increased understanding of the relatively simple *Drosophila* MB can inform broader lines of questioning within neurobiology.

5.0 Summary

Animals must integrate both internal and external sensory information. Moreover, external sensory information must be processed in the context of the internal sensory information in a way that allows animals to respond flexibly to both learned and immediate cues relevant to their survival. A structure in the *Drosophila* brain capable of performing such tasks is the MB. It receives the majority of its input from the primary olfactory processing neuropil, the AL. Its ~2000 KC interneurons form a sparse olfactory representation that propagates throughout its horizontal and vertical lobes where it outputs aversive or attractive behavioural drive respectively via MBONs. The modulatory DANs also innervating the MB lobes represent internal and external sensory information filtered on the basis of biological requirements such as hunger, thirst, high temperature avoidance, etc. The DANs modulate MBON output via dampening or exciting the KC presynaptic terminal (Figure 36), thus modulating the effective behavioural responses to environmental odours based on these biological requirements. The synapses between the KCs, DANs, and MBONs are also responsible for encoding lasting associations so that the fly's behaviour is an integration of both its past and present experiences. Presumably either the current or previous sensory information is sufficient to drive behaviour at a given choice point depending on their relative importance. The aim of this project and thesis was to build a case for the requirement of the *Drosophila* MB in facilitating instantaneous modification of behaviour using the same neural mechanisms underpinning learning, and to demonstrate that the two processes require the same types of sensory input relating to both the environment and internal state. My experimental work and that of my collaborators showed that prescient biologically important information, in the form of a $\beta'2$ region innervating PAM neuron representation of the food odour vinegar, is sufficient to dampen the fly's immediate aversive behavioural response to CO_2, an environmental odour important in the fly's ecology. Moreover, this dampening is likely similar to the process by which memories are expressed.

My data identified a specific subset of MBONs innervating the $\beta'2$ MB region as being necessary and sufficient for naïve behavioural avoidance of CO_2. This same region has also been specifically linked to the processing of other naïve behavioural responses, establishing it as a strong candidate either as a segregated MB sub-region dedicated to

processing naïve behavioural responses, or a region important for processing a specific type of naïve responses. It remains to be elucidated what the fine grain nature of DAN representation actually is, and how different internal and external circumstances impact on their modulation of MB output.

The MB field is now at a stage where real insight into its function is up for grabs. Much of the legwork relating to anatomical description has now been done, and the general impressions emerging from decades of behavioural analysis are beginning to fit together. What remains is the necessary description of the many physiological functions of the MB, and importantly, how that physiology relates to diverse internal and external sensory stimuli. It will be important for the MB field to not focus too heavily on established methods of investigation and the trains of thought surrounding the MB's function primarily as a centre of learning and memory. A broader characterisation of the MB in the context of the functioning fly brain demands a more open mind-set with regards to how its neural substrates might underpin a broader range of functions, only one of which is learning and memory.

6.0 References

Ache, B. W., & Young, J. M. (2005). Olfaction: Diverse species, conserved principles. *Neuron*, *48*(3), 417–430.

Asahina, K., Louis, M., Piccinotti, S., & Vosshall, L. B. (2009). A circuit supporting concentration-invariant odor perception in Drosophila. *Journal of biology*, *8*(1), 9.

Aso, Y., Hattori, D., Yu, Y., Johnston, R. M., Iyer, N. a, Ngo, T.-T., … Rubin, G. M. (2014). The neuronal architecture of the mushroom body provides a logic for associative learning. *eLife*, *3*, 1–47.

Aso, Y., Herb, A., Ogueta, M., Siwanowicz, I., Templier, T., Friedrich, A. B., … Tanimoto, H. (2012). Three Dopamine Pathways Induce Aversive Odor Memories with Different Stability. *PLoS Genetics*, *8*(7), e1002768.

Aso, Y., Sitaraman, D., Ichinose, T., Kaun, K. R., Vogt, K., Belliart-Guérin, G., … Rubin, G. M. (2014). Mushroom body output neurons encode valence and guide memory-based action selection in Drosophila. *eLife*, *3*(3), e04580.

Aso, Y., Siwanowicz, I., Bräcker, L., Ito, K., Kitamoto, T., & Tanimoto, H. (2010). Specific Dopaminergic Neurons for the Formation of Labile Aversive Memory. *Current Biology*, *20*(16), 1445–1451.

Awasaki, T., Lai, S.-L., Ito, K., & Lee, T. (2008). Organization and Postembryonic Development of Glial Cells in the Adult Central Brain of Drosophila. *Journal of Neuroscience*, *28*(51), 13742–13753.

Balkenius, A., & Hansson, B. (2012). Discrimination training with multimodal stimuli changes activity in the mushroom body of the hawkmoth manduca sexta. *PLoS ONE*, *7*(4), 1–7.

Bargmann, C. I. (2012). Beyond the connectome: How neuromodulators shape neural circuits. *BioEssays : news and reviews in molecular, cellular and developmental biology*, 1–8.

Barth, J., Dipt, S., Pech, U., Hermann, M., Riemensperger, T., & Fiala, A. (2014). Differential associative training enhances olfactory acuity in Drosophila melanogaster. *The Journal of neuroscience : the official journal of the Society for Neuroscience*, *34*(5), 1819–37.

Barth, M., Schultze, M., Schuster, C. M., & Strauss, R. (2010). Circadian plasticity in photoreceptor cells controls visual coding efficiency in Drosophila melanogaster. *PLoS ONE*, *5*(2).

Basu, J., Zaremba, J. D., Cheung, S. K., Hitti, F. L., Zemelman, B. V., Losonczy, A., & Siegelbaum, S. A. (2016). Gating of hippocampal activity, plasticity, and memory by entorhinal cortex long-range inhibition. *Science*, *351*(6269), aaa5694–aaa5694.

Becher, P. G., Flick, G., Rozpedowska, E., Schmidt, A., Hagman, A., Lebreton, S., … Bengtsson, M. (2012). Yeast, not fruit volatiles mediate Drosophila melanogaster attraction, oviposition and development. *Functional Ecology*, *26*(4), 822–828.

Bekinschtein, P., Katche, C., Slipczuk, L., Gonzalez, C., Dorman, G., Cammarota, M., … Medina, J. H. (2010). Persistence of long-term memory storage: New insights into its molecular signatures in the hippocampus and related structures. *Neurotoxicity*

Research, *18*(3-4), 377–385.

Bell, W. J., Roth, L. M., & Nalepa, C. A. (2007). *Cockroaches: Ecology, Behaviour and Natural History*.

Benton, R., Vannice, K. S., Gomez-Diaz, C., & Vosshall, L. B. (2009). Variant Ionotropic Glutamate Receptors as Chemosensory Receptors in Drosophila. *Cell*, *136*(1), 149–162.

Bhandawat, V., Olsen, S. R., Gouwens, N. W., Schlief, M. L., & Wilson, R. I. (2007). Sensory processing in the Drosophila antennal lobe increases reliability and separability of ensemble odor representations. *Nature Neuroscience*, *10*(11), 1474–1482.

Bilen, J., Atallah, J., Azanchi, R., Levine, J. D., & Riddiford, L. M. (2013). Regulation of onset of female mating and sex pheromone production by juvenile hormone in Drosophila melanogaster. *Proceedings of the National Academy of Sciences of the United States of America*, *110*(45), 18321–6.

Boeckh, J., Distler, P., Ernst, K. D., H"sl, M., & Malun, D. (1990). Olfactory bulb and antennal lobe. *Chemosensory Information Processing*, 201–227.

Bräcker, L. B., Siju, K. P., Arela, N., So, Y., Hang, M., Hein, I., … Grunwald Kadow, I. C. (2013). Essential role of the mushroom body in context-dependent CO2 avoidance in drosophila. *Current Biology*, *23*(13), 1228–1234.

Brand, A. H., & Perrimon, N. (1993). Targeted gene expression as a means of altering cell fates and generating dominant phenotypes. *Development (Cambridge, England)*, *118*(2), 401–15.

Buck, L., & Axel, R. (1991). A novel multigene family may encode odorant receptors: a molecular basis for odor recognition. *Cell*, *65*(1), 175–87.

Burke, C. J., Huetteroth, W., Owald, D., Perisse, E., Krashes, M. J., Das, G., … Waddell, S. (2012). Layered reward signalling through octopamine and dopamine in Drosophila. *Nature*, 2–10.

Burke, C. J., & Waddell, S. (2011). Remembering nutrient quality of sugar in Drosophila. *Current biology : CB*, *21*(9), 746–50.

Busch, S., Selcho, M., Ito, K., & Tanimoto, H. (2009). A map of octopaminergic neurons in the Drosophila brain. *The Journal of comparative neurology*, *513*(6), 643–67.

Buszewski, B., Kesy, M., Ligor, T., & Amann, A. (2007). Human exhaled air analytics: Biomarkers of diseases. *Biomedical Chromatography*.

Butcher, N. J., Friedrich, A. B., Lu, Z., Tanimoto, H., & Meinertzhagen, I. A. (2012). Different classes of input and output neurons reveal new features in microglomeruli of the adult Drosophila mushroom body calyx. *The Journal of comparative neurology*, *2201*(10), 2185–2201.

Byers, D., Davis, R. L., & Kiger, J. A. (1981). Defect in cyclic AMP phosphodiesterase due to the dunce mutation of learning in Drosophila melanogaster. *Nature*, *289*(5793), 79–81.

Campbell, R. A. A., Honegger, K. S., Qin, H., Li, W., Demir, E., & Turner, G. C. (2013). Imaging a Population Code for Odor Identity in the Drosophila Mushroom Body. *Journal of Neuroscience*, *33*(25), 10568–10581.

Cappe, C., Rouiller, E. M., & Barone, P. (2009). Multisensory anatomical pathways.

Hearing Research, *258*(1-2), 28–36.

Chittka, L., & Niven, J. (2009). Are Bigger Brains Better? *Current Biology*, *19*(21), R995–R1008.

Chou, Y.-H., Spletter, M. L., Yaksi, E., Leong, J. C. S., Wilson, R. I., & Luo, L. (2010). Diversity and wiring variability of olfactory local interneurons in the Drosophila antennal lobe. *Nature Neuroscience*, *13*(4), 439–449.

Choudhury, B. P. (1978). Retinotopic organization of the guinea pig's visual cortex. *Brain research*, *144*(1), 19–29.

Chow, D. M., Theobald, J. C., & Frye, M. a. (2011). An olfactory circuit increases the fidelity of visual behavior. *The Journal of neuroscience : the official journal of the Society for Neuroscience*, *31*(42), 15035–47.

Chyb, S. (2004). Drosophila gustatory receptors: from gene identification to functional expression. *Journal of insect physiology*, *50*(6), 469–77.

Claridge-Chang, A., Roorda, R. D., Vrontou, E., Sjulson, L., Li, H., Hirsh, J., & Miesenböck, G. (2009). Writing Memories with Light-Addressable Reinforcement Circuitry. *Cell*, *139*(2), 405–415.

Clyne, P. J. (2000). Candidate Taste Receptors in Drosophila. *Science*, *287*(5459), 1830–1834.

Clyne, P. J., Warr, C. G., Freeman, M. R., Lessing, D., Kim, J., & Carlson, J. R. (1999). A novel family of divergent seven-transmembrane proteins: candidate odorant receptors in Drosophila. *Neuron*, *22*(2), 327–38.

Cohn, R., Morantte, I., & Ruta, V. (2015). Coordinated and Compartmentalized Neuromodulation Shapes Sensory Processing in Drosophila. *Cell*, *163*(7), 1742–1755.

Colomb, J., Kaiser, L., Chabaud, M., & Preat, T. (2009). Parametric and genetic analysis of Drosophila appetitive long-term memory and sugar motivation. *Genes, brain, and behavior*, *8*(4), 407–15.

Crittenden, J. R., Skoulakis, E. M. C., Han, K., Crittenden, J. R., Skoulakis, E. M. C., Han, K., … Davis, R. L. (1998). Markers Tripartite Mushroom Body Architecture Revealed by Antigenic Markers, 38–51.

Dacks, A. M., Green, D. S., Root, C. M., Nighorn, A. J., & Wang, J. W. (2009). Serotonin modulates olfactory processing in the antennal lobe of Drosophila. *Journal of neurogenetics*, *23*(4), 366–77.

DasGupta, S., Ferreira, C. H., & Miesenböck, G. (2014). FoxP influences the speed and accuracy of a perceptual decision in Drosophila. *Science (New York, N.Y.)*, *344*(6186), 901–4.

de Belle, J. S., & Heisenberg, M. (1994). Associative odor learning in Drosophila abolished by chemical ablation of mushroom bodies. *Science (New York, N.Y.)*, *263*(5147), 692–695.

de Vries, H. S. M., Wasono, M. a. J., Harren, F. J. M., Woltering, E. J., van der Valk, H. C. P. M., & Reuss, J. (1996). Ethylene and CO_2 emission rates and pathways in harvested fruits investigated, in situ, by laser photothermal deflection and photoacoustic techniques. *Postharvest Biology and Technology*, *8*(1), 1–10.

Drugowitsch, J., Moreno-Bote, R., Churchland, A. K., Shadlen, M. N., & Pouget, A.

(2012). The Cost of Accumulating Evidence in Perceptual Decision Making. *Journal of Neuroscience*, *32*(11), 3612–3628.

Dudai, Y., Jan, Y. N., Byers, D., Quinn, W. G., & Benzer, S. (1976). Dunce, a mutant of Drosophila deficient in learning. *Proceedings of the National Academy of Sciences of the United States of America*, *73*(5), 1684–8.

Dunipace, L., Meister, S., McNealy, C., & Amrein, H. (2001). Spatially restricted expression of candidate taste receptors in the Drosophila gustatory system. *Current Biology*, *11*(11), 822–835.

Dweck, H. K. M., Ebrahim, S. a. M., Thoma, M., Mohamed, A. a. M., Keesey, I. W., Trona, F., … Hansson, B. S. (2015). Pheromones mediating copulation and attraction in *Drosophila*. *Proceedings of the National Academy of Sciences*, *112*(21), E2829–E2835.

Ehret, G., & Romand, R. (1994). Development of tonotopy in the inferior colliculus II: 2-DG measurements in the kitten. *European Journal of Neuroscience*, *6*(10), 1589–1595.

Ejima, A., Smith, B. P. C., Lucas, C., van der Goes van Naters, W., Miller, C. J., Carlson, J. R., … Griffith, L. C. (2007). Generalization of Courtship Learning in Drosophila Is Mediated by cis-Vaccenyl Acetate. *Current Biology*, *17*(7), 599–605.

Farris, S. M. (2011). Are mushroom bodies cerebellum-like structures? *Arthropod structure & development*, *40*(4), 368–79.

Farris, S. M. (2013). Evolution of complex higher brain centers and behaviors: Behavioral correlates of mushroom body elaboration in insects. *Brain, Behavior and Evolution*, *82*(1), 9–18.

Faucher, C., Forstreuter, M., Hilker, M., & de Bruyne, M. (2006). Behavioral responses of Drosophila to biogenic levels of carbon dioxide depend on life-stage, sex and olfactory context. *The Journal of experimental biology*, *209*(Pt 14), 2739–48.

Fischer, J. A., Giniger, E., Maniatis, T., & Ptashne, M. (1988). GAL4 activates transcription in Drosophila. *Nature*, *332*(6167), 853–856.

Frank, D. D., Jouandet, G. C., Kearney, P. J., Macpherson, L. J., & Gallio, M. (2015). Temperature representation in the Drosophila brain. *Nature*, *519*(7543), 358–61.

Friedrich, R. W., & Korsching, S. I. (1998). Chemotopic, combinatorial, and noncombinatorial odorant representations in the olfactory bulb revealed using a voltage-sensitive axon tracer. *The Journal of neuroscience : the official journal of the Society for Neuroscience*, *18*(23), 9977–9988.

Frye, M. A. (2010). Multisensory systems integration for high-performance motor control in flies. *Current Opinion in Neurobiology*, *20*(3), 347–352.

Galili, D. S., Dylla, K. V., Lüdke, A., Friedrich, A. B., Yamagata, N., Wong, J. Y. H., … Tanimoto, H. (2014). Converging circuits mediate temperature and shock aversive olfactory conditioning in Drosophila. *Current Biology*, *24*(15), 1712–1722.

Gish, M., Dafni, A., & Inbar, M. (2010). Mammalian herbivore breath alerts aphids to flee host plant. *Current biology : CB*, *20*(15), R628–9.

Gronenberg, W. (2001). Subdivisions of hymenopteran mushroom body calyces by their afferent supply. *Journal of Comparative Neurology*, *435*(4), 474–489.

Grosjean, Y., Rytz, R., Farine, J.-P., Abuin, L., Cortot, J., Jefferis, G. S. X. E., & Benton,

R. (2011). An olfactory receptor for food-derived odours promotes male courtship in Drosophila. *Nature*.

Gruntman, E., & Turner, G. C. (2013). Integration of the olfactory code across dendritic claws of single mushroom body neurons. *Nature Neuroscience*, *16*(12), 1821–1829.

Haehnel, M., & Menzel, R. (2012). Long-term memory and response generalization in mushroom body extrinsic neurons in the honeybee Apis mellifera. *Journal of Experimental Biology*, *215*(3), 559–565.

Hamada, F. N., Rosenzweig, M., Kang, K., Pulver, S. R., Ghezzi, A., Jegla, T. J., & Garrity, P. A. (2008). An internal thermal sensor controlling temperature preference in Drosophila. *Nature*, *454*(7201), 217–220.

Hammer, M. (1993). An identified neuron mediates the unconditioned stimulus in associative olfactory learning in honeybees. *Nature, 366*, 59–63.

Heimbeck, G., Bugnon, V., Gendre, N., Keller, a, & Stocker, R. F. (2001). A central neural circuit for experience-independent olfactory and courtship behavior in Drosophila melanogaster. *Proceedings of the National Academy of Sciences of the United States of America*, *98*(26), 15336–15341.

Hidaka, S., Teramoto, W., & Sugita, Y. (2015). Spatiotemporal Processing in Crossmodal Interactions for Perception of the External World: A Review. *Frontiers in Integrative Neuroscience*, *9*(December), 1–13.

Hige, T., Aso, Y., Modi, M. N., Rubin, G. M., Turner, G. C., Hige, T., … Turner, G. C. (2015). Heterosynaptic Plasticity Underlies Aversive Olfactory Learning in Drosophila Article Heterosynaptic Plasticity Underlies Aversive Olfactory Learning in Drosophila. *Neuron*, *88*(5), 985–998.

Hige, T., Aso, Y., Rubin, G. M., & Turner, G. C. (2015). Plasticity-driven individualization of olfactory coding in mushroom body output neurons. *Nature*.

Honegger, K. S., Campbell, R. A. A., & Turner, G. C. (2011). Cellular-Resolution Population Imaging Reveals Robust Sparse Coding in the Drosophila Mushroom Body. *Journal of Neuroscience*, *31*(33), 11772–11785.

Hong, E. J., & Wilson, R. I. (2015). Simultaneous Encoding of Odors by Channels with Diverse Sensitivity to Inhibition. *Neuron*, *85*(3), 573–589.

Huetteroth, W., Perisse, E., Lin, S., Klappenbach, M., Burke, C., & Waddell, S. (2015). Sweet Taste and Nutrient Value Subdivide Rewarding Dopaminergic Neurons in Drosophila. *Current biology : CB*, 751–758.

Huetteroth, W., & Waddell, S. (2011). Hungry flies tune to vinegar. *Cell*, *145*(1), 17–8.

Hughes, N. K., Price, C. J., & Banks, P. B. (2010). Predators are attracted to the olfactory signals of prey. *PLoS ONE*, *5*(9), 1–4.

Hunter, P. (2013). Your decisions are what you eat. Metabolic state can have a serious impact on risk-taking and decision-making in humans and animals. *EMBO reports*, *14*(6), 505–508.

Ichinose, T., Aso, Y., Yamagata, N., Abe, A., Rubin, G. M., & Tanimoto, H. (2015). Reward signal in a recurrent circuit drives appetitive long-term memory formation. *eLife*, *4*, 1–18.

Ito, K., Shinomiya, K., Ito, M., Armstrong, J. D., Boyan, G., Hartenstein, V., … Vosshall, L. B. (2014). A systematic nomenclature for the insect brain. *Neuron*, *81*(4), 755–

765.

Ito, K., Suzuki, K., Estes, P., Ramaswami, M., Yamamoto, D., & Strausfeld, N. J. (1998). The Organization of Extrinsic Neurons and Their Implications in the Functional Roles of the Mushroom Bodies in Drosophila melanogaster Meigen. *Spring*.

Jefferis, G. S. X. E., Potter, C. J., Chan, A. M., Marin, E. C., Rohlfing, T., Maurer, C. R., & Luo, L. (2007). Comprehensive maps of Drosophila higher olfactory centers: spatially segregated fruit and pheromone representation. *Cell*, *128*(6), 1187–203.

Johnson, B. A., & Leon, M. (2007). Chemotopic odorant coding in a mammalian olfactory system. *The Journal of comparative neurology*, *503*(1), 1–34.

Joiner, M. a, & Griffith, L. C. (2000). Visual input regulates circuit configuration in courtship conditioning of Drosophila melanogaster. *Learning & memory (Cold Spring Harbor, N.Y.)*, *7*(1), 32–42.

Joiner, M. a., & Griffith, L. C. (1999). Mapping of the Anatomical Circuit of CaM Kinase-Dependent Courtship Conditioning in Drosophila. *Learning & Memory*, *6*(2), 177–192.

Jones, W. D., Cayirlioglu, P., Kadow, I. G., & Vosshall, L. B. (2007). Two chemosensory receptors together mediate carbon dioxide detection in Drosophila. *Nature*, *445*(7123), 86–90.

Keeler, B. E., Lallemand, P., Patel, M. M., de Castro Bras, L. E., & Clemens, S. (2015). Opposing aging-related shift of excitatory dopamine D1 and inhibitory D3 receptor protein expression in striatum and spinal cord. *Journal of Neurophysiology*.

Kent, K. S., Hoskins, S. G., & Hildebrand, J. G. (1987). A Novel Serotonin-Immunoreactive Neuron in the Antenna1 Lobe of the Sphinx Moth Mandwca sexta Persists Throughout Postembryonic Life, *18*(5), 451–465.

Kim, Y.-C., Lee, H.-G., & Han, K.-A. (2007). D1 dopamine receptor dDA1 is required in the mushroom body neurons for aversive and appetitive learning in Drosophila. *The Journal of neuroscience : the official journal of the Society for Neuroscience*, *27*(29), 7640–7.

Kitamoto, T. (2001). Conditional modification of behavior inDrosophila by targeted expression of a temperature-sensitiveshibire allele in defined neurons. *Journal of Neurobiology*, *47*(2), 81–92.

Klapoetke, N. C., Murata, Y., Kim, S. S., Pulver, S. R., Birdsey-Benson, A., Cho, Y. K., … Boyden, E. S. (2014). Independent optical excitation of distinct neural populations. *Nature Methods*, *11*(3), 338–346.

Knaden, M., Strutz, A., Ahsan, J., Sachse, S., & Hansson, B. S. (2012). Spatial representation of odorant valence in an insect brain. *Cell reports*, *1*(4), 392–9.

Krashes, M. J., DasGupta, S., Vreede, A., White, B., Armstrong, J. D., & Waddell, S. (2009). A neural circuit mechanism integrating motivational state with memory expression in Drosophila. *Cell*, *139*(2), 416–27.

Kurtovic, A., Widmer, A., & Dickson, B. J. (2007). A single class of olfactory neurons mediates behavioural responses to a Drosophila sex pheromone. *Nature*, *446*(7135), 542–546.

Lachaise, D., Cariou, M.-L., David, J. R., Lemeunier, F., Tsacas, L., & Ashburner, M. (1988). Historical Biogeography of the Drosophila melanogaster Species Subgroup. In *Evolutionary Biology* (pp. 159–225). Boston, MA: Springer US.

Lai, S.-L., & Lee, T. (2006). Genetic mosaic with dual binary transcriptional systems in Drosophila. *Nature Neuroscience*, *9*(5), 703–709.

Larsson, M. C., Domingos, A. I., Jones, W. D., Chiappe, M. E., Amrein, H., & Vosshall, L. B. (2004). Or83b encodes a broadly expressed odorant receptor essential for Drosophila olfaction. *Neuron*, *43*(5), 703–714.

Laurent, G. (2002). Olfactory network dynamics and the coding of multidimensional signals. *Nature reviews. Neuroscience*, *3*(11), 884–895.

Lee, T., & Luo, L. (1999). Mosaic analysis with a repressible cell marker for studies of gene function in neuronal morphogenesis. *Neuron*, *22*(3), 451–61.

Lewis, L. P. C., Siju, K. P., Aso, Y., Friedrich, A. B., Bulteel, A. J. B., Rubin, G. M., & Grunwald Kadow, I. C. (2015). A Higher Brain Circuit for Immediate Integration of Conflicting Sensory Information in Drosophila. *Current biology : CB*, *25*(17), 2203–14.

Lin, H.-H., Chu, L.-A., Fu, T.-F., Dickson, B. J., & Chiang, A.-S. (2013). Parallel neural pathways mediate CO2 avoidance responses in Drosophila. *Science (New York, N.Y.)*, *340*(6138), 1338–41.

Lin, S., Owald, D., Chandra, V., Talbot, C., Huetteroth, W., & Waddell, S. (2014). Neural correlates of water reward in thirsty Drosophila. *Nature neuroscience*, *17*(11), 1536–42.

Liu, C., Plaçais, P.-Y., Yamagata, N., Pfeiffer, B. D., Aso, Y., Friedrich, A. B., … Tanimoto, H. (2012). A subset of dopamine neurons signals reward for odour memory in Drosophila. *Nature*, *488*(7412), 512–516.

Liu, W., Liang, X., Gong, J., Yang, Z., Zhang, Y.-H., Zhang, J.-X., & Rao, Y. (2011). Social regulation of aggression by pheromonal activation of Or65a olfactory neurons in Drosophila. *Nature Neuroscience*, *14*(7), 896–902.

Lourenço, C., & Turner, C. (2014). Breath Analysis in Disease Diagnosis: Methodological Considerations and Applications. *Metabolites*, *4*(2), 465–498.

Luan, H., Peabody, N. C., Vinson, C. R., & White, B. H. (2006). Refined spatial manipulation of neuronal function by combinatorial restriction of transgene expression. *Neuron*, *52*(3), 425–36.

Marder, E. (2012). Neuromodulation of Neuronal Circuits: Back to the Future. *Neuron*, *76*(1), 1–11.

Marin, E. C., Jefferis, G. S. X. E., Komiyama, T., Zhu, H., & Luo, L. (2002). Representation of the glomerular olfactory map in the Drosophila brain. *Cell*, *109*(2), 243–55.

McBride, S. M., Giuliani, G., Choi, C., Krause, P., Correale, D., Watson, K., … Siwicki, K. K. (1999). Mushroom body ablation impairs short-term memory and long-term memory of courtship conditioning in Drosophila melanogaster. *Neuron*, *24*(4), 967–977.

Mizunami, M., & Matsumoto, Y. (2010). Roles of Aminergic Neurons in Formation and Recall of Associative Memory in Crickets. *Frontiers in Behavioral Neuroscience*, *4*(November), 1–11.

Mizunami, M., Okada, R., Li, Y., & Strausfeld, N. J. (1998). Mushroom Bodies of the Cockroach : Activity and Identities of Neurons, *519*(July), 501–519.

Mizunami, M., Weibrecht, J. M., & Strausfeld, N. J. (1998). Mushroom bodies of the cockroach: Their participation in place memory. *Journal of Comparative Neurology*, *402*(4), 520–537.

Morgan, T. H. (1910). Sex limited inheritance in Drosophila. *Science*, *32*(812), 120–122.

Murthy, V. N. (2011). Olfactory maps in the brain. *Annual review of neuroscience*, *34*(May), 233–258.

Nakai, J., Ohkura, M., & Imoto, K. (2001). A high signal-to-noise Ca(2+) probe composed of a single green fluorescent protein. *Nature biotechnology*, *19*(2), 137–41.

Nayak, S. V., & Singh, R. N. (1983). Sensilla on the tarsal segments and mouthparts of adult Drosophila melanogaster meigen (Diptera : Drosophilidae). *International Journal of Insect Morphology and Embryology*, *12*(5-6), 273–291.

Neckameyer, W. S. (1998). Dopamine and Mushroom Bodies in Drosophila: Experience-Dependent and -Independent Aspects of Sexual Behavior. *Learning & Memory*, *5*, 157–165.

Nicolai, L. J. J., Ramaekers, a., Raemaekers, T., Drozdzecki, a., Mauss, a. S., Yan, J., … Hassan, B. a. (2010). Genetically encoded dendritic marker sheds light on neuronal connectivity in Drosophila. *Proceedings of the National Academy of Sciences*, *107*(47), 20553–20558.

Niven, J. E., & Laughlin, S. B. (2008). Energy limitation as a selective pressure on the evolution of sensory systems. *The Journal of experimental biology*, *211*(Pt 11), 1792–804.

Owald, D., Felsenberg, J., Talbot, C. B., Das, G., Perisse, E., Huetteroth, W., & Waddell, S. (2015a). Activity of Defined Mushroom Body Output Neurons Underlies Learned Olfactory Behavior in Drosophila. *Neuron*, 1–11.

Owald, D., Felsenberg, J., Talbot, C. B., Das, G., Perisse, E., Huetteroth, W., & Waddell, S. (2015b). Activity of Defined Mushroom Body Output Neurons Underlies Learned Olfactory Behavior in Drosophila. *Neuron*, *86*(2), 417–427.

Park, S., Sonn, J. Y., Oh, Y., Lim, C., & Choe, J. (2014). SIFamide and SIFamide Receptor Defines a Novel Neuropeptide Signaling to Promote Sleep in Drosophila. *Molecules and cells*, *37*(4), 295–301.

Parnas, M., Lin, A. C., Huetteroth, W., & Miesenböck, G. (2013). Odor discrimination in Drosophila: from neural population codes to behavior. *Neuron*, *79*(5), 932–44.

Pavlov, P. I. (1927). Conditioned reflexes: An investigation of the physiological activity of the cerebral cortex. *Annals of neurosciences*, *17*(3), 136–41.

Pech, U., Pooryasin, A., Birman, S., & Fiala, A. (2013). Localization of the contacts between Kenyon cells and aminergic neurons in the *Drosophila melanogaster* brain using splitGFP reconstitution. *Journal of Comparative Neurology*, *4026*, n/a–n/a.

Perisse, E., Yin, Y., Lin, A., Lin, S., Huetteroth, W., & Waddell, S. (2013). Different Kenyon Cell Populations Drive Learned Approach and Avoidance in Drosophila. *Neuron*, *79*(5), 945–956.

Pfeiffer, B. D., Truman, J. W., & Rubin, G. M. (2012). Using translational enhancers to increase transgene expression in Drosophila. *Proceedings of the National Academy of Sciences*, *109*(17), 6626–6631.

Préat, T. (1998). Decreased odor avoidance after electric shock in Drosophila mutants

biases learning and memory tests. *The Journal of neuroscience : the official journal of the Society for Neuroscience*, *18*(20), 8534–8.

Qi, C., & Lee, D. (2014). Pre- and Postsynaptic Role of Dopamine D2 Receptor DD2R in Drosophila Olfactory Associative Learning. *Biology*, *3*(4), 831–845.

Qin, H., Cressy, M., Li, W., Coravos, J. S., Izzi, S. A., & Dubnau, J. (2012). Gamma Neurons Mediate Dopaminergic Input during Aversive Olfactory Memory Formation in Drosophila. *Current Biology*, 1–7.

R. Menzel, J. Erber, T. M. (1974). Learning and memory in the honeybee. *Book chapter: Experimental analysis of insect behaviour*, *15*(3 Pt 1), 1617–30.

Randolf, M., & Giurfa, M. (2001). Cognitive architecture of a mini-brain : the honeybee, *5*(2), 62–71.

Recanzone, G. H. (2009). Interactions of auditory and visual stimuli in space and time. *Hearing research*, *258*(1-2), 89–99.

Robinson, B. G., Khurana, S., Kuperman, A., & Atkinson, N. S. (2012). Neural adaptation leads to cognitive ethanol dependence. *Current Biology*, *22*(24), 2338–2341.

Rolls, E. T. (2015). Taste, olfactory, and food reward value processing in the brain. *Progress in neurobiology*, *127-128*, 64–90.

Root, C. M., Ko, K. I., Jafari, A., & Wang, J. W. (2011). Presynaptic facilitation by neuropeptide signaling mediates odor-driven food search. *Cell*, *145*(1), 133–44.

Root, C. M., Semmelhack, J. L., Wong, A. M., Flores, J., & Wang, J. W. (2007). Propagation of olfactory information in Drosophila. *Proceedings of the National Academy of Sciences of the United States of America*, *104*(28), 11826–11831.

Rosenzweig, M., Brennan, K. M., Tayler, T. D., Phelps, P. O., Patapoutian, A., & Garrity, P. a. (2005). The Drosophila ortholog of vertebrate TRPA1 regulates thermotaxis. *Genes and Development*, *19*(4), 419–424.

Ruta, V., Datta, S. R., Vasconcelos, M. L., Freeland, J., Looger, L. L., & Axel, R. (2010). A dimorphic pheromone circuit in Drosophila from sensory input to descending output. *Nature*, *468*(7324), 686–90.

Sarlegna, F. R., & Mutha, P. K. (2014). The influence of visual target information on the online control of movements. *Vision Research*, *110*, 144–154.

Schloegl, H., Percik, R., Horstmann, A., Villringer, A., & Stumvoll, M. (2011). Peptide hormones regulating appetite-focus on neuroimaging studies in humans. *Diabetes/Metabolism Research and Reviews*, *27*(2), 104–112.

Schroll, C., Riemensperger, T., Bucher, D., Ehmer, J., Völler, T., Erbguth, K., … Fiala, A. (2006). Light-Induced Activation of Distinct Modulatory Neurons Triggers Appetitive or Aversive Learning in Drosophila Larvae. *Current Biology*, *16*(17), 1741–1747.

Schwaerzel, M., Monastirioti, M., Scholz, H., Friggi-Grelin, F., Birman, S., & Heisenberg, M. (2003). Dopamine and octopamine differentiate between aversive and appetitive olfactory memories in Drosophila. *The Journal of neuroscience : the official journal of the Society for Neuroscience*, *23*(33), 10495–502.

Scott, K., Brady, R., Cravchik, A., Morozov, P., Rzhetsky, A., Zuker, C., & Axel, R. (2001). A chemosensory gene family encoding candidate gustatory and olfactory receptors in Drosophila. *Cell*, *104*(5), 661–73.

Seeds, A. M., Ravbar, P., Chung, P., Hampel, S., Midgley, F. M., Mensh, B. D., & Simpson, J. H. (2014). A suppression hierarchy among competing motor programs drives sequential grooming in Drosophila. *eLife*, *3*, e02951.

Semmelhack, J. L., & Wang, J. W. (2009). Select Drosophila glomeruli mediate innate olfactory attraction and aversion. *Nature*, *459*(7244), 218–23.

Siegel, R. W., & Hall, J. C. (1979). Conditioned responses in courtship behavior of normal and mutant *Drosophila*. *Proceedings of the National Academy of Sciences of the United States of America*, *76*(7), 3430–3434.

Siju, K. P., Hill, S. R., Hansson, B. S., & Ignell, R. (2010). Influence of blood meal on the responsiveness of olfactory receptor neurons in antennal sensilla trichodea of the yellow fever mosquito, Aedes aegypti. *Journal of Insect Physiology*, *56*(6), 659–665.

Silbering, a. F., & Galizia, C. G. (2007). Processing of Odor Mixtures in the Drosophila Antennal Lobe Reveals both Global Inhibition and Glomerulus-Specific Interactions. *Journal of Neuroscience*, *27*(44), 11966–11977.

Silva, M. G., Lima, J. A. P., Sthel, M. S., Marín, E., Gatts, C. E. N., Cardoso, S. L., & Campostrini, E. (2001). Ethylene and CO_2 emission rates in tropical fruits investigated by infrared absorption techniques, *17*, 534–537.

Stensmyr, M. C., Dweck, H. K. M., Farhan, A., Ibba, I., Strutz, A., Mukunda, L., … Hansson, B. S. (2012). A conserved dedicated olfactory circuit for detecting harmful microbes in drosophila. *Cell*, *151*(6), 1345–1357.

Stewart, F. J., Baker, D. a., & Webb, B. (2010). A model of visual-olfactory integration for odour localisation in free-flying fruit flies. *Journal of Experimental Biology*, *213*(11), 1886–1900.

Stocker, R. F., Heimbeck, G., Gendre, N., & de Belle, J. S. (1997). Neuroblast ablation in Drosophila P[GAL4] lines reveals origins of olfactory interneurons. *Journal of Neurobiology*, *32*(5), 443–56.

Stortkuhl, K. F., & Kettler, R. (2001). Functional analysis of an olfactory receptor in Drosophila melanogaster. *Proc Natl Acad Sci U S A*, *98*(16), 9381–9385.

Strausfeld, N. J., Hansen, L., Li, Y., Gomez, R. S., & Ito, K. (1998). Evolution, Discovery, and Interpretations of Arthropod Mushroom Bodies. *Learning & Memory*, *5*(1), 11–37.

Strutz, A., Soelter, J., Baschwitz, A., Farhan, A., Grabe, V., Rybak, J., … Sachse, S. (2014). Decoding odor quality and intensity in the Drosophila brain. *eLife*, *3*, e04147.

Suh, G. S. B., Wong, A. M., Hergarden, A. C., Wang, J. W., Simon, A. F., Benzer, S., … Anderson, D. J. (2004). A single population of olfactory sensory neurons mediates an innate avoidance behaviour in Drosophila. *Nature*, *431*(7010), 854–9.

Szüts, D., & Bienz, M. (2000). LexA chimeras reveal the function of Drosophila Fos as a context-dependent transcriptional activator. *Proceedings of the National Academy of Sciences of the United States of America*, *97*(10), 5351–5356.

Tanaka, N. K., Awasaki, T., Shimada, T., & Ito, K. (2004). Integration of chemosensory pathways in the Drosophila second-order olfactory centers. *Current biology : CB*, *14*(6), 449–57.

Tanaka, N. K., Ito, K., & Stopfer, M. (2009). Odor-Evoked Neural Oscillations in Drosophila Are Mediated by Widely Branching Interneurons. *Journal of Neuroscience*, *29*(26), 8595–8603.

Tanaka, N. K., Tanimoto, H., & Ito, K. (2008). Neuronal assemblies of the Drosophila mushroom body. *The Journal of comparative neurology*, *508*(5), 711–55.

Terhzaz, S., Rosay, P., Goodwin, S. F., & Veenstra, J. A. (2007). The neuropeptide SIFamide modulates sexual behavior in Drosophila. *Biochemical and Biophysical Research Communications*, *352*(2), 305–310.

Tomchik, S. M. (2013). Dopaminergic neurons encode a distributed, asymmetric representation of temperature in Drosophila. *The Journal of neuroscience : the official journal of the Society for Neuroscience*, *33*(5), 2166–76a.

Tomer, R., Denes, A. S., Tessmar-Raible, K., & Arendt, D. (2010). Profiling by Image Registration Reveals Common Origin of Annelid Mushroom Bodies and Vertebrate Pallium. *Cell*, *142*(5), 800–809.

Tompkins, L., Siegel, R. W., Gailey, D. A., & Hall, J. C. (1983). Conditioned courtship in Drosophila and its mediation by association of chemical cues. *Behavior Genetics*, *13*(6), 565–578.

Tully, T., & Quinn, W. G. (1985). Classical conditioning and retention in normal and mutant Drosophila melanogaster. *Journal of comparative physiology. A, Sensory, neural, and behavioral physiology*, *157*(2), 263–277.

Turner, G. C., Bazhenov, M., & Laurent, G. (2008). Olfactory representations by Drosophila mushroom body neurons. *Journal of neurophysiology*, *99*(2), 734–46.

Turner, S. L., & Ray, A. (2009). Modification of CO2 avoidance behaviour in Drosophila by inhibitory odorants. *Nature*, *461*(7261), 277–81.

Venema, D. R. (2006). Enhancing undergraduate teaching and research with a Drosophila virginizing system. *CBE life sciences education*, *5*(4), 353–60.

Verleyen, P., Huybrechts, J., Baggerman, G., Van Lommel, A., De Loof, A., & Schoofs, L. (2004). SIFamide is a highly conserved neuropeptide: A comparative study in different insect species. *Biochemical and Biophysical Research Communications*, *320*(2), 334–341.

Vet, L. E. M., Lenteren, J. C. VAN, Heymans, M., & Meelis, E. (1983). An airflow olfactometer for measuring olfactory responses of hymenopterous parasitoids and other small insects. *Physiological Entomology*, *8*(1), 97–106.

Vogt, K., Schnaitmann, C., Dylla, K. V., Knapek, S., Aso, Y., Rubin, G. M., & Tanimoto, H. (2014). Shared mushroom body circuits operate visual and olfactory memories in Drosophila. *eLife*, 1–22.

Vosshall, L. B., Amrein, H., Morozov, P. S., Rzhetsky, A., Axel, R., Biophysics, M., & Dulac, C. (1999). A Spatial Map of Olfactory Receptor Expression in the, *96*, 725–736.

Wang, J. W. (2012). Presynaptic modulation of early olfactory processing in Drosophila. *Developmental Neurobiology*, *72*(1), 87–99.

Wang, J. W., Wong, A. M., Flores, J., Vosshall, L. B., & Axel, R. (2003). Two-photon calcium imaging reveals an odor-evoked map of activity in the fly brain. *Cell*, *112*(2), 271–282.

Wang, K., Gong, J., Wang, Q., Li, H., Cheng, Q., Liu, Y., … Wang, Z. (2014). Parallel pathways convey olfactory information with opposite polarities in Drosophila. *Proceedings of the National Academy of Sciences of the United States of America*, *111*(8), 3164–9.

Wasserman, S., Lu, P., Aptekar, J. W., & Frye, M. a. (2012). Flies dynamically anti-track, rather than ballistically escape, aversive odor during flight. *Journal of Experimental Biology*, *215*, 2833–2840.

Wasserman, S. M., Aptekar, J. W., Lu, P., Nguyen, J., Wang, A. L., Keles, M. F., … Frye, M. a. (2015). Olfactory neuromodulation of motion vision circuitry in Drosophila. *Current biology : CB*, *25*(4), 467–72.

Whittle, C. L., Fakharzadeh, S., Eades, J., & Preti, G. (2007). Human breath odors and their use in diagnosis. *Annals of the New York Academy of Sciences*, *1098*, 252–266.

Wise, R. A. (2004). Dopamine, learning and motivation. *Nature reviews. Neuroscience*, *5*(June), 483–494.

Wong, A. M., Wang, J. W., & Axel, R. (2002). Spatial representation of the glomerular map in the Drosophila protocerebrum. *Cell*, *109*(2), 229–41.

Xu, P., Atkinson, R., Jones, D. N. M., & Smith, D. P. (2005). Drosophila OBP LUSH Is Required for Activity of Pheromone-Sensitive Neurons. *Neuron*, *45*(2), 193–200.

Yamagata, N., Ichinose, T., Aso, Y., Plaçais, P.-Y., Friedrich, A. B., Sima, R. J., … Tanimoto, H. (2015). Distinct dopamine neurons mediate reward signals for short- and long-term memories. *Proceedings of the National Academy of Sciences*, *112*(2), 578–583.

Yamamoto, D., Jallon, J. M., & Komatsu, a. (1997). Genetic dissection of sexual behavior in Drosophila melanogaster. *Annual review of entomology*, *42*, 551–585.

Yanagawa, A., Guigue, A. M. a, & Marion-Poll, F. (2014). Hygienic grooming is induced by contact chemicals in Drosophila melanogaster. *Frontiers in behavioral neuroscience*, *8*(July), 254.

Yang, C.-H., He, R., & Stern, U. (2015). Behavioral and circuit basis of sucrose rejection by Drosophila females in a simple decision-making task. *The Journal of neuroscience : the official journal of the Society for Neuroscience*, *35*(4), 1396–410.

Yao Yang, M., Armstrong, J. D., Vilinsky, I., Strausfeld, N. J., & Kaiser, K. (1995). Subdivision of the Drosophila mushroom bodies by enhancer-trap expression patterns. *Neuron*, *15*(1), 45–54.

Yiu, A. P., Mercaldo, V., Yan, C., Richards, B., Rashid, A. J., Hsiang, H. L. L., … Josselyn, S. A. (2014). Neurons Are Recruited to a Memory Trace Based on Relative Neuronal Excitability Immediately before Training. *Neuron*, *83*(3), 722–735.

Young, R. E., Romani, R. J., & Biale, J. B. (1962). Carbon Dioxide Effects on Fruit Respiration . II. Response of Avocados, Bananas, & Lemons. *Plant physiology*, *37*(3), 416–422.

Zhu, J., Park, K. C., & Baker, T. C. (2003). Identification of odors from overripe mango that attract vinegar flies, Drosophila melanogaster. *Journal of Chemical Ecology*, *29*(4), 899–909.

7.0 Appendix

	Line	p65ADZp DNA fragment	ZpGdbd DNA fragment	KC γd	KC γmain	KC α'/β'ap	KC α'/β'm	KC α/βp	KC α/βs	KC α/βc
Broad KCs	MB010B	R13F02	R52H09	▒	▒	■	■	■	■	■
	MB152B	R19B03	R26E07	▒	▒	■	■	░	▒	░
	MB364B	R13F02	R21B06	■	■			▒	■	■
	MB417B	R26E07	R29G11			■	■	■	■	░
γ KCs	MB028B	R26E07	R16H11	▒						
	MB419B	R26E07	R39A11	▦						
	MB355B	R12E03	R26E07	▦	░					
	MB009B	R13F02	R45H04	▒	░					
	MB131B	R13F02	R89B01	░	▒					
α'/β' KCs	MB005B	R13F02	R34A03			▦	▦			
	MB461B	R35B12	R26E07			■	▦			
	MB463B	R35B12	R34A03			■	░			
	MB370B	R13F02	R41C07			░	▦			
	MB418B	R26E07	R30F02				▦			
α/β KCs	MB371B	R13F02	R85D07					▒		
	MB008B	R13F02	R44E04					■	■	■
	MB185B	R52H09	R18F09						▦	
	MB477B	R44E04	R26E07						▦	

Table 7. KC Split-GAL4 lines.

	Line	p65ADZp DNA fragment	ZpGdbd DNA fragment
Horizontal lobe MBONs	MB298B	R53C03	R24E12
	MB434B	R30E08	R53C10
	MB433B	R30E08	R11C07
	MB011B	R14C08	R15B01
	MB210B	R15B01	R27G01
	MB002B	R12C11	R14C08
	MB074C	R21D02	R12C11
	MB399B	R21D02	R22C12
	MB310C	R52G04	R17C11
	MB083C	R52G04	R94B10
	MB057B	R80G12	R53H03
	MB112C	R93D10	R13F04
	MB051B	R70B10	R19F09
	MB018B	R20G03	R19F09
	MB093C	R73H08	R40B08
	MB082C	R40B08	R23C06
Vertical lobe MBONs	MB052B	R71D08	R11F03
	MB552B	R71D08	R92B02
	MB543B	R65B09	R81E11
	MB542B	R65B09	R51D04
	MB027B	R24H08	R53F03
	MB050B	R65B09	R11F03
	MB549C	R71D08	R49C12
	MB080C	R33E02	R50A05
	MB242A	R64F07	R57C10

Column headers (matrix, left to right): MBON-γ4>γ1γ2; MBON-β1>α (MB-MV2); MBON-γ5β'2a (MB-M6); MBON-β'2mp (MB-M4); MBON-β'2mp_bilateral; MBON-β2β'2a; MBON-α1; MBON-γ3; MBON-γ3β'1; MBON-β'1; MBON-γ1pedc>α/β (MB-MVP2); MBON-γ2α'1; MBON-α'2 (MB-V4); MBON-α3 (MB-V3); MBON-α1; MBON-α2sc (MB-V2α); MBON-α2p3p; MBON-α3ap (MB-V2α3); MBON-α'3m (MB-V2α3); MBON-calyx (MB-CP1)

Table 8. MBON Split-GAL4 lines.

Table 9. DAN Split-GAL4 lines.

Column headers (heatmap matrix): PPL1-γ1pedc (MB-MP1), PPL1-γ2α'1 (MB-MV1), PPL1-α'2α2 (MB-V1), PPL1-α3, PPL1-α'3, PPL1-γ1, PAM-γ5, PAM-β'2a, PAM-β2β'2a, PAM-β2, PAM-β'2m, PAM-β'2p, PAM-γ4<γ1γ2, PAM-γ4, PAM-β1(MVP1), PAM-β1ped, PAM-α1, PAM-γ3, PAM-β'1ap, PAM-β'1m

	Line	p65ADZp DNA fragement	ZpGdbd DNA fragement
PPL1 cluster DANs	MB060B	R82C10	R72B05
	MB065B	TH	R72B05
	MB504B	R52H03	TH
	MB438B	R30E11	R22B12
	MB439B	R30E11	R82C10
	MB502B	R52H03	R14E06
	MB308B	TH	R26F01
	MB058B	R82C10	R50B03
	MB296B	R15B01	R26F01
	MB304B	R82C10	R26F01
PAM cluster DANs	MB315C	R58E02	R48H11
	MB109B	R76F05	R23C12
	MB087C	R61H03	R28E09
	MB301B	R71D01	R58F02
	MB213B	R76F05	R32G08
	MB299B	R58E02	R37E10
	MB056B	R76F05	R80G12
	MB312B	R58E02	R10G03
	MB043B	R58E02	R32D11
	MB188B	R58E02	R11A03
	MB195B	R58E02	R31F06
	MB025B	R24E12	R52H01
	MB042B	R58E02	R22E04
	MB040B	R58E02	R18D09
	MB196B	R58E02	R36B06
	MB032B	R30G08	TH
	MB047B	R58E02	R93A09
	MB194B	R58E02	R29G04
	MB316B	R58E02	R93G08

	Line	p65ADZp DNA fragement	ZpGdbd DNA fragement	OA-VPM3	OA-VPM4	CSD	MB-C1	SIFamide	DGI/DAL
Octopaminergic neurons	MB021B	R24E06	R95A10		▒				
	MB022B	R24E06	RTDC2	■	■				
	MB113C	TDC2	R95A10		■				
	MB465C	R37D04	R51B02			▒			
Other MB extrinsic neurons	MB380B	R17A04	R65D07				■		
	MB013B	R14F05	R14B03					■	
	MB460B	R34E09	R45E06						■

Table 10. Octopaminergic neurons and other MB extrinsic neuron Split-GAL4 lines.

Genotype	Stimulus		
	CO2	Vinegar	Vinegar + CO2
Shi/w-	-0.61	-0.11	0.51
GH146/Shi	-	-0.03	-0.58
Gr63a/Shi	0.05	-	0.38

Table 11. Olfactory channel blockade data. Preference indexes (16-20n).

	KC Screen Preference Index (PI) mean and p-values					
Genotype	CO2 PI	CO2 p-value	Vinegar PI	Vinegar p-value	CO2 + Vinegar PI	CO2 + Vinegar p-value
Shi/w-	-0.524	-	0.5922	-	0.5603	-
shi/MB005B	-0.1584	0.389	0.2754	0.5399	-0.005275	0.2411
shi/MB370B	0.2183	0.0025	0.6874	> 0.9999	0.9392	0.5995
shi/MB418B	-0.1766	0.5253	0.503	> 0.9999	0.4997	> 0.9999
shi/MB461B	0.03326	0.0142	0.7366	> 0.9999	0.7855	> 0.9999
shi/MB463B	-0.441	> 0.9999	0.5287	> 0.9999	0.5639	> 0.9999
shi/MB008B	-0.3398	> 0.9999	0.4716	> 0.9999	0.05011	0.434
shi/MB185B	-0.2843	> 0.9999	0.1175	0.0415	-0.0397	0.0187
shi/MB371B	0.2263	0.0019	0.3496	> 0.9999	0.8074	> 0.9999
shi/MB477B	-0.4149	> 0.9999	0.3706	> 0.9999	0.3067	> 0.9999
shi/MB009B	-0.4719	> 0.9999	0.2947	0.4238	-0.3243	0.0117
shi/MB028B	-0.3046	> 0.9999	0.3604	> 0.9999	-0.1938	0.0388
shi/MB131B	-0.3855	> 0.9999	0.04705	0.0129	-0.1705	0.0437
shi/MB355B	-0.3711	> 0.9999	0.2791	> 0.9999	0.07225	0.504
shi/MB419B	-0.4383	> 0.9999	0.63	> 0.9999	0.3136	> 0.9999
shi/MB010B	-0.5304	> 0.9999	0.5248	> 0.9999	0.5712	> 0.9999
shi/MB152B	0.02896	0.0179	0.5292	> 0.9999	0.6966	> 0.9999
shi/MB364B	-0.3177	> 0.9999	0.3076	0.6131	-0.02019	0.2132
shi/MB417B	-0.08524	0.1035	0.8286	> 0.9999	0.7061	> 0.9999

Table 12. KC primary screen data. p-values calculated via Kruskal-wallis non-parametric ANOVA with Dunn's post-hoc multicomparison test.

MBON Screen Preference Index (PI) mean and p-values						
Genotype	CO2 PI	CO2 p-value	Vinegar PI	Vinegar p-value	CO2 + Vinegar PI	CO2 + Vinegar p-value
Shi/w-	-0.5379	-	0.563	-	0.4887	-
Shi/MB002B	-0.3575	> 0.9999	0.5924	> 0.9999	0.4681	> 0.9999
Shi/MB011B	-0.01	0.0058	0.287	> 0.9999	0.5066	> 0.9999
Shi/MB057B	-0.41	> 0.9999	0.3945	> 0.9999	0.0007783	0.3812
Shi/MB074C	-0.03	0.0455	0.6221	> 0.9999	0.5221	> 0.9999
Shi/MB083C	-0.3275	> 0.9999	0.2612	> 0.9999	-0.4269	0.0048
Shi/MB210B	-0.4075	> 0.9999	0.1838	0.0057	0.3553	> 0.9999
Shi/MB298B	-0.5175	> 0.9999	0.3406	> 0.9999	0.3318	> 0.9999
Shi/MB399B	-0.095	0.0463	0.3085	> 0.9999	0.578	> 0.9999
Shi/MB433B	-0.245	0.8211	0.3663	> 0.9999	0.6993	> 0.9999
Shi/MB434B	-0.065	0.0151	0.5039	> 0.9999	0.385	> 0.9999
Shi/MB018B	-0.2925	> 0.9999	0.1514	0.3348	0.55	> 0.9999
Shi/MB027B	-0.0825	0.0613	0.1222	0.0953	0.5402	> 0.9999
Shi/MB050B	-0.1775	0.3453	0.02215	0.0249	-0.02848	0.1941
Shi/MB051B	-0.2125	0.0776	0.07133	0.07	0.2732	> 0.9999
Shi/MB052B	-0.2788	0.5333	0.03611	0.0641	-0.01224	0.2847
Shi/MB080C	-0.32	> 0.9999	0.05992	0.0342	0.1056	> 0.9999
Shi/MB082C	-0.1925	0.3673	0.2825	> 0.9999	-0.4062	0.0067
Shi/MB093C	-0.425	> 0.9999	0.3924	> 0.9999	-0.1989	0.0456
Shi/MB112C	-0.355	> 0.9999	-0.2184	0.003	-0.3983	0.0069
Shi/MB242A	-0.3925	> 0.9999	0.2927	> 0.9999	0.27	> 0.9999
Shi/MB310C	-0.225	0.8919	0.307	> 0.9999	0.6466	> 0.9999
Shi/MB542B	-0.3925	> 0.9999	0.3339	> 0.9999	0.5758	> 0.9999
Shi/MB543B	-0.2925	> 0.9999	0.4898	> 0.9999	0.6405	> 0.9999
Shi/MB549C	-0.245	> 0.9999	0.6667	> 0.9999	0.1013	> 0.9999
Shi/MB552B	-0.52	> 0.9999	0.5726	> 0.9999	0.2584	> 0.9999

Table 13. MBON primary screen data. p-values calculated via Kruskal-wallis non-parametric ANOVA with Dunn's post-hoc multicomparison test.

	PAM Screen Preference Index (PI) mean and p-values					
Genotype	CO2 PI	CO2 p-value	Vinegar PI	Vinegar p-value	CO2 + Vinegar PI	CO2 + Vinegar p-value
Shi/w-	-0.5505	-	0.5095	-	0.494	-
Shi/MB025B	-0.1266	0.0015	0.0914	0.1818	0.07958	0.5903
Shi/MB087C	-0.3158	> 0.9999	-0.03865	0.0185	-0.05003	0.123
Shi/MB109B	-0.4822	> 0.9999	0.244	> 0.9999	0.2474	> 0.9999
Shi/MB301B	-0.6591	> 0.9999	0.2129	> 0.9999	0.1507	> 0.9999
Shi/MB195B	-0.2513	0.0876	0.1225	0.0304	-0.003088	0.0084
Shi/MB312B	-0.3006	> 0.9999	0.05633	0.1001	0.1795	> 0.9999
Shi/MB315B	-0.4871	> 0.9999	0.2699	0.8408	0.1239	> 0.9999
Shi/MB032B	-0.2414	0.5066	0.2421	> 0.9999	-0.08395	0.2104
Shi/MB043B	-0.3567	> 0.9999	-0.1204	0.0096	0.1915	> 0.9999
Shi/MB047B	-0.3883	> 0.9999	-0.01638	0.0577	-0.00095	0.4081
Shi/MB188B	-0.4328	> 0.9999	0.4439	> 0.9999	0.271	> 0.9999
Shi/MB194B	-0.0437	0.1749	0.01868	0.0615	0.2438	> 0.9999
Shi/MB213B	-0.4203	> 0.9999	0.4701	> 0.9999	0.0117	0.1952
Shi/MB299B	-0.02223	0.0138	0.234	> 0.9999	0.4293	> 0.9999
Shi/MB316B	-0.6957	> 0.9999	0.1898	> 0.9999	0.1419	> 0.9999
Shi/MB040B	-0.5613	> 0.9999	0.04078	0.0035	0.3192	> 0.9999
Shi/MB042B	0.0099	0.0056	0.1828	> 0.9999	0.5047	> 0.9999
Shi/MB196B	-0.188	0.54	0.2297	> 0.9999	0.2032	> 0.9999

Table 14. PAM neuron primary screen data. p-values calculated via Kruskal-wallis non-parametric ANOVA with Dunn's post-hoc multicomparison test.

PPL1 Screen Preference Index (PI) mean and p-values

Genotype	CO2 PI	CO2 p-value	Vinegar PI	Vinegar p-value	CO2 + Vinegar PI	CO2 + Vinegar p-value
Shi/w-	-0.5124	-	0.6539	-	0.5807	-
Shi/MB058B	-0.1555	0.0716	0.0954	0.0199	0.05278	0.1297
Shi/MB060B	-0.7862	0.561	0.2032	0.0656	0.5558	> 0.9999
Shi/MB065B	-0.3016	> 0.9999	0.0919	0.0199	0.02068	0.09
Shi/MB296B	-0.4496	> 0.9999	0.3706	> 0.9999	0.2032	> 0.9999
Shi/MB304B	-0.5479	> 0.9999	0.08643	0.0183	0.2603	> 0.9999
Shi/MB308B	-0.5787	> 0.9999	0.2147	0.0707	-0.1354	0.0151
Shi/MB438B	-0.2776	0.8106	0.6344	> 0.9999	0.4717	> 0.9999
Shi/MB439B	-0.2067	0.2266	0.6928	> 0.9999	0.5988	> 0.9999
Shi/MB502B	-0.4274	> 0.9999	0.3618	0.9412	0.6254	> 0.9999
Shi/MB504B	-0.4767	> 0.9999	0.4893	> 0.9999	0.3893	> 0.9999

Octopamine Screen Preference Index (PI) mean and p-values

Genotype	CO2 PI	CO2 p-value	Vinegar PI	Vinegar p-value	CO2 + Vinegar PI	CO2 + Vinegar p-value
Shi/w-	-0.4498	-	0.5268	-	0.627	-
Shi/MB021B	-0.3451	> 0.9999	0.2647	0.4137	0.1841	0.2023
Shi/MB022B	-0.3289	> 0.9999	0.3029	0.9511	-0.06569	0.029
Shi/MB113C	-0.4304	> 0.9999	0.1464	0.2023	-0.04921	0.0237

Other Screen neuron Preference Index (PI) mean and p-values

Genotype	CO2 PI	CO2 p-value	Vinegar PI	Vinegar p-value	CO2 + Vinegar PI	CO2 + Vinegar p-value
Shi/w-	-0.4911	-	0.8091	-	0.8797	-
Shi/MB013B	-0.5404	> 0.9999	0.2583	0.0073	0.41	0.0613
Shi/MB380B	-0.132	0.2958	0.301	0.0129	0.3147	0.0073
Shi/MB460B	-0.1007	0.1088	0.535	0.5333	0.2816	0.004
Shi/MB465C	-0.4609	> 0.9999	0.3926	0.0522	0.5211	0.0974

Table 15. PPL1, octopaminergic, and extrinsic neuron primary screen data. p-values calculated via Kruskal-wallis non-parametric ANOVA with Dunn's post-hoc multicomparison test.

MB011B confirmation experiments Preference Index (PI) mean and p-values (12n)

Genotype	Starved				Fed			
	32		25		32		25	
	CO2 PI	CO2 p-value	CO2 PI	CO2 p-value	CO2 PI	CO2 p-value	CO2 PI	CO2 p-value
Shi/w-	-0.8142	-	-0.775	-	-0.815	-	-0.7733	-
Shi/MB011B	-0.3075	< 0.0001	-0.72	0.5843	-0.535	0.0002	-0.755	> 0.9999
w-/MB011B	-0.717	0.2865	-0.666	0.1031	-0.783	> 0.9999	-0.703	0.3621

MB002B confirmation experiments Preference Index (PI) mean and p-values (12n)

Genotype	Starved				Fed			
	32		25		32		25	
	CO2 PI	CO2 p-value	CO2 PI	CO2 p-value	CO2 PI	CO2 p-value	CO2 PI	CO2 p-value
Shi/w-	-0.8142	-	-0.775	-	-0.815	-	-0.7733	-
Shi/MB002B	-0.4558	0.0002	-0.7783	> 0.9999	-0.6633	0.0401	-0.7992	> 0.9999
w-/M002B	-0.819	> 0.9999	-0.697	0.3476	-0.842	> 0.9999	-0.763	> 0.9999

MB109B dTrpA1 activation experiments Preference Index (PI) mean and p-values (10n)

Genotype	Starved				Fed			
	32		25		32		25	
	CO2 PI	CO2 p-value	CO2 PI	CO2 p-value	CO2 PI	CO2 p-value	CO2 PI	CO2 p-value
dTrpA1/w-	-0.862	-	-0.821	-	-0.789	-	-0.771	-
dTrpA1/MB109B	-0.528	< 0.0001	-0.724	0.0789	-0.686	0.2274	-0.674	0.1671
w+/M109B	-0.857	> 0.9999	-0.81	> 0.9999	-0.866	0.4645	-0.671	0.1499

MB056B dTrpA1 activation experiments Preference Index (PI) mean and p-values (8n)

Genotype	32		25	
	CO2 PI	CO2 p-value	CO2 PI	CO2 p-value
dTrpA1/w-	-0.745	-	-0.775	-
dTrpA1/MB056B	-0.3063	0.0052	-0.6988	0.7826
w+/MB056B	-0.7363	> 0.9999	-0.8075	> 0.9999

MB434B confirmation experiments Preference Index (PI) mean and p-values (8n)

Genotype	32		25	
	CO2 PI	CO2 p-value	CO2 PI	CO2 p-value
Shi/w-	-0.6188	-	-0.5113	-
Shi/MB434B	-0.5313	0.5936	-0.67	0.0601
w-/MB434B	-0.58	> 0.9999	-0.4	0.2357

Table 16. MBON confirmation data, and PAM DAN activation data. p-values calculated via one-way ANOVA with Bonferroni's post-hoc multicomparison test.

MBON optogenetic activation experiments Preference Index (PI) mean and p-values (10-13n)		
Genotype	Light-aversion PI	p-value
Empty/Chr	0.008192	-
Chr/MB002B	-0.06364	0.4841
Chr/MB011B	-0.1812	0.0082
Empty/w-	-0.03878	-
w-/MB002B	0.05592	0.0725
w-/MB011B	-0.06125	> 0.9999

PAM optogenetic activation experiments Preference Index (PI) mean and p-values (9-15n)		
Genotype	Light-attraction PI	p-value
Empty/Chr	0.008192	-
Chr/MB056B	0.1309	0.4468
Chr/MB047B	0.1105	0.8751
Chr/MB109B	0.1857	0.0356
Chr/MB316B	0.2186	0.0129
Chr/MB042B	0.1882	0.0488
Chr/MB040B	0.1904	0.038
Empty/w-	-0.03878	> 0.9999
w-/MB056B	0.01106	> 0.9999
w-/MB047B	-0.1052	> 0.9999
w-/MB109B	0.04863	0.6439
w-/MB316B	-0.0897	> 0.9999
w-/MB042B	0.03823	> 0.9999
w-/MB040B	0.04026	> 0.9999

Table 17. MBON and PAM DAN optogenetic activation data. p-values calculated via one-way ANOVA with Bonferroni's post-hoc multicomparison test.

CS conditioning test Preference Index (PI) mean and p-values (16n)

Genotype	Conditioning Pis			p-values	
	Air	CO2	Vinegar + CO2	Air v. CO2 p-value	Air v. conflict p-value
CS	-0.5828	-0.5776	-0.6651	> 0.9999	0.6792

MB109B activation and odour pairing 2 mins Preference Index (PI) mean and p-values (10n)

Genotype	CO2 2 min condition	p-value
dTrpA1/w-	-0.775	-
dTrpA1/MB109B	-0.728	0.6289
w+/dTrpA1	-0.735	0.7815

Table 18. CS and PAM DAN (MB109B) 3 minute memory data. p-values calculated via one-way ANOVA with Bonferroni's post-hoc multicomparison test.

Stimulus	Peak delta f/f %	p-value	Statistical test
humidified air (fed)	8.021	0.002	air (fed) vs vinegar (fed) : Wilcoxon matched-pairs signed rank test
humidified air (starved)	25.38	0.0001	air (starved) vs vinegar (starved) : Paired t-test
vinegar (fed)	113.7	0.0232	vinegar (fed vs vinegar (starved) : Mann Whitney test
vinegar (starved)	232.7	-	
CO2 (fed)	13.73	0.8944	CO2 (fed) vs CO2 (starved) : unparied t-test
CO2 (starved)	8.152	-	
Stimulus	Peak delta f/f %	p-value	
paraffin oil (fed)	16.7	-	
paraffin oil (starved)	22.77	-	
acetoin acetate (fed)	72.9	-	
acetoin acetate (starved)	172	0.0006	paraffin (starved) vs acetoin acetate (starved) : Paired t-test
isoamyl acetate (fed)	14.83	-	
isoamyl acetate (starved)	66.44	-	
benzaldehyde (fed)	30.55	-	
benzaldehyde (starved)	69.39	-	
Stimulus	Peak delta f/f %	p-value	
humidified air (fed)	1.475	-	
humidified air (starved)	2.139	-	
CO2 (fed)	46.87	0.0178	CO2 (fed) vs vinegar (fed) : Paired t-test
CO2 (starved)	38.84	-	
vinegar (fed)	13.53	-	
vinegar (starved)	25.49	-	
CO2 + vinegar (fed)	17.35	0.0344	CO2 (fed) vs CO2 + vinegar (fed) : Paired t-test
CO2 + vinegar (starved)	16.91	-	

Table 19. Calcium imaging data and statistical tests.

Acknowledgements

Firstly I would like to thank Dr. Ilona Grunwald Kadow for hosting me in her lab for the duration of my PhD, and for her excellent scientific and technical support over the course of my project. Our many discussions have shaped how I now understand brains.

I would also like to thank my thesis advisory committee, Prof. Dr. Hiromu Tanimoto, and Prof. Dr. Axel Borst who gave useful and critical feedback on the progress of my project.

It was my pleasure to work with the members of the Kadow lab and Max Planck Institute of Neurobiology. I have had many fruitful and inspiring conversations over the years that fed directly into my project. In this regard I would particularly like to thank Dr. Katrin Vogt and other members of the Tanimoto lab for their invaluable intellectual and technical input and advice during the early stages of my project. I am also grateful to the Graduate School of Systemic Neuroscience for providing an excellent academic framework for my PhD.

Thanks to our collaborators Dr. Yoshinori Aso and and Dr. Gerald Rubin at Janelia Farm Research Campus for providing me with the excellent library of fly lines and for organising the MB screening project that has been central to my research. I am also grateful to Dr. Yoshinori Aso for the opportunity to work with his behavioural setups at JFRC.

Special thanks to Dr. Siju Purayil for lending his experience in calcium imaging to this project, and to Anja Friedrich for her excellent confocal data.

Finally, I would like to thank Olivia Haas for her love and unwavering intellectual and emotional support through rough and smooth. Without her everything would have been harder. I also want to thank my family for their support from afar throughout the last five years.

Publication

A higher brain circuit for immediate integration of conflicting sensory information in *Drosophila*

Laurence P.C. Lewis, K.P. Siju, Yoshinori Aso, Anja B. Freidrich, Alexander J.B. Bulteel, Gerald M. Rubin, and Ilona C. Grunwald Kadow. Current Biology 2015 August 31;25(17):2203-14.

Curriculum Vitae

Laurence Lewis

Personal information

Date of birth: 26th July 1984

Nationality: British

Place of birth: Newport, Isle of Wight, United Kingdom

Languages: English, German

Education

2011 – 2015   **LMU, Munich, Germany**

PhD at the Max Planck Institute of Neurobiology in the lab of Dr. Ilona Kadow on olfactory conflict resolution in *Drosophila*.

2010 – 2011   **LMU, Munich, Germany**

GSN PhD Fast-Track year

2003 – 2006   **The University of Reading, Reading, United Kingdom**

BSc (hons) Biological Sciences

1997 – 2002   **Ryde School, Isle of Wight, United Kingdom**

British A-levels: Physics, Biology, Design Technology

Professional experience

2007 – 2010   **Senior Scientific Officer, Cancer Research UK,
                      London, United Kingdom**

Carried out individual and collaborative research projects, managed laboratory resources, equipment, and budgeting, and trained new laboratory members in standard techniques.

2003 – 2006   **Mental Health Care Worker, Warby House Hospital,
                      Reading, UK**

Provided individual compassionate care for patients suffering from a range of illnesses and coordinated care programmes with in-house medical professionals.

Teaching experience

2011 – 2015   Theoretical and practical supervision of yearly masters practical course in molecular neurobiology

2015   Supervision of Sarvarinder Gill during a six month internship from UCSF.

2015   Supervision of Alexander Bulteel during a three month internship from Dartmouth.

2013 – 2015   Supervision of Ketura Berry during an initial Fullbright scholarship and then as an intern.

2013   Supervision of Lidia Castro during a one month student internship.

2012-2015   Training of student lab helpers in fly handling and rearing techniques.

Publications

Lewis LPC, KP Siju, Aso Y, Freidrich AB, Bulteel Aj, Rubin GM, and Grunwald Kadow IC. A higher brain circuit for immediate integration of conflicting sensory information in *Drosophila*. Curr Biol. Aug 2015 ; 25(17): 2203-14. 2015

Hodson C, Cole AR, **Lewis LPC**, Miles JA, Purkiss A. and Walden H. Structural analysis of human FANCL, the E3 ligase in the Fanconi anemia pathway. J Biol Chem. Sept 2011 ; 286, pp. 32628-32637. 2011

Marshall KE, Morris KL, Charlton D, O'Reilly N, **Lewis LPC**, Walden H, Serpell LC. Hydrophobic, aromatic, and electrostatic interactions play a central role in amyloid fibril formation and stability. Biochemistry. March 2011 ; 50(12): 2061-71. 2011

Cole AR, **Lewis LPC**, Walden H. The structure of the catalytic subunit FANCL of the Fanconi anemia core complex. Nat Struct Mol Biol. March 2010 ; 17(3): 294-298. 2010

Conference talks and posters

2011   Oral presentation: Joint Kadow and Louis lab retreat

2012   Oral presentation: MB mini-olympiad meeting, Janelia Farm Research Campus, Virginia, United States

2013   Oral presentation: "Munich Fly Retreat", Ringerg castle, Tegernsee, Germany

2014   Poster: Cold Spring Harbour Neuronal Circuits meeting, New York, United States

2015   Poster: QBI / MCN Symposium, Brisbane, Australia

2015   Oral presentation: Joint lab retreat with Louis, Portugues, and Zimmer groups.

Declaration (Eidesstattliche Versicherung / Affidavit)

Eidesstattliche Versicherung/Affidavit

Hiermit versichere ich an Eides statt, dass ich die vorliegende Dissertation 'A neural circuit for resolving sensory conflict in *Drosophila*' selbstständig angefertigt habe, mich außer der angegebenen keiner weiteren Hilfsmittel bedient und alle Erkenntnisse, die aus dem Schrifttum ganz oder annähernd übernommen sind, als solche kenntlich gemacht und nach ihrer Herkunft unter Bezeichnung der Fundstelle einzeln nachgewiesen habe.

I hereby confirm that the dissertation 'A neural circuit for resolving sensory conflict in *Drosophila*' is the result of my own work and that I have only used sources or materials listed and specified in the dissertation.

München, den / Munich, date   Unterschrift / signature

Declaration of author contributions

I designed and carried out all behaviour experiments with the exception of those in Figure 33B. This includes all behavioural screening and subsequent behavioural experiments.

Dr. Ilona Kadow, Dr. Siju Purayil and myself designed the calcium imaging experiments. Dr. Siju Purayil carried out the calcium imaging experiments (Figures 27, 28, 30, and 32).

Anja Friedrich performed all immunohistochemical staining and confocal imaging (Figures 23, 24, 26, 27A, and 29).

Author ……………………………………………………

Supervisor ………………………………………….